2010-03-02

A Mathematical Model Describing the Early Development of Multiple Myeloma

Joaquin Zabalo
University of Miami, jzabalo@bellsouth.net

UNIVERSITY OF MIAMI

A MATHEMATICAL MODEL DESCRIBING THE EARLY DEVELOPMENT OF MULTIPLE MYELOMA

By

Joaquin Zabalo

A DISSERTATION

Submitted to the Faculty
of the University of Miami
in partial fulfillment of the requirements for
the degree of Doctor of Philosophy

Coral Gables, Florida

May 2010

UNIVERSITY OF MIAMI

A dissertation submitted in partial fulfillment of
the requirements for the degree of
Doctor of Philosophy

A MATHEMATICAL MODEL DESCRIBING THE EARLY DEVELOPMENT OF MULTIPLE MYELOMA

Joaquin Zabalo

Approved:

_____	_____
Chris Cosner, Ph.D.	Terri A. Scandura, Ph.D.
Professor of Mathematics	Dean of the Graduate School
_____	_____
Huseyin Kocak, Ph.D.	Shigui Ruan, Ph.D.
Professor of Mathematics	Professor of Mathematics

_____
Lawrence Boise, Ph.D.
Professor of Hematology and
Medical Oncology
Emory University
Winship Cancer Institute

ZABALO, JOAQUIN (Ph.D., Mathematics)

A Mathematical Model Describing the Early Development of Multiple Myeloma (May 2010)

Abstract of a dissertation at the University of Miami.

Dissertation supervised by Professor Chris Cosner.
No. of pages in text. (182)

Multiple myeloma is a malignant bone marrow plasma cell tumor which is responsible for approximately 12,000 deaths per year in the United States and two percent of all cancer deaths. It is recognized clinically by the presence of more than ten percent bone marrow plasma cells, the detection of a monoclonal protein (M-protein), anemia, hypercalcemia, renal insufficiency, and lytic bone lesions. The disease is usually preceded by a premalignant tumor called monoclonal gammopathy of undetermined significance (MGUS), which is present in one percent of adults over the age of fifty, three percent over the age of seventy and ten percent of those in the tenth decade. MGUS is also recognized by the detection of M-protein, but with less than ten percent bone marrow plasma cells and without the other features exhibited by myeloma. The majority of MGUS patients remain stable for long periods without ever developing myeloma. Only a small percentage of patients with MGUS eventually develop multiple myeloma. However, the reason for this is not yet known. Once the myeloma stage is reached, a sequence of well-understood mutational evets eventually lead to the escape of the tumor from the control of the immune system.

We propose a mathematical model of tumor-immune system interactions at the onset of the disease in an effort to better understand the early events that take place and their

influence on the outcome of the disease. The model is calibrated with parameter values obtained from available data and we study the resulting dynamics. Next, we study how the behavior of the system is affected as parameters are varied. Finally, we interpret the results and draw some conclusions.

ACKNOWLEDGMENTS

I would like to express my deepest gratitude to my advisor, Dr. Chris Cosner, for giving me the opportunity to pursue my interest in cancer modeling and for his constant guidance throughout the process. I would also like to thank Dr. Kocak and Dr. Ruan for their many helpful suggestions and Dr. Boise for his help with the medical literature. Also, I would like to thank my wife Esther for all her encouragement and patience and my parents for teaching me the value of an education.

TABLE OF CONTENTS

LIST OF FIGURES

LIST OF TABLES

Chapter 1

Introduction

1.1 General Overview of the Immune System

The immune system is the body's natural defense against foreign substances or altered self substances. It is a two-tier line of defense consisting of *innate immunity* and *adaptive immunity*. *Innate immunity* refers to the non-specific first line of defense against the foreign substance. It consists of cells which can attack a wide variety of invading substances, even if the host has never been exposed to them before. *Adaptive immunity* refers to a specific immune response mounted against a previously encountered foreign substance called an antigen. With each successive encounter of the same antigen, the adaptive immune response improves. This behavior is called the *immune memory*.

The cells of the immune system arise from pluripotent hematopoeietic (generate cellular elements of blood) stem cells residing in the bone marrow. These stem cells produce either common lymphoid progenitor cells, which give rise to T-lymphocytes

(T-cells) and B-lymphocytes (B-cells) involved in *adaptive immunity*, or common myeloid progenitor cells which give rise to other types of cells including dendritic cells and macrophages involved in *innate immunity*.

Innate immunity begins with antigen-presenting cells (APC), such as macrophages (MAC) and dendritic cells (DC), and natural killer (NK) cells, which are circulating throughout the body looking for foreign substances. MAC are primarily phagocytic cells that engulf and destroy pathogens. They also secrete cytokines (proteins that affect the behavior of other cells), and induce inflamatory response and fever. NK cells, although not lymphocytes, are large granular lymphocyte-like cells that can detect and attack certain infected cells. Primarily, they attack tumor cells and help protect against a variety of viruses. They also secrete lymphokines (cytokines secreted by T-cells), such as interferon-gamma ($IFN-\gamma$). These chemical signals stimulate other components of the immune system to enter into action. DC are phagocytic when they are immature and take up pathogens. After maturing, they act as APC to T-cells, initiating adaptive immune responses. In order for this to occur, ingested antigens are fragmented into small particles called peptides. Part of these peptides bind to molecules called the major histocompatibility complex (MHC) which are in turn presented in the APC cell surface as an MHC/peptide complex. The T-cells carry surface receptors that allow them to recognize different MHC/peptide complexes. Once the T-cells are activated by the MHC/peptide recognition, they divide and secrete lymphokines. T-cells mature in the thymus. The two subgroups of T-cells are helper T-cells ($CD4^{+}T$) that help B-cells produce antibodies in response to antigens and induce the development of $CD8^{+}T$ cells, which later become cytotoxic T-cells (CTL). In contrast, the B-cells have receptors with the ability to recognize parts of

the antigens free in solution without the assistance of MHC molecules. These surface receptors on these B-cells respond to a specific antigen. When a signal is received by these B-cell receptors, the B-cells are activated and will proliferate and differentiate into plasma cells that secrete antibody molecules in high volumes. Plasma cells are terminally differentiated B-cells that provide protective immunity through the continuous production of antibodies. These released antibodies (which are soluble forms of the B-cell receptors) are used to neutralize the invading pathogen, leading to their destruction. There is a population of short-lived plasma cells which resides primarily in the nonlymphoid area of the spleen or lymph nodes. However, many migrate to the bone marrow where the majority enter a long-lived population of plasma cells. Some of the activated B- and T-cells will differentiate into memory cells. These will remain circulating through the organism for long periods of time, thus guaranteeing future protection against the same (or a similar) antigen that elicited the immune response. For a more detailed explanation, refer to [48].

1.2 The Immune System, Cancer and Immunoediting

Normally, during the first stages of a tumor, the immune system responds as follows. First, the antigenicity (how different it is from self) of tumor cells causes the recruitment of NK cells, NKT cells, and DC of the innate immune system to the tumor site. The NK cells attack the tumor and both NK and NKT cells start producing $IFN-\gamma$, which induces the production of chemokines. These are chemoattractant proteins that stimulate the migration and activation of cells. Chemokines recruit

more NK and DC, MAC, and other immune effector cells to the tumor site and activates MAC and NK cells to attack the tumor. Dead tumor cell debris is ingested by DC and carried to the lymph nodes where tumor-specific $CD4^{+}T$ cells develop and induce the development of tumor-specific $CD8^{+}T$ cells, which later become CTL. These cells of the adaptive immune system migrate to the tumor site where they produce $IFN-\gamma$ and attack the tumor. This first stage was originally referred to as *Immunosurveillance*. Now, it is seen as part of a larger picture, *Immunoediting*, where the selective pressure of the immune system on the mutating cancer cells is considered. In the *Immunoediting* hypothesis, this first stage is referred to as *Elimination*, since the cancer cells have been recognized and are being destroyed by the immune system. The cancer cells continue to mutate and the immune system attempts to destroy them once they are recognized. The second stage is *Equilibrium*, where an equilibrium is reached in the number of cancer cells. Eventually, an escape mutant is selected for, leading to the escape of the cancer cells from immune control. This final stage is therefore referred to as *Escape*. For a more detailed explanation, refer to [22, 23, 91].

1.3 Monoclonal Gammopathy of Undetermined Significance and Multiple Myeoloma

Multiple myeloma (MM) is a malignant plasma cell tumor recognized clinically by the proliferation of malignant plasma cells in the bone marrow, the detection of a serum or urine monoclonal (produced by a single clone) protein, anemia, hypercalcemia, renal insufficiency, and lytic bone lesions (see [67]). It accounts for approximately

12,000 deaths per year in the United States alone and approximately 2% of all cancer deaths (see [62]). The disease is usually preceded by a premalignant tumor called *monoclonal gammopathy of undetermined significance* (MGUS), which is present in 1% of adults over the age of 50, 3% over the age of 70, and 10% in the tenth decade (see [67, 62]). MGUS is characterized by a monoclonal protein (M-protein) in the serum or urine without other clinical features of MM (see [67]).

Genetically, there is not much difference between MGUS cells and MM cells . The majority of MGUS patients remain stable for long periods without ever developing MM (see [19]). It is believed that the progression of the disease from MGUS to MM, which constitutes the first stage of the disease, is mostly due to a failure of the immune system rather than the usual *immunoediting*. Refer to Figure 1.1 for a graphic representation of the events that occur at this stage. However, once the MM stage is reached, a sequence of mutational events ultimately lead to the escape of the cancer from immune control. This constitutes the second stage of the disease. Figure 1.2 depicts disease progression from normal plasma cell to MM escape mutant.

MGUS cells undergo chromosomal instability (CIN) mutations (IgH translocations). This process is ongoing throughout the disease. Since normal plasma cells are genetically unstable during the production of antibodies, they are therefore somewhat more tolerant to DNA damage than other cells. Primary Ig translocations ($cyclinD1$ or $D3$, $FGFR3$ and $MMSET$, $cMAF$), which are oncogene mutations requiring one mutational hit, provide immortalizing events in 50% of the tumors. $CyclinD1$ or $D3$ mutations allow cells to grow in response to $interleukin-6$ ($IL-6$) by making them more susceptible to proliferative stimuli. MGUS cells grow in response to

$IL-6$, while normal plasma cells produce antibodies but do not proliferate (see [67]). $IL-6$ is produced by bone marrow stromal cells and its production rate is increased by the presence of tumor cells (see [58, 59, 77]). Also, MGUS cells are continually producing M-protein (monoclonal antibody). T-cells tolerate M-protein produced by the MGUS cells, since it is normally produced by plasma cells. This monoclonal immunoglobulin (Ig) that can serve as a patient-specific tumor antigen, secreted largely as a soluble antigen, can lead to deletion of Ig-reactive $CD4^+T$ cells by the same mechanism which is responsible for the prevention of autoimmunity (see [19]). This might explain the reduction in the number of $CD4^+T$ cells found in patients with MM and the reduction in the number of $CD4^+T$ and $CD8^+T$ cells in patients with either MGUS or MM (although in later stages of MM, $CD4^+T$ cell numbers continue to decline and $CD8^+T$ cell numbers increase slightly) (see [13]). M-protein is a marker which is used during diagnosis. The increase in the amount of M-protein as the disease progresses is caused by an increase in the number of MGUS and/or MM cells. The bone marrows of patients with MGUS contain less than 10% plasma cells while those of patients with MM contain greater than 10% plasma cells (see [67]). When glycolipid is normally presented by DC, it stimulates the production of $IFN-\gamma$ and $interleukin-4$ ($IL-4$) and regulates autoimmunity and resistance to infections and tumors. However, when glycolipid is presented by non-dendritic cells, such as MGUS cells, it causes the loss of ligand-dependent $IFN-\gamma$ production by NKT cells. However, this NKT cell disfunction is thought to be medically reversible by stimulating the cells with $\alpha-galactosylcerabide$ ($\alpha-GalCer$) pulsed DC (see [18]). $IFN-\gamma$ production also contributes to growth control of *myeloma* by initially inducing the production of chemokines that recruit more immune cells to the tumor site, and later by mediating angiostasis (the body's normal regulation over

the creation of new blood vessels), controlling tumor growth via decreased $IL-6$ or $STAT-3$-mediated transcription, and inhibiting osteoclastogenesis (bone destruction). So its decrease also has an effect on later stages of cancer progression. For a graphic representation of the cell processes described above, refer to Figure 1.1. Karyotypic instability is maintained througout the progression of the disease. Activating oncogene mutations ($NRAS$, $KRAS$, $FGFR3$), requiring one mutational hit, occur mostly in MM. The *Ras* mutation causes abnormal signaling inside the MM cell, taking the place of $IL-6$, and results in enhancing the growth of the cancer cells and decreasing the amount of $IL-6$ that is required for their survival and growth. However, this does not necessarily result in $IL-6$ independence. Angiogenesis (the process involving the formation of new blood vessels) begins at this stage in order to provide nutrients to the cancer cells. Secondary Ig translocations occur. These include two TSP (tumor-suppressor gene) mutations, deletion of $p-53$ and inactivation of *Rb*, each requiring two mutational hits. These accomplish two things. First, they prevent normal TSP function, which would cause the destruction of the cell if DNA mutations are occurring. Second, they knock out the ability of the TSP to inhibit $IL-6$ expression, thus leading to the autocrine (affects the function of the same cell type) production of $IL-6$, in which the cells stimulate their own growth. For a more detailed explanation on the sequence of mutational events and their affect, refer to [40, 62].

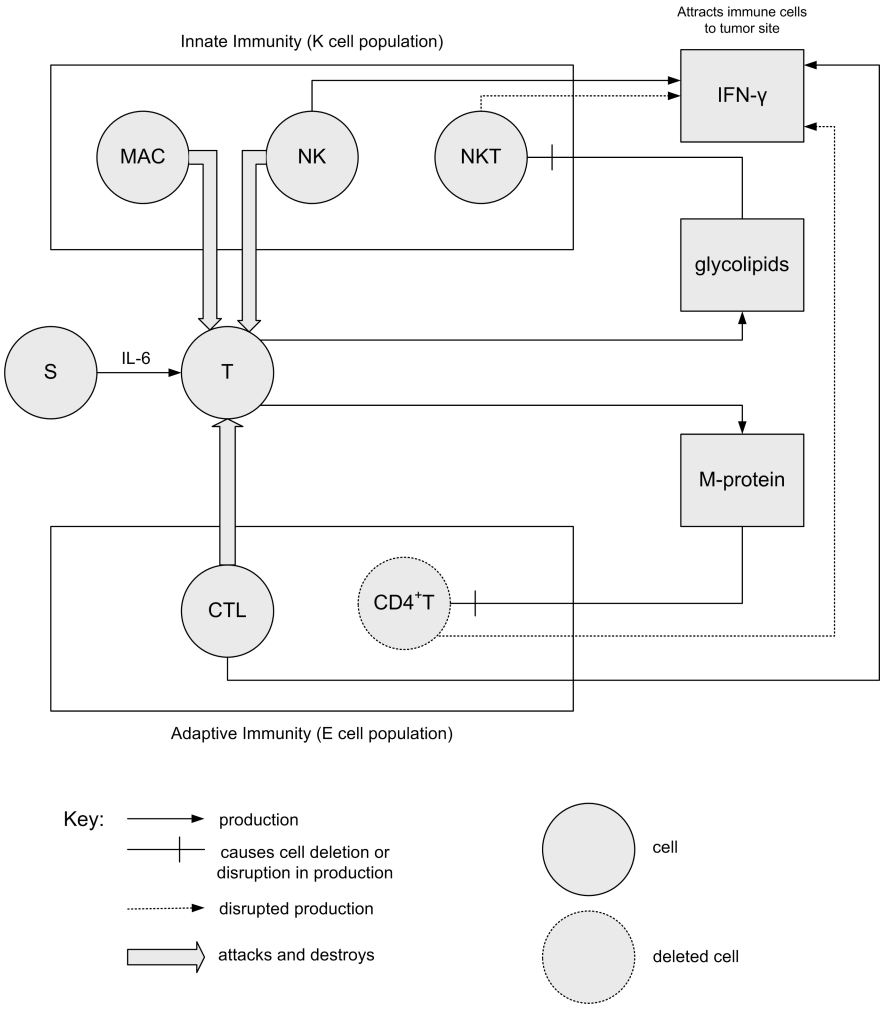

Figure 1.1: This flowchart shows the interactions between stromal cells (S), tumor cells (T), macrophages (MAC), natural killer cells (NK), natural killer T-cells (NKT), cytotoxic T-cells (CTL), helper T-cells ($CD4^{+}T$), interferon-gamma ($IFN-\gamma$), glycolipids, and M-protein, during the MGUS phase of the disease, which eventually lead to MM.

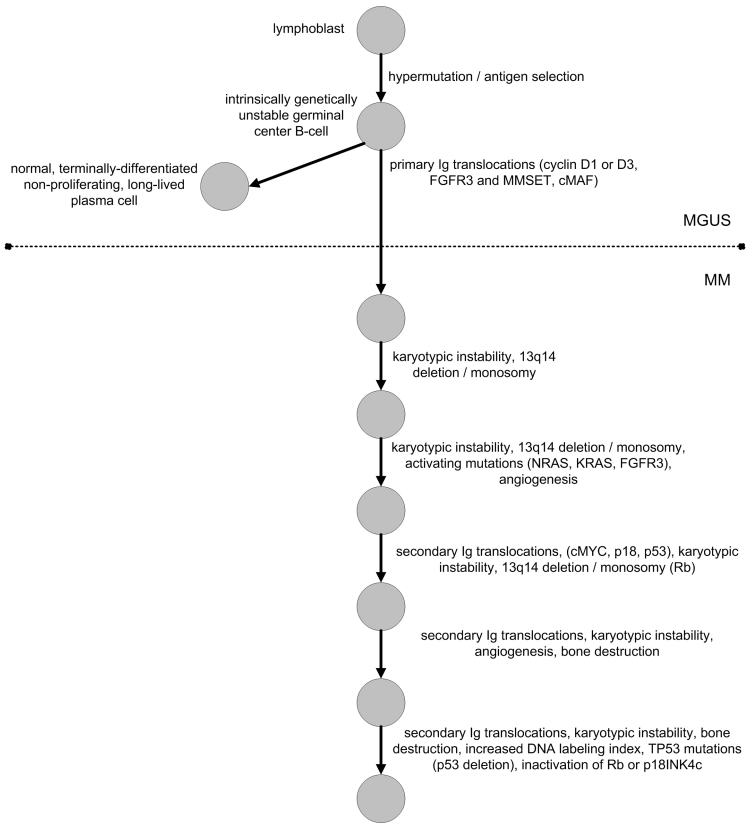

Figure 1.2: This flowchart shows the sequence of mutational events that are necessary for the disease to progress from normal to MGUS, from MGUS to MM, and finally to escape from the control of the immune system.

Chapter 2

Construction of the Model

The model (see Figure 1.1) deals with the transition from normal to MGUS and possibly MM. This is thought to be mostly due to a failure of the immune system. The interaction between the cancer cells, the normal plasma cells, the stromal cells, and the immune system is captured by a system of differential equations. As seen in Figure 1.1, certain cell populations were grouped together either as cells of the innate immune system or cells of the adaptive immune system in order to reduce the number of equations in the model. However, not all cells of the same group have the same function. For instance, some cells in one group produce $IFN - \gamma$ while other cells in the same group do not. Also, the functions of cells in different groups sometimes overlap. For example, certain cells in both groups produce $IFN - \gamma$. This issue will be addressed at a later time. Also, grouping cells into the two groups mentioned above results in a built-in time delay in the model. The model attempts to capture the dynamics of interacting processes in an effort to understand how they influence the outcome of the disease.

This is a first attempt at a crude model using the data that is available at the moment. As more is known about the disease, the model can be refined.

The motivation for such a model is that it might lead to a better understanding of disease progression. This, in turn, can lead to better treatment protocols. As mentioned in Section 1.3, the majority of MGUS patients remain stable for long periods without ever developing MM. Only a small percentage of patients with MGUS develops MM (see [67]). If the reason for this is known, it can lead to more effective treatments that, although might not lead to a cure, might keep an MGUS patient from eventually developing MM, or push a patient with MM back to the MGUS stage.

We would like the model to answer several questions. For one thing, how much of an influence does the production of M-protein and glycolipids by the cancer cells have on the development of the disease? This is clinically significant, since the disfunction in the ability of NKT cells to produce $IFN - \gamma$ (which attracts immune cells to the tumor site) is medically reversible, as mentioned earlier. What else, if anything, influences the progression or outcome of the disease? Since this disease usually occurs late in life, prolonging the increase in tumor cells to the levels seen in MGUS or MM long enough might be as good as a cure.

Figure 1.2 shows the the sequence of mutational events that are necessary for the progression from MGUS to MM and which ultimately results in the escape of the cancer from the control of the immune system. The process is fairly well understood and to capture this behavior, stochastic models such as the ones used in [46] and [47], which use a branching process, or in [73], can be utilized.

The model that we are proposing, however, is not concerned with the later stages of the disease. Instead, we are attempting to model the early occurrences that take place from the start, beginning with one MGUS cell.

2.1 The Model Equations

The variables listed below represent densities as either cells per milliliter (in the first four cases) or picograms per milliliter (in the last four cases) as a function of time t in days.

Variables:

$T(t)$ = MGUS tumor cells

$N(t)$ = Normal bone marrow plasma cells

$K(t)$ = Cells of the innate immune system

$E(t)$ = Cells of the adaptive immune system

$P(t)$ = M-protein produced by tumor cells

$G(t)$ = glycolipids produced by tumor cells

$I(t) = IL-6$ produced by stromal cells

$F(t) = IFN-\gamma$ produced by immune system cells

The behavior of the biological system is described by the following system of differential equations:

$$
\begin{cases}
\dfrac{dT}{dt} = \dfrac{k_T I}{e_T + I}\left(1 - \dfrac{T+N}{K_T}\right)T - \dfrac{d_T(K+E)T}{g_T + T} \\[2ex]
\dfrac{dN}{dt} = l_N\left(1 - \dfrac{N}{K_N} - \dfrac{T}{K_T}\right) \\[2ex]
\dfrac{dK}{dt} = r_K\left(1 - \dfrac{K}{K_K}\right)K + \dfrac{k_{KE}F}{e_{KE} + F} \\[2ex]
\dfrac{dE}{dt} = \dfrac{k_{KE}F}{(e_{KE} + F)(1 + \beta P)} - d_E E \\[2ex]
\dfrac{dP}{dt} = l_P T - d_P P \\[2ex]
\dfrac{dG}{dt} = l_G T - d_G G \\[2ex]
\dfrac{dI}{dt} = l_I\left(1 + \dfrac{7T}{e_I + T}\right)s - d_I I \\[2ex]
\dfrac{dF}{dt} = \dfrac{l_F}{e_F + T}\left(\dfrac{1}{3}K + \dfrac{1}{3}\dfrac{1}{1 + \alpha G}K + E\right)T - d_F F
\end{cases}
\tag{2.1}
$$

In the first and third equations, logistic growth is assumed. In general, if A is the population density, then assuming that the per capita birth rate decreases with density and the per capita death rate increases with density, we obtain the following differential equation for the population growth rate:

$$\begin{aligned}
\frac{dA}{dt} &= [(b - b_1 A) - (d + d_1 A)]A \text{ , for some parameters } b, b_1, d, d_1 > 0 \\
&= (b - d)\left[1 - \frac{A}{\frac{b-d}{b_1+d_1}}\right] A \\
&= r\left[1 - \frac{A}{K}\right] A \text{ , where } r = b - d \text{ is the net proliferation rate and} \\
&\qquad\qquad K = \tfrac{b-d}{b_1+d_1} = \tfrac{r}{b_1+d_1} \text{ is the carrying capacity}
\end{aligned}$$

Therefore r and K are directly proportional and are related as explained above. This must be kept in mind if either one is varied in the model.

In the first equation of system (2.1), the first factor in the first term represents the growth of tumor cells in response to $IL-6$. It is of Michaelis-Menten type to indicate the limited response of tumor cells to the growth-stimulatory effects of $IL-6$. The second factor in the first term represents the competition for resources between tumor and normal plasma cells within the bone marrow, where K_T is the carrying capacity of tumor cells. The second term represents the destruction of tumor cells by cells of both the innate immune system and the adaptive immune system. It is modelled by Michaelis-Menten to indicate the limited immune response to the tumor. d_T represents the maximum rate of destruction of tumor cells by the immune system and g_T is a half-saturation constant. That is, g_T is the tumor density at which the destruction rate of tumor cells is equal to one half the maximum destruction rate.

This equation and the next do not include an intrinsic death rate of the cells, since MGUS cells, and plasma cells in general, are long-lived, usually accumulating over a patient's lifetime (see [109, 110]), their role being to secrete antibodies.

In the second equation, the first factor, l_N, represents the influx of normal plasma cells during a patient's lifetime. B cells, activated by antigen exposure, either differentiate into long-lived, antigen-secreting plasma cells, which reside mainly in the bone marrow, or into short-lived plasma cells, which reside mainly in the spleen or lymph nodes. The second factor represents the competition for resources between normal and tumor cells within the bone marrow, where K_N and K_T are the carrying capacities of normal bone marrow plasma cells and $MGUS$ cells, respectively. This form was used instead of $1-(N+T)/K_N$ to prevent the density of normal plasma cells from becoming negative over time (if $N=0$ and $T>K_N$).

In the third equation, the first term represents the background density of innate immune system cells (the K cell population consisting of NKT and NK cells, and MAC) that are ready to attack invading pathogens. Although these cells mature outside the bone marrow, they then circulate throughout the body and a number of them are found in a normal bone marrow (see [20, 32, 79], resp.), forming the first line of defense against the tumor. Logistic growth is assumed with net proliferation rate (birth rate minus death rate) r_K and the carrying capacity K_K of the K cell population the same as the initial value $K(0)$, calculated later, since $K(0)$ is the value for a healthy individual before the tumor. These cells also secrete $IFN-\gamma$, which induces the production of chemokines, which in turn attract more immune cells.

The second term represents the recruitment of innate immune system cells to the tumor site in response to the presence of $IFN - \gamma$. A Michaelis-Menten form was used to indicate the saturation effect of $IFN - \gamma$.

The fourth equations models the adaptive immune response. Since this is an antigen-specific immune response, any adaptive immune cells that were present before the tumor was encountered do not recognize the tumor and we can assume that there is no background density of these cells initially. Once exposed to the tumor, a tumor-specific immune response is mounted. The first term in the equation represents the recruitment of adaptive immune system cells ($CD4^+T$ ($Th1$), $CD8^+T$ (CTL)) to the tumor site in response to the presence of $IFN - \gamma$. Again, a Michaelis-Menten form was used to indicate the saturation effect of $IFN-\gamma$. The β in the denominator is an inhibition parameter which indicates the reduction in the number of $CD4^+T$ cells that react to the tumor due to the presence of M-protein, as explained earlier. When no longer exposed to the same antigen, adaptive immunity slowly decreases over time. Therefore, in the case that the tumor is eradicated, the second term represents the rate of decrease of these cells.

In the fifth equation, the first term represents the soluble M-protein produced by tumor cells and the second term represents the degradation of the M-protein.

In the sixth equation, the first term represents the glycolipids produced by tumor cells and the second term represents the degradation of the glycolipids.

In the seventh equation, the first term represents the production of $IL-6$ by bone marrow stromal cells and the increased production rate in response to the presence of tumor cells. A factor of 7 is used to indicate that as more tumor cells come into contact with bone marrow stromal cells, the $IL-6$ production rate by stromal cells will increase up to eight times the original amount. This eightfold increase in $IL-6$ secretion by bone marrow stromal cells caused by the adherence of myeloma cells to the stromal cells was stated in [103]. It is modelled by Michaelis-Menten to account for the self-limiting production of $IL-6$ by stromal cells stimulated by their interaction with tumor cells. The stromal cell population is assumed to be constant. The second term represents the degradation of $IL-6$.

In the eighth equation, the first term represents the production of $IFN-\gamma$ by cells of both the innate and adaptive immune system. The second factor of the first term consists of $\frac{1}{3}K$ for the NK cell contribution, $\frac{1}{3}\frac{1}{1+\alpha G}K$ for the NKT cell contribution, and E for the CTL and $CD4^{+}T$ cell contributions to the production of $IFN-\gamma$. The α in the denominator is an inhibition parameter which indicates that the presence of tumor-derived glycolipids causes a disfunction in $IFN-\gamma$ production by NKT cells, which are a subset of the cells of the innate immune system. Michaelis-Menten kinetics was used to account for the self-limiting production of $IFN-\gamma$ by immune cells stimulated by their interaction with tumor cells. The second term represents the degradation of $IFN-\gamma$. The details leading to the current form of this equation will be given later during the estimation of parameters.

Tables 2.1 and 2.2 give the units, dimensions, and a short description of the variables and parameters appearing in the model and Table 2.3 gives the initial conditions at the onset of the disease.

As explained in Section 3.2, the accuracy of parameter g_T is questionable and is suspected of possibly being incorrect. The value of $g_T = 1 \times 10^5 \frac{cells}{ml}$ given in Table 2.2 did not allow for tumor development. Instead, a value of $g_T = 5 \times 10^9 \frac{cells}{ml}$ was used initially and later the parameter was varied to study its effect on the behavior of the system. g_T turned out to be an important bifurcation parameter.

Table 2.1: Variables

Variable	Units	Dimensions	Description
T	$\frac{cells}{ml}$	$\frac{c}{v}$	*MGUS tumor cell density*
N	$\frac{cells}{ml}$	$\frac{c}{v}$	*normal plasma cell density*
K	$\frac{cells}{ml}$	$\frac{c}{v}$	*innate immune system cell density*
E	$\frac{cells}{ml}$	$\frac{c}{v}$	*adaptive immune system cell density*
P	$\frac{pg}{ml}$	$\frac{m}{v}$	*density of M-protein produced by tumor cells*
G	$\frac{pg}{ml}$	$\frac{m}{v}$	*density of glycolipids produced by tumor cells*
I	$\frac{pg}{ml}$	$\frac{m}{v}$	*density of* $IL-6$ *produced by stromal cells*
F	$\frac{pg}{ml}$	$\frac{m}{v}$	*density of* $IFN-\gamma$ *produced by immune system cells*

where c=cells, m=mass, v=volume, t=time

Table 2.2: Parameters

Parameter	Units	Dim	Description
k_T	$\frac{.44}{day}$	$\frac{1}{t}$	*net proliferation rate of tumor cells*
e_T	$\frac{2\times10^4 pg}{ml}$	$\frac{m}{v}$	*half-saturation of* $IL-6$
K_T	$\frac{7.7\times10^7 cells}{ml}$	$\frac{c}{v}$	*carrying capacity of tumor cells*
d_T	$\frac{1}{day}$	$\frac{1}{t}$	*destruction of tumor cells*
g_T	$\frac{1\times10^5 cells}{ml}$	$\frac{c}{v}$	*half-saturation constant*
l_N	$\frac{983.77 cells}{ml\times day}$	$\frac{c}{vt}$	*influx of plasma cells*
K_N	$\frac{1.23\times10^7 cells}{ml}$	$\frac{c}{v}$	*carrying capacity of plasma cells*
$k_N=\frac{l_N}{K_N}$	$\frac{8.00\times10^{-5}}{day}$	$\frac{1}{t}$	*influx of plasma cells*
k_K	$\frac{.1245}{day}$	$\frac{1}{t}$	*proliferation rate of innate immune cells*
d_K	$\frac{.03}{day}$	$\frac{1}{t}$	*death rate of innate immune cells*
$r_K=k_K-d_K$	$\frac{.09}{day}$	$\frac{1}{t}$	*net proliferation rate of innate immune cells*
K_K	$\frac{2.30\times10^7 cells}{ml}$	$\frac{c}{v}$	*carrying capacity of innate immune cells*
k_{KE}	$\frac{8.64\times10^6 cells}{ml\times day}$	$\frac{c}{vt}$	*recruitment rate of immune cells*
e_{KE}	$\frac{70pg}{ml}$	$\frac{m}{v}$	*half-saturation of* $IFN-\gamma$
β	$\frac{1.05\times10^{-10}ml}{pg}$	$\frac{v}{m}$	*inhibitory parameter*
d_E	$\frac{.03}{day}$	$\frac{1}{t}$	*decrease rate of adaptive immune cells*
l_P	$\frac{14.5pg}{cells\times day}$	$\frac{m}{ct}$	*M-protein production rate by tumor cells*
d_P	$\frac{.1172}{day}$	$\frac{1}{t}$	*M-protein degradation rate*
l_G	$\frac{8.92\times10^{-2}pg}{cells\times day}$	$\frac{m}{ct}$	*glycolipid production rate by tumor cells*
d_G	$\frac{.283}{day}$	$\frac{1}{t}$	*glycolipid degradation rate*
l_I	$\frac{1.0pg}{cells\times day}$	$\frac{m}{ct}$	*rate of* $IL-6$ *production by stromal cells*
e_I	$\frac{1\times10^3 cells}{ml}$	$\frac{c}{v}$	*half-saturation constant*
s	$\frac{7.7\times10^4 cells}{ml}$	$\frac{c}{v}$	*constant stromal cell density*
d_I	$\frac{10}{day}$	$\frac{1}{t}$	*rate of* $IL-6$ *degradation*
l_F	$\frac{50pg}{cells\times day}$	$\frac{m}{ct}$	*rate of* $IFN-\gamma$ *production by immune cells*
e_F	$\frac{1\times10^3 cells}{ml}$	$\frac{c}{v}$	*half-saturation constant*
α	$\frac{1.33\times10^{-6}ml}{pg}$	$\frac{v}{m}$	*inhibitory parameter*
d_F	$\frac{2.16}{day}$	$\frac{1}{t}$	*rate of* $IFN-\gamma$ *degradation*

Table 2.3: Initial Conditions

Variable	Initial Value
$T(0)$	$\frac{9.60\times10^{-4}cells}{ml}$
$N(0)$	$\frac{1.14\times10^{7}cells}{ml}$
$K(0)$	$\frac{2.30\times10^{7}cells}{ml}$
$E(0)$	$\frac{0cells}{ml}$
$P(0)$	$\frac{0pg}{ml}$
$G(0)$	$\frac{0pg}{ml}$
$I(0)$	$\frac{7.70\times10^{3}pg}{ml}$
$F(0)$	$\frac{0pg}{ml}$

In Section 3.1, we stated that we wanted the starting values to correspond to a stable, healthy, tumor-free individual before being afflicted with the disease. Therefore, the tumor-free equilibrium of the system was calculated and used as the initial conditions. All values agreed with those in Table 2.3 except for $N(0)$, which was $1.23 \times 10^{7}\frac{cells}{ml}$ at equilibrium. This is the value that was actually used in the model.

2.2 Estimation of Parameters

Due to the lack of available data, certain parameter estimates had to be made.

MGUS begins with a single clone. Since the volume of the active bone marrow of a healthy 35 year old adult male is approximately $1042ml$ (see [35]), then the initial cell density of tumor cells is

$$T(0) = \frac{1cell}{1042ml} = 9.60 \times 10^{-4}\frac{cells}{ml}$$

The total marrow cellularity of a healthy adult consists of approximately $.7 - .9 \times 10^{12}$ cells (see [39]), so $.8 \times 10^{12}$ cells will be used for this estimate. An average of 1.3% of these cells are plasma cells (see [45]). Therefore, an adult bone marrow consists of approximately

$$(.013)(.8 \times 10^{12}) = 1.04 \times 10^{10} \text{ plasma cells}$$

This value will be used later to calculate the carrying capacity K_N of bone marrow plasma cells and the initial plasma cell density at the onset of the disease $N(0)$.

We will assume that $E(0) = 0$, since initially, no adaptive immune response has been triggered by the tumor. Adaptive immune system cells that existed prior to the tumor will not detect and hence will not attack the newly formed tumor.

$K(0)$ was obtained as follows:

The K cell population consists of NKT cells, NK cells, and macrophages. According to [20], $HNK1^+$ (human natural killer) cells generally make up less that 1% and never greater that 2% of all nucleated bone marrow cells. Therefore, 1% was used as the percent of NKT cells in the bone marrow. 1% was used as the percent of NK cells in the bone marrow, since according to [32], NK precursor cells make up approximately 1% of all bone marrow progenitor cells. According to [79], $0 - 2\%$ of all nucleated bone marrow cells are macrophages, so we used 1% for our estimate.

Using a bone marrow cellularity of $.8 \times 10^{12}$ cells, we get

number of NKT cells $= (.01)(.8 \times 10^{12}) = .8 \times 10^{10}$ cells

number of NK cells $= (.01)(.8 \times 10^{12}) = .8 \times 10^{10}$ cells

number of $macrophages = (.01)(.8 \times 10^{12}) = .8 \times 10^{10}$ cells

Since, the K cell population consists of NKT cells, NK cells, and macrophages, then by adding the above, we get 2.4×10^{10} cells in the K cell population initially. Expressed as a cell density, we get

$$K(0) = \frac{2.4 \times 10^{10} cells}{1042 ml} = 2.30 \times 10^{7} \frac{cells}{ml}$$

This value will also be used as the carrying capacity K_K of the K cell population (in the absence of $IFN - \gamma$).

We will assume that $P(0) = 0$, $G(0) = 0$, and $F(0) = 0$. $I(0)$ was obtained as follows:

The seventh equation of the system is

$$\frac{dI}{dt} = l_I \left(1 + \frac{7T}{e_I + T}\right) s - d_I I,$$

where s is assumed to be constant.

For a healthy individual ($T = 0$), this equation becomes

$$\frac{dI}{dt} = l_I s - d_I I$$

Finding the equilibrium gives the steady-state background density of $IL-6$ at the onset of the disease. We will use this as the value of $I(0)$.

$$l_I s - d_I I(0) = 0$$

$$\implies l_I s = d_I I(0)$$

$$\implies I(0) = \frac{l_I s}{d_I}$$

Substituting $l_I = \frac{1.0pg}{cells \times day}$, $d_I = \frac{10}{day}$, and $s = \frac{7.7 \times 10^4 cells}{ml}$ (obtained later in the discussion of the seventh equation), gives

$$I(0) = \frac{(1.0)(7.7 \times 10^4)}{(10)} = 7.70 \times 10^3 \frac{pg}{ml}$$

In the first equation, the birth rate of tumor cells in response to $IL-6$ is given by k_T. The value of this parameter was calculated from the growth rate of MGUS cells given in [97], since this growth rate can be attributed mainly to the influence of $IL-6$. It was obtained by taking the reciprocal of the mean myeloma cell generation time (1 cell generated in 2.29 days $\implies$ birth rate$= \frac{1}{2.29day} = \frac{.44}{day}$). For the value of the half-saturation of $IL-6$ (which was not available) given by e_T, the half-saturation of $IL-2$ during effector cell proliferation given in [3] was used.

Next, the the carrying capacity K_T of tumor cells needed to be calculated. Patients with MGUS maintain an elevated plasma cell count (sometimes for years), but are not classified as having MM until a certain threshold is reached. This value is 10% plasma cells in the bone marrow (see [67]). The corresponding cell number is

$$(.10)(.8 \times 10^{12}) = 8.0 \times 10^{10} \text{ cells}$$

which corresponds to a plasma cell density of

$$\frac{8.0 \times 10^{10} cells}{1042 ml} = 7.7 \times 10^{7} \frac{cells}{ml}$$

We have been using a bone marrow cellularity of $.8 \times 10^{12}$ cells, which corresponds to a bone marrow cell density of

$$\frac{.8 \times 10^{12}}{1042} = 7.68 \times 10^{8} \frac{cells}{ml}$$

This will be used as the bone marrow carrying capacity.

In the MM case, besides having greater than 10% plasma cells, the patients also exhibit osteolytic bone lesions (which make room for more tumor cells) and other complications (see [67]). The patient is classified as having *smoldering MM* if he has a greater that 10% plasma cell content, but none of the other complications (see [67], [62]).

Therefore, assuming that osteolytic bone lesions have not occurred yet, the carrying capacity of tumor cells cannot exceed the bone marrow carrying capacity and therefore should lie somewhere between 7.7×10^7 and $7.68 \times 10^8 \frac{cells}{ml}$. This agrees with the fact that clinical presentation of MM usually occurs from 10^{11} to 10^{12} cells (see [97]), which is equivalent to a cell density between 9.60×10^7 and $9.60 \times 10^8 \frac{cells}{ml}$. For now, the lower value will be used. This is approximately equal to the 10% total bone marrow plasma cell content which is the threshold value that distinguishes MGUS from MM. At a later time in the analysis of the model, the value can be increased numerically to see if the outcome is altered.

Therefore, let the carrying capacity of tumor cells be set to

$$K_T = 7.7 \times 10^7 \frac{cells}{ml}$$

The parameter value of d_T, corresponding to the destruction rate of tumor cells by cells of the innate (K) and adaptive (E) immune system, and the half-saturation constan g_T, were obtained from [3].

In the second equation, in order to estimate the values of the influx of normal bone marrow plasma cells l_N as the patient ages and the carrying capacity K_N, several observations had to be made. As mentioned earlier, antibody-secreting plasma cells are produced in response to an invading pathogen. Therefore, rather than a constant influx into the bone marrow, each time a person is exposed to an infection (or cancer in our case), new plasma cells are produced to combat it.

However, the best that can be done in this model is to determine an average influx rate l_N of bone marrow plasma cells throughout the person's lifetime.

According to [99], the number of Ig-G containing cells increases rapidly until the third decade of an individual's life and gradually until the ninth decade. The number of Ig-A containing cells increases rapidly during the first decade, moderately until the sixth decade, and levels off after the seventh decade. The number of Ig-M containing cells increases slightly until the third decade and levels off thereafter. This behavior is captured qualitatively by the second equation. In our model, the time $t = 0$ represents the time at the onset of the disease, when the first MGUS cell appears, where time is measured in days. Since the bone marrow volume of a 35 year old adult male was used to calculate densities and, as noted above, the increase of the number of bone marrow plasma cells slows down after the third decade, we will assume an adult age of 35 years.

In [99], human bone marrow specimens were obtained from different groups, observed under a microscope, and the number of immunoglobulin containing cells were counted. The values of l_N and K_N will be obtained from the graph in Figure 1, on page 246 of this paper, as follows:

In the second equation

$$\frac{dN}{dt} = l_N \left(1 - \frac{N}{K_N} - \frac{T}{K_T}\right)$$

Let $T = 0$ for a healthy individual and solve the differential equation to get

$$\frac{dN}{dt} = l_N - \frac{l_N}{K_N}N$$
$$\implies \frac{dN}{dt} + \frac{l_N}{K_N}N = l_N$$

$$\implies e^{\frac{l_N}{K_N}t}\frac{dN}{dt} + \frac{l_N}{K_N}e^{\frac{l_N}{K_N}t}N = l_N e^{\frac{l_N}{K_N}t}$$

$$\implies \frac{d}{dt}\left(e^{\frac{l_N}{K_N}t}N\right) = l_N e^{\frac{l_N}{K_N}t}$$

$$\implies e^{\frac{l_N}{K_N}t}N = K_N e^{\frac{l_N}{K_N}t} + C, \text{ where } C \text{ is a constant}$$

$$\implies$$

$$N = K_N + Ce^{-\frac{l_N}{K_N}t} \tag{2.2}$$

To obtain the values of K_N, C, and l_N from the graph mentioned above, the plot of age versus plasma cell count corresponding to Ig-G containing plasma cells will be used, since many multiple myelomas are of the type that contain Ig-G. In the graph, the x-axis contains age intervals. For our estimates, the greatest integer less than or equal to the midpoint of each interval was used. For the interval ≥ 80, 84 was used. Estimates for the points were obtained by overlaying a transparent grid over a blown-up copy of the graph and rounding to the nearest integer. Table 2.4 contains this information.

Table 2.4: Age-Dependent Cell Densities

age interval	age used	$\frac{cells}{unitfield}$	cells in BM	cell density ($\frac{cells}{ml}$)
0-1	.5	5	4.00×10^9	3.84×10^6
2-4	3	7	5.60×10^9	5.37×10^6
5-9	7	9	7.20×10^9	6.91×10^6
10-19	14	12	9.60×10^9	9.21×10^6
20-29	24	14	1.12×10^{10}	1.07×10^7
30-39	34	13	1.04×10^{10}	9.98×10^6
40-49	44	15	1.20×10^{10}	1.15×10^7
50-59	54	14	1.12×10^{10}	1.07×10^7
60-69	64	14	1.12×10^{10}	1.07×10^7
70-79	74	15	1.20×10^{10}	1.15×10^7
80-	84	16	1.28×10^{10}	1.23×10^7

The numbers in the third column of Table 2.4 represent the number of plasma cells counted per unit field under a microscope. We need the density of plasma cells in the bone marrow. However, we can assume that the numbers given in the table are representative of the entire population. As stated earlier, we will use an adult (assumed to be 35 years old) plasma cell count of 1.04×10^{10} cells. If we equate this with 13 plasma cells per unit field obtained from the table (corresponding to an age of 35), we get the following ratio of cells in the bone marrow per cells per unit field

$$\frac{1.04\times10^{10}}{13} = 8.00 \times 10^8 \frac{cells\ in\ BM}{cells\ per\ unit\ field}$$

Using this conversion factor gives the entries in the fourth column. The densities in the last column were obtained by dividing each entry in the fourth column by 1042 ml (the volume of the active bone marrow for a 35 year old healthy adult male) as done before on several occasions.

For the carrying capacity of normal bone marrow plasma cells, we will use the last entry in the table corresponding to ≥ 80 years of age. So we have

$$K_N = 1.23 \times 10^7 \frac{cells}{ml}$$

Our goal is to approximate these experimentally obtained points by equation (2.2).

In the following derivation, we have to keep in mind that $N(t_i)$ denotes the normal plasma cell density at t_i years of age. In this case $N(0)$ denotes the cell density at birth, in contrast to the model, where $N(0)$ denotes the cell density at the onset of the disease.

To estimate the influx l_N of normal bone marrow plasma cells, we will use the first, second, fourth, sixth, eighth, and tenth points from Table 2.4, since these give a smoother curve. These values are given in Table 2.5.

Table 2.5: Values of t_i and $N(t_i)$ Used

t_i	$N(t_i)$
.5	3.84×10^6
3	5.37×10^6
14	9.21×10^6
34	9.98×10^6
54	1.07×10^7
74	1.15×10^7

Returning to equation (2.2)

$N(t_i) = K_N + Ce^{-\frac{l_N}{K_N}t_i}$, where the value of K_N and points $(t_i, N(t_i))$ for

$$i = 1, \ldots, 6 \text{ are known}$$

$$\implies K_N - N(t_i) = -Ce^{-\frac{l_N}{K_N}t_i}, \text{ where } K_N - N(t_i) > 0 \forall i$$

$$\implies ln(K_N - N(t_i)) = ln(-C) - \frac{l_N}{K_N}t_i$$

$$\implies f(t_i) = \Gamma - \frac{l_N}{K_N}t_i, \text{ where } f(t_i) = ln(K_N - N(t_i)) \text{ and } \Gamma = ln(-C)$$

A *least squares* approximation is used to determine the values of Γ (and hence C) and l_N that best fit the experimental data.

Let

$$F(\Gamma, l_N) = \sum_{i=1}^{6} \left[\Gamma - \frac{l_N}{K_N}t_i - f(t_i)\right]^2$$

The values of Γ and l_N that minimize F will satisfy

$$\frac{\partial F}{\partial \Gamma} = \sum_{i=1}^{6} \left[\Gamma - \frac{l_N}{K_N}t_i - f(t_i)\right] = 0$$

$$\implies 6\Gamma - \frac{1}{K_N}\left(\sum_{i=1}^{6} t_i\right) l_N - \sum_{i=1}^{6} f(t_i) = 0$$

and

$$\frac{\partial F}{\partial l_N} = \sum_{i=1}^{6} \left[\Gamma - \frac{l_N}{K_N} t_i - f(t_i) \right] \frac{t_i}{K_N} = 0$$

$$\implies \frac{1}{K_N} \left(\sum_{i=1}^{6} t_i \right) \Gamma - \frac{1}{K_N^2} \left(\sum_{i=1}^{6} t_i^2 \right) l_N - \frac{1}{K_N} \sum_{i=1}^{6} t_i f(t_i) = 0$$

$$\implies \left(\sum_{i=1}^{6} t_i \right) \Gamma - \frac{1}{K_N} \left(\sum_{i=1}^{6} t_i^2 \right) l_N - \sum_{i=1}^{6} t_i f(t_i) = 0$$

Therefore, the following system needs to be solved for Γ and l_N

$$\begin{cases} 6\Gamma - \dfrac{1}{K_N} \left(\displaystyle\sum_{i=1}^{6} t_i \right) l_N - \sum_{i=1}^{6} f(t_i) = 0 \\ \left(\displaystyle\sum_{i=1}^{6} t_i \right) \Gamma - \dfrac{1}{K_N} \left(\displaystyle\sum_{i=1}^{6} t_i^2 \right) l_N - \displaystyle\sum_{i=1}^{6} t_i f(t_i) = 0 \end{cases} \tag{2.3}$$

Substituting the values of t_i and $f(t_i) = ln(K_N - N(t_i))$ for $i = 1, \ldots, 6$ (obtained from Table 2.5) and $K_N = 1.23 \times 10^7$ gives

$\sum_{i=1}^{6} t_i = 179.5$

$\sum_{i=1}^{6} t_i^2 = 9753.25$

$\sum_{i=1}^{6} f(t_i) = 89.180871$

$\sum_{i=1}^{6} t_i f(t_i) = 2540.0347$

Using these values in system (2.3) and solving the system gives

$l_N = 359075.87 \frac{cells}{ml \times year}$

and

$\Gamma = 15.736841$

$\implies ln(-C) = 15.736841$

$\implies C = -e^{15.736841}$

$\implies C = -6830039.4$

Therefore, the experimental data can be approximated by the function

$N = K_N + Ce^{-\frac{l_N}{K_N}t}$, where $K_N = 1.23 \times 10^7 \frac{cells}{ml}$, $C = -6830039.4$,

and $l_N = 359075.87 \frac{cells}{ml \times year}$

That is

$$N = 1.23 \times 10^7 - 6830039.4e^{-.0291931t}$$

In our model, as noted earlier, $N(0)$ denotes the normal plasma cell density at the onset of the disease. MGUS occurs in 1% of the population over age 50, 3% over age 70 (see [67]), and in 10% of the population in their tenth decade (see [62]). Therefore, since MGUS usually occurs later in the life of an individual, we will assume in our model that the onset of the disease occurs at 70 years of age. At $t = 70$ years of age, the above equation gives

$$N(70) = 1.14 \times 10^7 \frac{cells}{ml}$$

So in our model, the normal plasma cell density at the onset of the disease (at $t = 0$ days) is given by

$$N(0) = 1.14 \times 10^7 \frac{cell}{ml}$$

We determined that $l_N = 359075.87 \frac{cells}{ml \times year}$. However, in our model, t=days from onset of disease. Therefore, we need l_N to be in units $\frac{cells}{ml \times day}$. Ignoring leap years and assuming 365 days per year, we can rewrite l_N in the desired units by multiplying it by $\frac{1year}{365days}$. This gives

$$l_N = \frac{983.77cells}{ml \times day}$$

In the third equation, the net proliferation rate of innate immune system cells is given by $r_K = k_K - d_K$, where k_K is the maximum proliferation rate and d_K is the death rate. The values of these parameters where obtained from effector cell proliferation and death rates given in [3]. The carrying capacity K_K of the innate immune system cell population K (in the absence of $IFN - \gamma$) was set equal to the initial value $K(0)$, as mentioned earlier. Note that we are allowing this tumor-free carrying capacity to be exceeded if more K cells are recruited (due to the presence of $IFN-\gamma$) to fight the tumor. The second term contains parameters k_{KE} and e_{KE}, which are also found in the fourth equation. For recruitment parameter k_{KE}, the value given in [105] as the maximum recruitment rate ($\frac{100cells}{ml \times sec} = \frac{8.64 \times 10^6 cells}{ml \times day}$) was used. The half-saturation of $IFN - \gamma$, given by e_{KE} was obtained from the half-saturation of $IFN - \gamma$ during the activation of resting macrophages given in [96].

In the fourth equation, parameters k_{KE} and e_{KE} are as in the third equation above. The inhibitory parameter β represents the decrease in the number of reactive adaptive immune system cells (specifically $CD4^+T$ cells) due to the presence of soluble M-protein produced by tumor cells, as discussed earlier. β was obtained as follows:

T_{max} occurs when $T = K_T$. Let $T = K_T$ and solve the fifth equation for P to obtain P_{max}.

$$\frac{dP}{dt} = l_P T - d_P P$$

$$\implies \frac{dP}{dt} = l_P K_T - d_P P$$

$$\implies \frac{dP}{dt} + d_P P = l_P K_T$$

$$\implies e^{d_P t}\frac{dP}{dt} + d_P e^{d_P t} P = l_P K_T e^{d_P t}$$

$$\implies \frac{d}{dt}\left(e^{d_P t} P\right) = l_P K_T e^{d_P t}$$

$$\implies e^{d_P t} P = \frac{l_P K_T}{d_P} e^{d_P t} + C, \text{ where C is a constant}$$

$$\implies P = \frac{l_P K_T}{d_P} + C e^{-d_P t}$$

$$P(0) = 0 \implies C = -\frac{l_P K_T}{d_P}$$

Therefore,

$$P = \frac{l_P K_T}{d_P} - \frac{l_P K_T}{d_P} e^{-d_P t}$$

$$\implies P = \frac{l_P K_T}{d_P}\left(1 - e^{-d_P t}\right)$$

Substituting $l_P = \frac{14.5pg}{cells \times day}$, $K_T = \frac{7.7 \times 10^7 cells}{ml}$, and $d_P = \frac{.1172}{day}$ (where parameters l_P and d_P will be explained later in the discussion of the fifth equation) gives

$$P = \frac{(14.5)(7.7 \times 10^7)}{.1172}\left(1 - e^{-.1172t}\right)$$

$$\implies P = 9.53 \times 10^9 \left(1 - e^{-.1172t}\right) \frac{pg}{ml}$$

As $t \to \infty$, $P \to 9.53 \times 10^9$. So $P_{max} = 9.53 \times 10^9 \frac{pg}{ml}$

The E cell population consists of CTL and $CD4^+T$ cells, where CTL cells make up approximately .037 of the total bone marrow cellularity and $CD4^+T$ cells make up approximately .038 of the total bone marrow cellularity (see [20]). Since they occur in roughly the same amount, we can say that approximately one half of the E cell population consists of $CD4^+T$ cells. We assume that at $P = P_{max}$, all the reactive $CD4^+T$ cells are deleted (as discussed earlier). Therefore, we assume that at $P = P_{max}$, the E cell population decreases to $.5E$, leaving only CTL cells. So to find β, we solve

$$\frac{1}{1 + \beta P_{max}} = .5$$

$$\implies \beta = \frac{\frac{1}{.5} - 1}{P_{max}}$$

$$\implies \beta = \frac{1}{P_{max}}$$

Substituting $P_{max} = 9.53 \times 10^9 \frac{pg}{ml}$, gives

$$\beta = \frac{1}{9.53 \times 10^9}$$

$$\implies \beta = 1.05 \times 10^{-10} \frac{ml}{pg}$$

The value of parameter d_E, which represents the rate of decrease of adaptive immune system cells, was obtained from the effector cell death rate given in [3]. This parameter is used to represent the fact that, as mentioned earlier, adaptive immunity decreases over time if no longer exposed to the tumor.

In the fifth equation, l_P and d_P represent the rate of M-protein production by tumor cells and degradation, respectively. The values of these parameters were obtained from [97]. For l_P, the mean synthetic rate was used, and for d_P, the mean of the fractional catabolic rates given in Table I in the cited paper was used.

In the sixth equation, l_G and d_G represent the rate of glycolipid production by tumor cells and degradation, respectively. Neither of these rates were available. To estimate the rate of glycolipid production by tumor cells, the amount of glycolipid ($LacCer$) produced by leukocytes when stimulated with HDL_3 was used. This was calculated from the data given in [63] as follows:

$LacCer$ has a molecular weight of 880. In the above experiment, 40 flasks, each with a volume of 2.5 milliliters were used, and .2 milligrams of HDL_3 per milliliter was used. Before incubation,

$$\frac{1.2\mu mol\ LacCer}{1g\ HDL_3}$$

was present. So the initial density of $LacCer$ is given by

$$\frac{1.2\mu mol\ LacCer}{1g\ HDL_3} \times \frac{1g\ HDL_3}{1\times10^3 mg\ HDL_3} \times \frac{.2mg\ HDL_3}{1ml} = \frac{.24\mu mol\ LacCer}{1\times10^3 ml}$$

In picograms per milliliter, this becomes

$$\frac{.24\mu mol\ \ LacCer}{1\times10^{3}ml} \times \frac{1\times10^{-6}mol\ \ LacCer}{1\mu mol\ \ LacCer} \times \frac{880g\ \ LacCer}{1mol\ \ LacCer} \times \frac{1\times10^{12}pg\ \ LacCer}{1g\ \ LacCer}$$

$$= 2.11 \times 10^{5} \frac{pg\ \ LacCer}{ml}$$

Incubation with leukocytes (10^7 cells/ml in 40 flasks of volume 2.5 ml each) for 18 hours (.75 days) at 37° C, resulted in

$$\frac{5.0\mu mol\ \ LacCer}{1g\ \ HDL_3}$$

So the final density of $LacCer$ after .75 days is given by

$$\frac{5.0\mu mol\ \ LacCer}{1g\ \ HDL_3} \times \frac{1g\ \ HDL_3}{1\times10^{3}mg\ \ HDL_3} \times \frac{.2mg\ \ HDL_3}{1ml} = \frac{1\mu mol\ \ LacCer}{1\times10^{3}ml}$$

In picograms per milliliter, this becomes

$$\frac{1\mu mol\ \ LacCer}{1\times10^{3}ml} \times \frac{1\times10^{-6}mol\ \ LacCer}{1\mu mol\ \ LacCer} \times \frac{880g\ \ LacCer}{1mol\ \ LacCer} \times \frac{1\times10^{12}pg\ \ LacCer}{1g\ \ LacCer}$$

$$= 8.80 \times 10^{5} \frac{pg\ \ LacCer}{ml}$$

Therefore, the increase in $LacCer$ content in .75 days is

$$8.80 \times 10^{5} - 2.11 \times 10^{5} = \frac{6.69\times10^{5}pg\ \ LacCer}{ml}$$

The leukocyte density is $10^7 cells/ml$, so the $LacCer$ production per cell is given by

$$\frac{6.69\times10^5 pg\ \ LacCer}{ml} \times \frac{1ml}{1\times10^7 cells} = \frac{6.69\times10^{-2} pg\ \ LacCer}{cells}$$

Therefore, the rate of $LacCer$ production by leukocytes stimulated by HDL_3 is given by

$$\frac{6.69\times10^{-2} pg}{.75 cells\times da} = 8.92\times10^{-2}\frac{pg}{cells\times da}$$

This is the value used for parameter l_G in the model.

For the glycolipid degradation rate, d_G, the average turnover rate (percent degradation) of blood group glycolipid A-6-2 given in [4] was used. This value is $\frac{.283}{day}$.

In the seventh equation, l_I represents the rate of $IL-6$ production by bone marrow stromal cells. This was calculated from the data given in Table 2 in [103]. First, for six patients, the average $IL-6$ production by bone marrow stromal cells per day was calculated to be

$$avg = \frac{17+264+360+410+152+44}{6} = 207.8\frac{ng}{ml\times day} = 207.8\times10^3\frac{pg}{ml\times day}$$

The bone marrow stromal cell density used in the above experiment ([103]) was

$$\frac{2\times10^4 cells}{100\mu l} = \frac{2\times10^5 cells}{ml}$$

Therefore, the rate of $IL-6$ production is given by

$$l_I = \frac{207.8\times10^3 pg}{ml\times day} \times \frac{1ml}{2\times10^5 cells} = 1.0\frac{pg}{cells\times day}$$

For e_I (which was not available), the half-saturation constant for self-limiting $IL-2$ production under similar circumstances given in [3] was used.

A constant stromal cell density s is assumed. The frequency of fibroblast colony-forming cells in the bone marrow is approximately 10^{-4} (see [92]). So the number of bone marrow stromal cells is approximately

$$(10^{-4})(.8\times10^{12}) = 8.0\times10^7 \text{ cells}$$

This gives a constant stromal cell density of

$$s = \frac{8.0\times10^7 cells}{1042ml} = 7.7\times10^4\frac{cells}{ml}$$

For the rate of $IL-6$ degradation d_I (which was not available), the value corresponding to $IL-2$ degradation obtained from [3] was used.

In the eighth equation, parameter l_F represents the rate of $IFN-\gamma$ production by cells of the innate and adaptive immune system in response to the presence of the tumor and d_F represents the degradation of $IFN-\gamma$. The values of l_F and d_F were obtained from [96]. Parameter e_F (which was not available) is a half-saturation

constant due to the fact that the process is self-limiting. For this parameter, the half-saturation constant for self-limiting $IL-2$ production under similar circumstances given in [3] was used. Parameter α represents the inhibition of $IFN-\gamma$ production by cells of the innate immune system (specifically NKT cells) due to the presence of tumor-derived glycolipids (as discussed earlier). This parameter was obtained as follows:

T_{max} occurs when $T = K_T$, so let $T = K_T$ in the sixth equation and solve it for G to obtain G_{max}.

$$\frac{dG}{dt} = l_G T - d_G G$$

$$\implies \frac{dG}{dt} = l_G K_T - d_G G$$

$$\implies \frac{dG}{dt} + d_G G = l_G K_T$$

$$\implies e^{d_G t}\frac{dG}{dt} + d_G e^{d_G t} G = l_G K_T e^{d_G t}$$

$$\implies \frac{d}{dt}(e^{d_G t} G) = l_G K_T e^{d_G t}$$

$$\implies e^{d_G t} G = \frac{l_G K_T}{d_G} e^{d_G t} + C, \text{ where } C \text{ is a constant}$$

$$\implies G = \frac{l_G K_T}{d_G} + C e^{-d_G t}$$

$$G(0) = 0 \implies C = -\frac{l_G K_T}{d_G}$$

Therefore,

$$G = \frac{l_G K_T}{d_G} - \frac{l_G K_T}{d_G} e^{-d_G t}$$

$$\implies G = \frac{l_G K_T}{d_G}(1 - e^{-d_G t})$$

Substituting $l_G = \frac{8.92 \times 10^{-2} pg}{cells \times day}$, $K_T = \frac{7.7 \times 10^7 cells}{ml}$, and $d_G = \frac{.283}{day}$ gives

$$G = \frac{(8.92 \times 10^{-2})(7.7 \times 10^7)}{(.283)}(1 - e^{-.283t})$$

$$\implies G = 2.43 \times 10^7 (1 - e^{-.283t}) \frac{pg}{ml}$$

As $t \to \infty$, $G \to 2.43 \times 10^7$. So $G_{max} = 2.43 \times 10^7 \frac{pg}{ml}$.

The K cell population consists of MAC, NKT cells, and NK cells, and each of these make up .01 of the total bone marrow cellularity (see [79, 20, 32], resp.). If K denotes the density of the K cell population, then this population consists of roughly $\frac{1}{3}K$ MAC, $\frac{1}{3}K$ NKT, and $\frac{1}{3}K$ NK cells. NK and NKT cells, which account for $\frac{2}{3}$ of the K cell population, produce $IFN - \gamma$. Therefore, if there are no tumor-derived glycolipids in the system ($G = 0$), $\frac{2}{3}K$ cells contribute to $IFN - \gamma$ production. As mentioned earlier, tumor-derived glycolipids cause a disfunction in the ability of NKT cells to produce $IFN - \gamma$. The cells are not destroyed, many simply lose their ability

to produce $IFN-\gamma$. According to [18], the number of glycolipid reactive $IFN-\gamma$-producing cells drops from a mean of 65 per 10^6 peripheral blood mononuclear cells in healthy controls to a mean of 1.8 per 10^6 in patients with progressive myeloma. Therefore, we assume that at $G = G_{max}$, the number of $IFN-\gamma$-producing NKT cells is

$$\frac{1.8}{65} \times (number\ of\ NKT\ cells)$$

$$= .03 \times (number\ of\ NKT\ cells)$$

Since the density of NKT cells is $\frac{1}{3}K$, then we assume that at $G = G_{max}$, the $IFN-\gamma$-producing NKT cell subpopulation decreases from $\frac{1}{3}K$ to $(.03)(\frac{1}{3}K)$.

So to find α, we solve

$$\frac{1}{1+\alpha G_{max}} = .03$$

$$\implies \alpha = \frac{\frac{1}{.03}-1}{G_{max}} = \frac{32.33}{G_{max}}$$

Substituting $G_{max} = 2.43 \times 10^7 \frac{pg}{ml}$, gives

$$\alpha = \frac{32.33}{2.43\times 10^7}$$

$$\implies \alpha = 1.33 \times 10^{-6}$$

2.3 Nondimensionalization of the System

The first equation of system (2.1):

$$\frac{dT}{dt} = \frac{k_T I}{e_T + I}\left(1 - \frac{T+N}{K_T}\right)T - \frac{d_T(K+E)T}{g_T + T}$$

Let $I^* = \dfrac{I}{K_I}$, where $K_I = \dfrac{l_I s}{d_I}$. Then, I^* is nondimensional. The reason for this choice will become apparent during the nondimensionalization of the seventh equation.

The first term becomes

$$\frac{k_T I}{e_T + I}\left(1 - \frac{T+N}{K_T}\right)T = \frac{k_T \dfrac{I}{K_I}}{\dfrac{e_T}{K_I} + \dfrac{I}{K_I}}\left(1 - \frac{T+N}{K_T}\right)T = \frac{k_T I^*}{\frac{e_T}{K_I} + I^*}\left(1 - \frac{T+N}{K_T}\right)T$$

So the above equation becomes

$$\begin{aligned}\frac{dT}{dt} &= \frac{k_T I^*}{\frac{e_T}{K_I} + I^*}\left(1 - \frac{T+N}{K_T}\right)T - \frac{d_T(K+E)T}{g_T + T} \\ &= \frac{k_T I^*}{\frac{e_T}{K_I} + I^*}\left(1 - \frac{T}{K_T} - \frac{N}{K_T}\right)T - \frac{d_T(K+E)T}{g_T + T}\end{aligned}$$

Let $T^* = \dfrac{T}{K_T} \implies \dfrac{dT^*}{dt} = \dfrac{1}{K_T}\dfrac{dT}{dt}$ and $N^* = \dfrac{N}{K_T}$, both nondimensional.

Dividing by K_T gives

$$\frac{1}{K_T}\frac{dT}{dt} = \frac{k_T I^*}{\frac{e_T}{K_I} + I^*}\left(1 - \frac{T}{K_T} - \frac{N}{K_T}\right)\frac{T}{K_T} - \frac{d_T(K+E)}{K_T}\frac{\frac{T}{K_T}}{\frac{g_T}{K_T} + \frac{T}{K_T}}$$

$$\Longrightarrow \frac{dT^*}{dt} = \frac{k_T I^*}{\frac{e_T}{K_I} + I^*}(1 - T^* - N^*)T^* - d_T\left(\frac{K}{K_T} + \frac{E}{K_T}\right)\frac{T^*}{\frac{g_T}{K_T} + T^*}$$

Let $K^* = \dfrac{K}{K_T}$ and $E^* = \dfrac{E}{K_T}$, which are both nondimensional.

Then, we get

$$\begin{aligned}
\frac{dT^*}{dt} &= \frac{k_T I^*}{\frac{e_T}{K_I} + I^*}(1 - T^* - N^*)T^* - d_T(K^* + E^*)\frac{T^*}{\frac{g_T}{K_T} + T^*} \\
&= \frac{k_T I^*}{\frac{e_T}{(\frac{l_I s}{d_I})} + I^*}(1 - T^* - N^*)T^* - d_T(K^* + E^*)\frac{T^*}{\frac{g_T}{K_T} + T^*} \\
&= \frac{k_T I^*}{\frac{d_I e_T}{l_I s} + I^*}(1 - T^* - N^*)T^* - d_T(K^* + E^*)\frac{T^*}{\frac{g_T}{K_T} + T^*}
\end{aligned}$$

Dividing by k_T gives

$$\frac{1}{k_T}\frac{dT^*}{dt} = \frac{I^*}{\frac{d_I e_T}{l_I s} + I^*}(1 - T^* - N^*)T^* - \frac{d_T}{k_T}(K^* + E^*)\frac{T^*}{\frac{g_T}{K_T} + T^*}$$

We want $\frac{1}{k_T}\frac{d}{dt} = \frac{d}{dt^*}$. In order to obtain this, let $t = \frac{1}{k_T}t^*$. Then, by the Chain Rule, $\frac{d}{dt^*} = \frac{d}{dt}\frac{dt}{dt^*} = \frac{1}{k_T}\frac{d}{dt}$.

Therefore, the nondimensional version of the first equation of system (2.1) is given by

$$\frac{dT^*}{dt^*} = \frac{I^*}{\frac{d_I e_T}{l_I s} + I^*}(1 - T^* - N^*)T^* - \frac{d_T}{k_T}(K^* + E^*)\frac{T^*}{\frac{g_T}{K_T} + T^*} \tag{2.4}$$

The second equation of system (2.1):

$$\frac{dN}{dt} = l_N\left(1 - \frac{N}{K_N} - \frac{T}{K_T}\right)$$

Recall that $N^* = \frac{N}{K_T} \implies \frac{dN^*}{dt} = \frac{1}{K_T}\frac{dN}{dt}$ and $T^* = \frac{T}{K_T}$. So this equation becomes

$$\begin{aligned}\frac{dN}{dt} &= l_N\left[1 - \frac{\left(\frac{N}{K_T}\right)}{\left(\frac{K_N}{K_T}\right)} - \frac{T}{K_T}\right] \\ &= l_N\left[1 - \frac{K_T}{K_N}N^* - T^*\right]\end{aligned}$$

Dividing by K_T gives

$$\frac{1}{K_T}\frac{dN}{dt} = \frac{l_N}{K_T}\left[1 - \frac{K_T}{K_N}N^* - T^*\right]$$

$$\implies \frac{dN^*}{dt} = \frac{l_N}{K_T}\left[1 - \frac{K_T}{K_N}N^* - T^*\right]$$

Dividing by k_T gives

$$\frac{1}{k_T}\frac{dN^*}{dt} = \frac{l_N}{k_T K_T}\left[1 - \frac{K_T}{K_N}N^* - T^*\right]$$

$$\implies \frac{dN^*}{dt^*} = \frac{l_N}{k_T K_T}\left[1 - \frac{K_T}{K_N}N^* - T^*\right]$$

It would be desirable to express l_N in terms of a new variable k_N of dimension $\frac{1}{t}$. This will simplify the analysis of time scales later on. To achieve this end, let $k_N = \frac{l_N}{K_N}$. Then, $l_N = k_N K_N$, so the equation becomes

$$\frac{dN^*}{dt^*} = \frac{k_N K_N}{k_T K_T}\left[1 - \frac{K_T}{K_N}N^* - T^*\right]$$

Therefore, the nondimensional version of the second equation of system (2.1) is given by

$$\frac{dN^*}{dt^*} = \frac{k_N}{k_T}\left(\frac{K_N}{K_T} - N^* - \frac{K_N}{K_T}T^*\right) \tag{2.5}$$

The third equation of system (2.1):

$$\frac{dK}{dt} = r_K \left(1 - \frac{K}{K_K}\right) K + \frac{k_{KE} F}{e_{KE} + F}$$

Let $F^* = \dfrac{F}{K_F}$, where $K_F = \dfrac{l_F K_T}{d_F}$. Then, F^* is nondimensional. The reason for this choice of F^* will become apparent during the nondimensionalization of the eighth equation.

The second term becomes

$$\frac{k_{KE} F}{e_{KE} + F} = \frac{k_{KE} \dfrac{F}{K_F}}{\dfrac{e_{KE}}{K_F} + \dfrac{F}{K_F}} = \frac{k_{KE} F^*}{\dfrac{e_{KE}}{K_F} + F^*}$$

So the above equation becomes

$$\frac{dK}{dt} = r_K \left(1 - \frac{K}{K_K}\right) K + \frac{k_{KE} F^*}{\dfrac{e_{KE}}{K_F} + F^*}$$

Recall that $K^* = \dfrac{K}{K_T} \implies \dfrac{dK^*}{dt} = \dfrac{1}{K_T}\dfrac{dK}{dt}$ and $K = K^* K_T$. So dividing by K_T gives

$$\frac{1}{K_T}\frac{dK}{dt} = r_K \left(1 - \frac{K}{K_K}\right) \frac{K}{K_T} + \frac{k_{KE} F^*}{K_T(\frac{e_{KE}}{K_F} + F^*)}$$

$$\begin{aligned} \Longrightarrow \frac{dK^*}{dt} &= r_K\left(1-\frac{K}{K_K}\right)K^* + \frac{k_{KE}}{K_T}\frac{F^*}{\frac{e_{KE}}{K_F}+F^*} \\ &= r_K\left(1-\frac{K_TK^*}{K_K}\right)K^* + \frac{k_{KE}}{K_T}\frac{F^*}{\frac{e_{KE}}{K_F}+F^*} \end{aligned}$$

Dividing by k_T gives

$$\frac{1}{k_T}\frac{dK^*}{dt} = \frac{r_K}{k_T}\left(1-\frac{K_TK^*}{K_K}\right)K^* + \frac{k_{KE}}{k_TK_T}\frac{F^*}{\frac{e_{KE}}{K_F}+F^*}$$

$$\begin{aligned} \Longrightarrow \frac{dK^*}{dt^*} &= \frac{r_K}{k_T}\left(1-\frac{K_T}{K_K}K^*\right)K^* + \frac{k_{KE}}{k_TK_T}\frac{F^*}{\frac{e_{KE}}{K_F}+F^*} \\ &= \frac{r_K}{k_T}\left(1-\frac{K_T}{K_K}K^*\right)K^* + \frac{k_{KE}}{k_TK_T}\frac{F^*}{\frac{e_{KE}}{(\frac{l_FK_T}{d_F})}+F^*} \end{aligned}$$

Therefore, the nondimensional version of the third equation of system (2.1) is given by

$$\frac{dK^*}{dt^*} = \frac{r_K}{k_T}\left(1-\frac{K_T}{K_K}K^*\right)K^* + \frac{k_{KE}}{k_TK_T}\frac{F^*}{\frac{d_Fe_{KE}}{l_FK_T}+F^*} \tag{2.6}$$

The fourth equation of system (2.1):

$$\frac{dE}{dt} = \frac{k_{KE}F}{(e_{KE}+F)(1+\beta P)} - d_E E$$

Recall that $F^* = \dfrac{F}{K_F}$, where $K_F = \dfrac{l_F K_T}{d_F}$.

The first term becomes

$$\frac{k_{KE}F}{(e_{KE}+F)(1+\beta P)} = \frac{k_{KE}\dfrac{F}{K_F}}{\left(\dfrac{e_{KE}}{K_F}+\dfrac{F}{K_F}\right)(1+\beta P)} = \frac{k_{KE}F^*}{(\frac{e_{KE}}{K_F}+F^*)(1+\beta P)}$$

So the above equation becomes

$$\frac{dE}{dt} = \frac{k_{KE}F^*}{(\frac{e_{KE}}{K_F}+F^*)(1+\beta P)} - d_E E$$

Recall that $E^* = \dfrac{E}{K_T} \implies \dfrac{dE^*}{dt} = \dfrac{1}{K_T}\dfrac{dE}{dt}$.

Dividing by K_T gives

$$\frac{1}{K_T}\frac{dE}{dt} = \frac{k_{KE}F^*}{K_T(\frac{e_{KE}}{K_F}+F^*)(1+\beta P)} - d_E\frac{E}{K_T}$$

$$\implies \frac{dE^*}{dt} = \frac{k_{KE}F^*}{K_T(\frac{e_{KE}}{K_F} + F^*)(1+\beta P)} - d_E E^*$$

Dividing by k_T gives

$$\frac{1}{k_T}\frac{dE^*}{dt} = \frac{k_{KE}}{k_T K_T}\frac{F^*}{(\frac{e_{KE}}{K_F} + F^*)(1+\beta P)} - \frac{d_E}{k_T}E^*$$

$$\implies \frac{dE^*}{dt^*} = \frac{k_{KE}}{k_T K_T}\frac{F^*}{(\frac{e_{KE}}{K_F} + F^*)(1+\beta P)} - \frac{d_E}{k_T}E^*$$

Let $P^* = \dfrac{P}{K_P}$, where $K_P = \dfrac{l_P K_T}{d_P}$. Then, P^* is nondimensional. The reason for this choice of P^* will become apparent during the nondimensionalization of the fifth equation. Also, recall that $K_F = \dfrac{l_F K_T}{d_F}$. Then, the equation becomes

$$\begin{aligned}
\frac{dE^*}{dt^*} &= \frac{k_{KE}}{k_T K_T}\frac{F^*}{(\frac{e_{KE}}{K_F} + F^*)(1+\beta K_P P^*)} - \frac{d_E}{k_T}E^* \\
&= \frac{k_{KE}}{k_T K_T}\frac{F^*}{\left(\frac{e_{KE}}{(\frac{l_F K_T}{d_F})} + F^*\right)\left(1+\beta(\frac{l_P K_T}{d_P})P^*\right)} - \frac{d_E}{k_T}E^*
\end{aligned}$$

Therefore, the nondimensional version of the fourth equation of system (2.1) is given by

$$\frac{dE^*}{dt^*} = \frac{k_{KE}}{k_T K_T} \frac{F^*}{(\frac{d_F e_{KE}}{l_F K_T} + F^*)(1 + \beta \frac{l_P K_T}{d_P} P^*)} - \frac{d_E}{k_T} E^* \tag{2.7}$$

The fifth equation of system (2.1):

$$\frac{dP}{dt} = l_P T - d_P P$$

Recall that $T^* = \dfrac{T}{K_T}$.

At equilibrium, we get

$$\begin{aligned} l_P T - d_P P = 0 \implies P &= \frac{l_P}{d_P} T \\ &= \frac{l_P K_T}{d_P} T^* \end{aligned}$$

Let $K_P = \dfrac{l_P K_T}{d_P}$, which has dimension $\frac{m}{v}$, and $P^* = \dfrac{P}{K_P}$, which is nondimensional. Then, $\dfrac{dP^*}{dt} = \dfrac{1}{K_P} \dfrac{dP}{dt}$. So if T^* is an equilibrium value, then $P^* = T^*$ are terms of the same order.

Going back to the original equation, we have

$$\begin{aligned} \frac{dP}{dt} &= l_P T - d_P P \\ &= l_P K_T T^* - d_P P \end{aligned}$$

Dividing by K_P gives

$$\frac{1}{K_P}\frac{dP}{dt} = \frac{l_P K_T}{K_P} T^* - d_P \frac{P}{K_P} \implies \begin{aligned} \frac{dP^*}{dt} &= \frac{l_P K_T}{K_P} T^* - d_P P^* \\ &= \frac{l_P K_T}{(\frac{l_P K_T}{d_P})} T^* - d_P P^* \\ &= d_P T^* - d_P P^* \\ &= d_P (T^* - P^*) \end{aligned}$$

Dividing by k_t gives

$$\frac{1}{k_T}\frac{dP^*}{dt} = \frac{d_P}{k_T}(T^* - P^*)$$

Therefore, the nondimensional version of the fifth equation of system (2.1) is given by

$$\frac{dP^*}{dt^*} = \frac{d_P}{k_T}(T^* - P^*) \tag{2.8}$$

The sixth equation of system (2.1):

$$\frac{dG}{dt} = l_G T - d_G G$$

Recall that $T^* = \frac{T}{K_T}$.

At equilibrium, we get

$$\begin{aligned} l_G T - d_G G = 0 \implies G &= \frac{l_G}{d_G} T \\ &= \frac{l_G K_T}{d_G} T^* \end{aligned}$$

Let $K_G = \frac{l_G K_T}{d_G}$, which has dimension $\frac{m}{v}$, and $G^* = \frac{G}{K_G}$, which is nondimensional. Then, $\frac{dG^*}{dt} = \frac{1}{K_G}\frac{dG}{dt}$.

Going back to the original equation, we have

$$\begin{aligned} \frac{dG}{dt} &= l_G T - d_G G \\ &= l_G K_T T^* - d_G G \end{aligned}$$

Dividing by K_G gives

$$\frac{1}{K_G}\frac{dG}{dt} = \frac{l_G K_T}{K_G}T^* - d_G\frac{G}{K_G} \implies \frac{dG^*}{dt} = \frac{l_G K_T}{K_G}T^* - d_G G^*$$

$$= \frac{l_G K_T}{(\frac{l_G K_T}{d_G})}T^* - d_G G^*$$

$$= d_G T^* - d_G G^*$$

$$= d_G(T^* - G^*)$$

Dividing by k_t gives

$$\frac{1}{k_T}\frac{dG^*}{dt} = \frac{d_G}{k_T}(T^* - G^*)$$

Therefore, the nondimensional version of the sixth equation of system (2.1) is given by

$$\frac{dG^*}{dt^*} = \frac{d_G}{k_T}(T^* - G^*) \tag{2.9}$$

The seventh equation of system (2.1):

$$\frac{dI}{dt} = l_I\left(1 + \frac{7T}{e_I + T}\right)s - d_I I$$

Recall that $T^* = \dfrac{T}{K_T}$.

At equilibrium, we get

$$
\begin{aligned}
l_I\left(1+\frac{7T}{e_I+T}\right)s-d_II=0 \implies I &= \frac{l_Is}{d_I}\left(1+\frac{7T}{e_I+T}\right)\\
&= \frac{l_Is}{d_I}\left(1+\frac{7\frac{T}{K_T}}{\frac{e_I}{K_T}+\frac{T}{K_T}}\right)\\
&= \frac{l_Is}{d_I}\left(1+\frac{7T^*}{\frac{e_I}{K_T}+T^*}\right)
\end{aligned}
$$

Let $K_I=\dfrac{l_Is}{d_I}$, which has dimension $\frac{m}{v}$, and $I^*=\dfrac{I}{K_I}$, which is nondimensional. Then, $\dfrac{dI^*}{dt}=\dfrac{1}{K_I}\dfrac{dI}{dt}$.

Going back to the original equation, we have

$$
\begin{aligned}
\frac{dI}{dt} &= l_I\left(1+\frac{7T}{e_I+T}\right)s-d_II\\
&= l_I\left(1+\frac{7T^*}{\frac{e_I}{K_T}+T^*}\right)s-d_II
\end{aligned}
$$

Dividing by K_I gives

$$\frac{1}{K_I}\frac{dI}{dt} = \frac{l_I s}{K_I}\left(1 + \frac{7T^*}{\frac{e_I}{K_T} + T^*}\right) - d_I\frac{I}{K_I} \implies \begin{aligned} \frac{dI^*}{dt} &= \frac{l_I s}{K_I}\left(1 + \frac{7T^*}{\frac{e_I}{K_T} + T^*}\right) - d_I I^* \\ &= \frac{l_I s}{(\frac{l_I s}{d_I})}\left(1 + \frac{7T^*}{\frac{e_I}{K_T} + T^*}\right) - d_I I^* \\ &= d_I\left(1 + \frac{7T^*}{\frac{e_I}{K_T} + T^*}\right) - d_I I^* \\ &= d_I\left(1 + \frac{7T^*}{\frac{e_I}{K_T} + T^*} - I^*\right) \end{aligned}$$

Dividing by k_T gives

$$\frac{1}{k_T}\frac{dI^*}{dt} = \frac{d_I}{k_T}\left(1 + \frac{7T^*}{\frac{e_I}{K_T} + T^*} - I^*\right)$$

Therefore, the nondimensional version of the seventh equation of system (2.1) is given by

$$\frac{dI^*}{dt^*} = \frac{d_I}{k_T}\left(1 + \frac{7T^*}{\frac{e_I}{K_T} + T^*} - I^*\right) \tag{2.10}$$

The eighth and last equation of system (2.1):

$$\frac{dF}{dt} = \frac{l_F}{e_F + T}\left(\frac{1}{3}K + \frac{1}{3}\frac{1}{1+\alpha G}K + E\right)T - d_F F$$

Recall that $T^* = \frac{T}{K_T}$, $K^* = \frac{K}{K_T}$, $E^* = \frac{E}{K_T}$, and $G^* = \frac{G}{K_G}$, where $K_G = \frac{l_G K_T}{d_G}$.

At equilibrium, we get

$$\frac{l_F}{e_F + T}\left(\frac{1}{3}K + \frac{1}{3}\frac{1}{1+\alpha G}K + E\right)T - d_F F = 0$$

$$\begin{aligned}
\implies F &= \frac{l_F T}{d_F(e_F + T)}\left(\frac{1}{3}K + \frac{1}{3}\frac{1}{1+\alpha G}K + E\right) \\
&= \frac{l_F}{d_F}\frac{\frac{T}{K_T}}{\frac{e_F}{K_T} + \frac{T}{K_T}}\left(\frac{1}{3}K + \frac{1}{3}\frac{1}{1+\alpha G}K + E\right) \\
&= \frac{l_F}{d_F}\frac{T^*}{\frac{e_F}{K_T} + T^*}\left(\frac{1}{3}K + \frac{1}{3}\frac{1}{1+\alpha G}K + E\right) \\
&= \frac{l_F}{d_F}\left(\frac{1}{3}K_T K^* + \frac{1}{3}\frac{K_T K^*}{1+\alpha K_G G^*} + K_T E^*\right)\frac{T^*}{\frac{e_F}{K_T} + T^*} \\
&= \frac{l_F K_T}{d_F}\left(\frac{1}{3}K^* + \frac{1}{3}\frac{K^*}{1+\alpha K_G G^*} + E^*\right)\frac{T^*}{\frac{e_F}{K_T} + T^*}
\end{aligned}$$

Let $K_F = \frac{l_F K_T}{d_F}$, which has dimension $\frac{m}{v}$, and $F^* = \frac{F}{K_F}$, which is nondimensional. Then, $\frac{dF^*}{dt} = \frac{1}{K_F}\frac{dF}{dt}$.

Going back to the original equation, we have

$$\begin{aligned}
\frac{dF}{dt} &= \frac{l_F}{e_F + T}\left(\frac{1}{3}K + \frac{1}{3}\frac{1}{1+\alpha G}K + E\right)T - d_F F \\
&= l_F\left(\frac{1}{3}K + \frac{1}{3}\frac{1}{1+\alpha G}K + E\right)\frac{T^*}{\frac{e_F}{K_T} + T^*} - d_F F \\
&= l_F\left(\frac{1}{3}K_T K^* + \frac{1}{3}\frac{K_T K^*}{1+\alpha K_G G^*} + K_T E^*\right)\frac{T^*}{\frac{e_F}{K_T} + T^*} - d_F F \\
&= l_F K_T\left(\frac{1}{3}K^* + \frac{1}{3}\frac{K^*}{1+\alpha K_G G^*} + E^*\right)\frac{T^*}{\frac{e_F}{K_T} + T^*} - d_F F
\end{aligned}$$

Dividing by K_F gives

$$\frac{1}{K_F}\frac{dF}{dt} = \frac{l_F K_T}{K_F}\left(\frac{1}{3}K^* + \frac{1}{3}\frac{K^*}{1+\alpha K_G G^*} + E^*\right)\frac{T^*}{\frac{e_F}{K_T} + T^*} - d_F\frac{F}{K_F}$$

$$\begin{aligned}
\Longrightarrow \frac{dF^*}{dt} &= \frac{l_F K_T}{K_F}\left(\frac{1}{3}K^* + \frac{1}{3}\frac{K^*}{1+\alpha K_G G^*} + E^*\right)\frac{T^*}{\frac{e_F}{K_T} + T^*} - d_F F^* \\
&= \frac{l_F K_T}{(\frac{l_F K_T}{d_F})}\left(\frac{1}{3}K^* + \frac{1}{3}\frac{K^*}{1+\alpha K_G G^*} + E^*\right)\frac{T^*}{\frac{e_F}{K_T} + T^*} - d_F F^* \\
&= d_F\left(\frac{1}{3}K^* + \frac{1}{3}\frac{K^*}{1+\alpha K_G G^*} + E^*\right)\frac{T^*}{\frac{e_F}{K_T} + T^*} - d_F F^*
\end{aligned}$$

Dividing by k_T gives

$$\frac{1}{k_T}\frac{dF^*}{dt} = \frac{d_F}{k_T}\left(\frac{1}{3}K^* + \frac{1}{3}\frac{K^*}{1+\alpha K_G G^*} + E^*\right)\frac{T^*}{\frac{e_F}{K_T}+T^*} - \frac{d_F}{k_T}F^*$$

$$\begin{aligned}\Longrightarrow \frac{dF^*}{dt^*} &= \frac{d_F}{k_T}\left(\frac{1}{3}K^* + \frac{1}{3}\frac{K^*}{1+\alpha K_G G^*} + E^*\right)\frac{T^*}{\frac{e_F}{K_T}+T^*} - \frac{d_F}{k_T}F^* \\ &= \frac{d_F}{k_T}\left(\frac{1}{3}K^* + \frac{1}{3}\frac{K^*}{1+\alpha(\frac{l_G K_T}{d_G})G^*} + E^*\right)\frac{T^*}{\frac{e_F}{K_T}+T^*} - \frac{d_F}{k_T}F^*\end{aligned}$$

Therefore, the nondimensional version of the eighth equation of system (2.1) is given by

$$\frac{dF^*}{dt^*} = \frac{d_F}{k_T}\left(\frac{1}{3}K^* + \frac{1}{3}\frac{K^*}{1+\alpha\frac{l_G K_T}{d_G}G^*} + E^*\right)\frac{T^*}{\frac{e_F}{K_T}+T^*} - \frac{d_F}{k_T}F^* \tag{2.11}$$

In summary, using the nondimensionalization in Table 2.6 gives rise to the nondimensional system of differential equations (2.12).

Table 2.6: Nondimensional Variables

$$T^* = \frac{T}{K_T} \quad N^* = \frac{N}{K_T} \quad K^* = \frac{K}{K_T} \quad E^* = \frac{E}{K_T}$$

$$P^* = \frac{P}{K_P} \quad G^* = \frac{G}{K_G} \quad I^* = \frac{I}{K_I} \quad F^* = \frac{F}{K_F}$$

$$t^* = k_T t$$

where $K_P = \frac{l_P K_T}{d_P}$, $K_G = \frac{l_G K_T}{d_G}$, $K_I = \frac{l_I s}{d_I}$, and $K_F = \frac{l_F K_T}{d_F}$,

$$
\begin{cases}
\dfrac{dT^*}{dt^*} = \dfrac{I^*}{\frac{d_I e_T}{l_I s} + I^*}(1 - T^* - N^*)T^* - \dfrac{d_T}{k_T}(K^* + E^*)\dfrac{T^*}{\frac{g_T}{K_T} + T^*} \\
\dfrac{dN^*}{dt^*} = \dfrac{k_N}{k_T}\left(\dfrac{K_N}{K_T} - N^* - \dfrac{K_N}{K_T}T^*\right) \\
\dfrac{dK^*}{dt^*} = \dfrac{r_K}{k_T}\left(1 - \dfrac{K_T}{K_K}K^*\right)K^* + \dfrac{k_{KE}}{k_T K_T}\dfrac{F^*}{\frac{d_F e_{KE}}{l_F K_T} + F^*} \\
\dfrac{dE^*}{dt^*} = \dfrac{k_{KE}}{k_T K_T}\dfrac{F^*}{(\frac{d_F e_{KE}}{l_F K_T} + F^*)(1 + \beta\frac{l_P K_T}{d_P}P^*)} - \dfrac{d_E}{k_T}E^* \\
\dfrac{dP^*}{dt^*} = \dfrac{d_P}{k_T}(T^* - P^*) \\
\dfrac{dG^*}{dt^*} = \dfrac{d_G}{k_T}(T^* - G^*) \\
\dfrac{dI^*}{dt^*} = \dfrac{d_I}{k_T}\left(1 + \dfrac{7T^*}{\frac{e_I}{K_T} + T^*} - I^*\right) \\
\dfrac{dF^*}{dt^*} = \dfrac{d_F}{k_T}\left(\dfrac{1}{3}K^* + \dfrac{1}{3}\dfrac{K^*}{1 + \alpha\frac{l_G K_T}{d_G}G^*} + E^*\right)\dfrac{T^*}{\frac{e_F}{K_T} + T^*} - \dfrac{d_F}{k_T}F^*
\end{cases}
\tag{2.12}
$$

Chapter 3

Analysis of the Model

The behavior of the system will be analyzed numerically with the aid of several software packages, including *XPPAUT*, *Matlab* and *Maple*. Also, the system will be studied analytically to see what results can be obtained. However, before this can be done, the number of equations must be reduced in order to make it more manageable.

Numerical tests were performed on the original system (2.1), whenever possible, and repeated on the reduced and/or nondimensionalized systems to verify their accuracy at capturing the dynamics.

3.1 Initial Conditions

Consider the tumor-free state of the original system (2.1) obtained by setting $T = 0$ and finding the equilibria of the resulting system.

$$\frac{dN}{dt} = l_N \left(1 - \frac{N}{K_N}\right) = 0 \implies N = K_N = 1.23 \times 10^7$$

$$\frac{dK}{dt} = r_K \left(1 - \frac{K}{K_K}\right) K + \frac{k_{KE} F}{e_{KE} + F} = 0$$

$$\implies r_K \left(1 - \frac{K}{K_K}\right) K = 0 \ ,$$

$$\text{since } F(0) = 0 \text{ and } T \equiv 0 \implies \frac{dF}{dt} = 0 \text{ , so } F \equiv 0$$

$$\implies K = 0 \text{ or } K = K_K = 2.30 \times 10^7$$

$K = 0$ represents immune system failure, since it indicates that the individual has no innate immunity, and $K = 2.30 \times 10^7 \frac{cells}{ml}$ corresponds to a healthy individual with a normal immune system and therefore, this was the value that was used for $K(0)$.

$$\frac{dE}{dt} = \frac{k_{KE} F}{(e_{KE} + F)(1 + \beta P)} - d_E E = 0 \implies E = 0 \text{ , since } F \equiv 0$$

$$\frac{dP}{dt} = -d_P P = 0 \implies P = 0$$

$$\frac{dG}{dt} = -d_G G = 0 \implies G = 0$$

$$\frac{dI}{dt} = l_I s - d_I I = 0 \implies I = \frac{l_I s}{d_I} = \frac{(1.0)(7.7 \times 10^4)}{10} = 7.7 \times 10^3$$

$$\frac{dF}{dt} = -d_F F = 0 \implies F = 0$$

These values correspond to a stable, healthy, tumor-free individual before being afflicted with the disease and are good starting values for the model.

By comparing the equilibrium values just obtained with the initial conditions in Table 2.3, we can see that they pretty much agree. For the remainder of the analysis, the newly obtained equilibrium values above, along with $T(0) = 9.60 \times 10^{-4}$ (as given in Table 2.3), will be used as the initial conditions of the system. These values are summarized in Table 3.1.

Table 3.1: New Initial Conditions

Variable	Initial Value
$T(0)$	$\frac{9.60\times10^{-4}cells}{ml}$
$N(0)$	$\frac{1.23\times10^{7}cells}{ml}$
$K(0)$	$\frac{2.30\times10^{7}cells}{ml}$
$E(0)$	$\frac{0cells}{ml}$
$P(0)$	$\frac{0pg}{ml}$
$G(0)$	$\frac{0pg}{ml}$
$I(0)$	$\frac{7.70\times10^{3}pg}{ml}$
$F(0)$	$\frac{0pg}{ml}$

The corresponding nondimensional version of the initial conditions can be obtained from Table 3.1 by using the nondimensionalization in Table 2.6 as follows:

$$T^*(0) = \frac{T(0)}{K_T} = \frac{9.60 \times 10^{-4}}{7.7 \times 10^7} = 1.25 \times 10^{-11}$$

$$N^*(0) = \frac{N(0)}{K_T} = \frac{1.23 \times 10^7}{7.7 \times 10^7} = .16$$

$$K^*(0) = \frac{K(0)}{K_T} = \frac{2.30 \times 10^7}{7.7 \times 10^7} = .30$$

$$E^*(0) = \frac{E(0)}{K_T} = 0$$

$$P^*(0) = \frac{P(0)}{K_P} = 0$$

$$G^*(0) = \frac{G(0)}{K_G} = 0$$

$$I^*(0) = \frac{I(0)}{K_I} = \frac{I(0)}{\frac{l_I s}{d_I}} = \frac{I(0)d_I}{l_I s} = \frac{(7.7 \times 10^3)(10)}{(1)(7.7 \times 10^4)} = 1$$

$$F^*(0) = \frac{F(0)}{K_F} = 0$$

These are summarized in Table 3.2.

Table 3.2: Nondimensional Version of Initial Conditions

Variable	Initial Value
$T^*(0)$	1.25×10^{-11}
$N^*(0)$	.16
$K^*(0)$	.30
$E^*(0)$	0
$P^*(0)$	0
$G^*(0)$	0
$I^*(0)$	1
$F^*(0)$	0

3.2 Preliminary Numerical Results

The system appears to be stiff. *Stiffness* is a phenomenon sometimes exhibited by a system when some of its components are changing much more rapidly than others. In order to accurately solve the equations of such a system using classical numerical methods, it is necessary to take an extremely small integration step size, slowing down the calculations tremendously. In these cases, an *adaptive step size integrator* should be used. A numerical integration method of this type varies the step size as necessary. For instance, a small step size is used during periods of rapid change and a larger step size is used during periods of slower change. Due to the apparent stiffness of the system, it became necessary to use the adaptive stepsize integrator *Gear*, available in *XPPAUT*.

Numerical results based on the original system (2.1) revealed that either of several parameters had to be varied (sometimes several orders of magnitude) to obtain sustained tumor growth. One such parameter in question, half-saturation constant g_T (refer to Figure 3.1), is suspected of possibly being wrong for two reasons. First, it was estimated from a generic model [3] and not calculated for this model specifically. Second, the *law of mass action* does not apply initially, since the model begins with only one tumor cell ($\frac{9.60\times10^{-4}cells}{ml}$) in the entire BM and many immune cells distributed over the entire BM. So the tumor and immune cells are not uniformly distributed throughout the BM. Therefore, the last term

$$\frac{d_T(K+E)T}{g_T+T}$$

in the first equation in system (2.1) was modified. Suppose the units of K, E and T are cells rather than cell densities. Then, a way in which to obtain a more realistic result will be as follows. Since immune cells are restricted by the speed at which they can move, not all cells in the BM attack the tumor simultaneously. Only cells within a small volume surrounding the tumor cell can attack it in one day. According to [53], page 496, leukocytes move $2 - 20\frac{\mu m}{min}$. If we let

$$r = \frac{2 \times 10^{-6} m}{min} = .29 \frac{cm}{day}$$

and

$$V = \frac{4}{3}\pi(.29)^3 = .10 cm^3$$

then only immune cells within this volume surrounding the tumor cell can attack the cell in one day. So the fraction of BM cells that can attack each tumor cell in one day is

$$\frac{V}{V_{BM}} = \frac{.10ml}{1042ml} = 9.6 \times 10^{-5}$$

So initially, we want to replace $K + E$ by $9.6 \times 10^{-5}(K + E)$ to reduce the number of immune cells that attack the tumor cell. Replacing g_T in the denominator by

$$\frac{1}{9.6 \times 10^{-5}} g_T = (1.04 \times 10^4)(1 \times 10^5 \frac{cells}{ml}) = 1.04 \times 10^9 \frac{cells}{ml}$$

has the desired effect, and when T is large, this change is negligible.

This value is of the same order of magnitude as a value such as 3.5×10^9 or 5×10^9 which gives sustained tumor growth according to the numerical experiments

that were performed, as indicated in Figure 3.1. Since there is no way to medically determine the time it takes for the sharp increase in T starting from the time that the first tumor cell appears, we cannot determine which value gives a more biologically realistic result. When $g_T = 3.4 \times 10^9$, the figure seems to indicate that there is no tumor growth. However, calculating the equilibria using $Maple$ (done in greater detail later) yields a positive tumor equilibrium of $T = 5.924491790 \times 10^7$. So decreasing g_T delays the increase of T. However, g_T has a threshold effect on T. Performing the same equilibria calculation using $g_T = 1 \times 10^5$ results in no positive tumor equilibrium and hence no tumor growth. From this point on, we chose to use

$$g_T = 5 \times 10^9 \frac{cells}{ml}$$

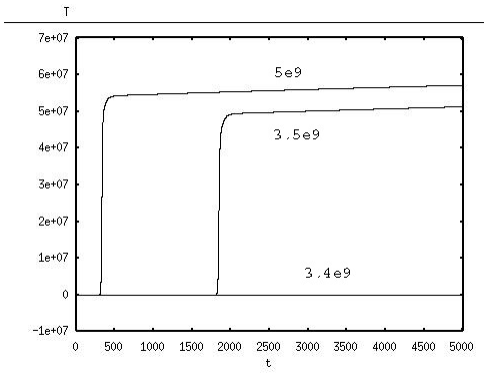

Figure 3.1: Plot of T versus time t for various values of g_T, using system (2.1).

Other numerical tests showed the expected behavior of the system. For instance, Figure 3.2 shows an initial increase in the number or E cells as the immune system tries to fight the tumor, followed by a decrease in the number of E cells due to an increase in M-protein. Also shown is a decrease in $IFN - \gamma$ (F) as the immune system tries to fight the tumor, followed by a decrease in $IFN - \gamma$ due to the effects

of tumor-derived glycolipids (G) and M-protein (P). Interestingly, the reduction in $IFN-\gamma$ production due to the tumor-derived glycolipids (which cause a disfunction in the ability of NKT cells to produce $IFN-\gamma$) is not as significant as expected. This is probably due to the fact that other immune cells also produce $IFN-\gamma$. However, the reduction in the number of E cells due to the increase in M-protein causes a more significant drop in the production of $IFN-\gamma$.

Repeating the same numerical tests on the nondimensional system (2.12) revealed no change in the qualitative behavior of the system.

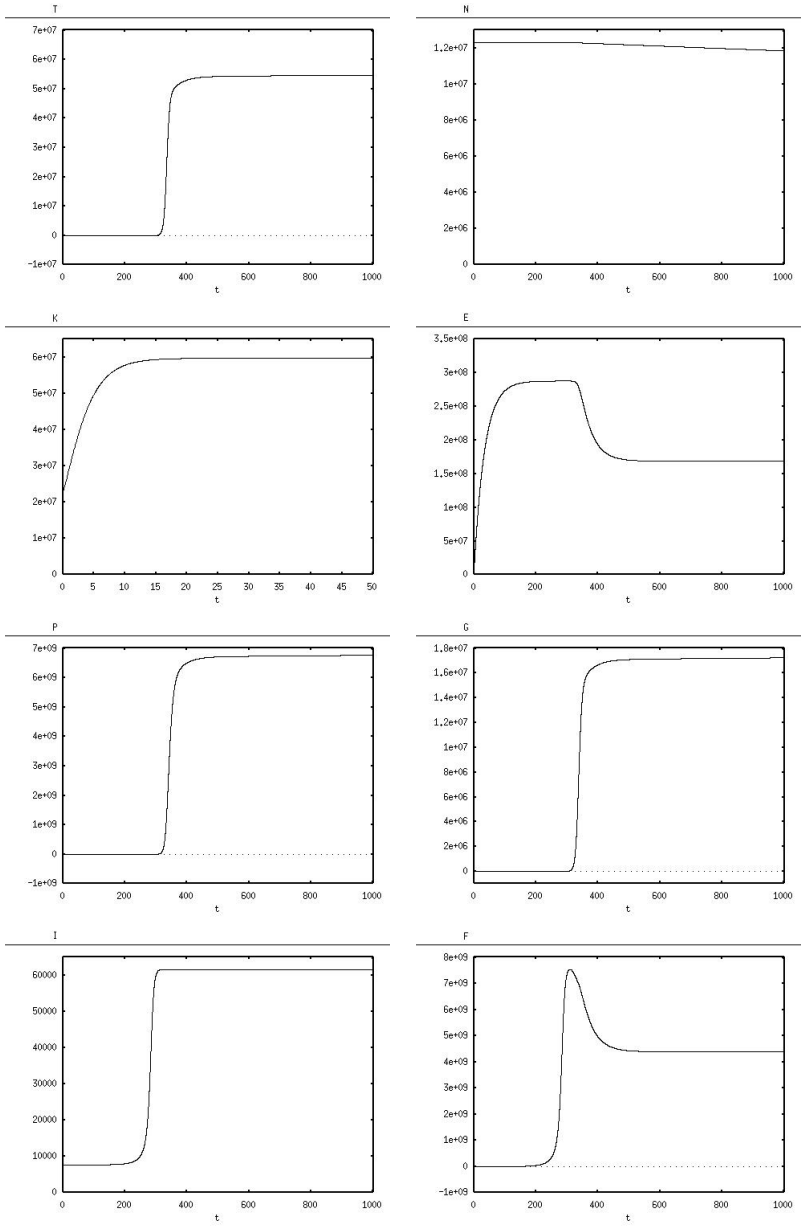

Figure 3.2: Plots of T, N, K, E, P, G, I, and F versus time t, using system (2.1).

3.3 Reduction of the Original System

In order to work with the system analytically, the number of equations must first be reduced. We will begin by working with the original system (2.1). Note that the

fifth and sixth equations are simple compared to the rest. Assuming that they are at equilibrium should not affect the outcome much, other than perhaps causing the loss of the built-in time delay, so events might occur at an earlier time, but the behavior should remain qualitatively the same. We will assume that both equations are at equilibrium and perform numerical tests to see if these assumptions are valid. This gives

$$\frac{dP}{dt} = l_P T - d_P P = 0 \implies P = \frac{l_P}{d_P} T \tag{3.1}$$

and

$$\frac{dG}{dt} = l_G T - d_G G = 0 \implies G = \frac{l_G}{d_G} T \tag{3.2}$$

This will eliminate the fifth and sixth equations of the system.

Substituting (3.1) and (3.2) into the fourth and eighth equations of system (2.1) gives

$$\frac{dE}{dt} = \frac{k_{KE} F}{(e_{KE} + F)(1 + \frac{\beta l_P}{d_P} T)} - d_E E \tag{3.3}$$

and

$$\frac{dF}{dt} = \frac{l_F}{e_F + T} \left(\frac{1}{3} K + \frac{1}{3} \frac{1}{1 + \frac{\alpha l_G}{d_G} T} K + E \right) T - d_F F \tag{3.4}$$

Making these changes in system (2.1) gives rise to the following simpler system:

$$\begin{cases} \dfrac{dT}{dt} = \dfrac{k_T I}{e_T + I}\left(1 - \dfrac{T+N}{K_T}\right)T - \dfrac{d_T(K+E)T}{g_T + T} \\ \\ \dfrac{dN}{dt} = l_N\left(1 - \dfrac{N}{K_N} - \dfrac{T}{K_T}\right) \\ \\ \dfrac{dK}{dt} = r_K\left(1 - \dfrac{K}{K_K}\right)K + \dfrac{k_{KE}F}{e_{KE} + F} \\ \\ \dfrac{dE}{dt} = \dfrac{k_{KE}F}{(e_{KE} + F)(1 + \frac{\beta l_P}{d_P}T)} - d_E E \\ \\ \dfrac{dI}{dt} = l_I\left(1 + \dfrac{7T}{e_I + T}\right)s - d_I I \\ \\ \dfrac{dF}{dt} = \dfrac{l_F}{e_F + T}\left(\dfrac{1}{3}K + \dfrac{1}{3}\dfrac{1}{1 + \frac{\alpha l_G}{d_G}T}K + E\right)T - d_F F \end{cases} \tag{3.5}$$

Numerical tests revealed no change in the qualitative behavior of the above reduced system.

Next, we will compare time scales using nondimensional system (2.12) to see if a time scale argument can be used to justify applying a pseudo-equilibrium hypothesis (assuming that some processes reach equilibrium much sooner that others) in order to reduce the system further. After substituting parameter values into the nondimensional system (2.12) using *Maple*, we obtain the following:

$$
\begin{cases}
\dfrac{dT^*}{dt^*} = \dfrac{I^*(1-T^*-N^*)T^*}{2.597402597+I^*} - \dfrac{2.272727273(K^*+E^*)T^*}{64.93506494+T^*} \\[2ex]
\dfrac{dN^*}{dt^*} = .00002904368358 - .0001818181818N^* - .00002904368358T^* \\[2ex]
\dfrac{dK^*}{dt^*} = .2045454545(1-3.347826087K^*)K^* + \dfrac{.2550177096F^*}{3.927272727\times 10^{-8}+F^*} \\[2ex]
\dfrac{dE^*}{dt^*} = \dfrac{.2550177096F^*}{(3.927272727\times 10^{-8}+F^*)(1+1.000277304P^*)} - .06818181818E^* \\[2ex]
\dfrac{dP^*}{dt^*} = .2663636364T^* - .2663636364P^* \\[2ex]
\dfrac{dG^*}{dt^*} = .6431818182T^* - .6431818182G^* \\[2ex]
\dfrac{dI^*}{dt^*} = 22.72727273 + \dfrac{159.0909091T^*}{.00001298701299+T^*} - 22.72727273I^* \\[2ex]
\dfrac{dF^*}{dt^*} = \dfrac{4.909090909T^*\left(\dfrac{K^*}{3}+\dfrac{K^*}{3+96.83715900G^*}+E^*\right)}{.00001298701299+T^*} - 4.909090909F^*
\end{cases}
\tag{3.6}
$$

From these results, it seems that some processes are occurring at a faster rate than others. This is partly responsible for the stiffness observed in the system. Therefore, we can apply a pseudo-equilibrium hypothesis by assuming that the faster processes

are at equilibrium, since they reach equilibrium at an earlier time than the slower processes. However, since we want to study the interaction between the cancer cells and the immune system, we want to keep the equations for tumor cells T and for immune cells K and E in our system. Therefore, we will only eliminate the I and F equations by assuming that the last two equations of the original system (2.1) are at equilibrium. As before, once these changes are applied, numerical tests are performed on the resulting system to make sure that it still behaves the same qualitatively.

Finding the equilibrium values of these equations gives

$$\frac{dI}{dt} = l_I \left(1 + \frac{7T}{e_I + T}\right) s - d_I I = 0 \implies I = \frac{l_I}{d_I}\left(1 + \frac{7T}{e_I + T}\right) s \tag{3.7}$$

$$\frac{dF}{dt} = \frac{l_F}{e_F + T}\left(\frac{1}{3}K + \frac{1}{3}\frac{1}{1+\alpha G}K + E\right) T - d_F F = 0$$

$$\implies F = \frac{l_F}{d_F(e_F + T)}\left(\frac{1}{3}K + \frac{1}{3}\frac{1}{1+\alpha G}K + E\right) T \tag{3.8}$$

Next, these results are substituted into the first, third and fourth equations of system (2.1). Substituting (3.7) into the first equation gives

$$\begin{aligned}
\frac{dT}{dt} &= \frac{k_T \dfrac{l_I}{d_I}\left(1+\dfrac{7T}{e_I+T}\right)s}{e_T+\dfrac{l_I}{d_I}\left(1+\dfrac{7T}{e_I+T}\right)s}\left(1-\frac{T+N}{K_T}\right)T-\frac{d_T(K+E)T}{g_T+T} \\
&= \frac{k_T \dfrac{l_I}{d_I}\left(\dfrac{e_I+8T}{e_I+T}\right)s}{e_T+\dfrac{l_I}{d_I}\left(\dfrac{e_I+8T}{e_I+T}\right)s}\left(1-\frac{T+N}{K_T}\right)T-\frac{d_T(K+E)T}{g_T+T} \\
&= \frac{k_T \dfrac{l_I}{d_I}\left(\dfrac{e_I+8T}{e_I+T}\right)s}{\dfrac{l_I}{d_I}\left(\dfrac{e_I+8T}{e_I+T}\right)\left[\dfrac{e_T d_I}{s l_I}\left(\dfrac{e_I+T}{e_I+8T}\right)+1\right]s}\left(1-\frac{T+N}{K_T}\right)T-\frac{d_T(K+E)T}{g_T+T} \\
&= \frac{k_T}{\dfrac{e_T d_I}{s l_I}\left(\dfrac{e_I+T}{e_I+8T}\right)+1}\left(1-\frac{T+N}{K_T}\right)T-\frac{d_T(K+E)T}{g_T+T}
\end{aligned}$$

Substituting (3.8) into the third equation gives

$$\begin{aligned}
\frac{dK}{dt} &= r_K\left(1-\frac{K}{K_K}\right)K + \frac{\frac{k_{KE}l_F}{d_F(e_F+T)}\left(\frac{1}{3}K+\frac{1}{3}\frac{1}{1+\alpha G}K+E\right)T}{e_{KE}+\frac{l_F}{d_F(e_F+T)}\left(\frac{1}{3}K+\frac{1}{3}\frac{1}{1+\alpha G}K+E\right)T} \\
&= r_K\left(1-\frac{K}{K_K}\right)K + \frac{\frac{k_{KE}l_F}{d_F(e_F+T)}\left(\frac{2K+\alpha GK+3E+3\alpha GE}{3(1+\alpha G)}\right)T}{e_{KE}+\frac{l_F}{d_F(e_F+T)}\left(\frac{2K+\alpha GK+3E+3\alpha GE}{3(1+\alpha G)}\right)T} \\
&= r_K\left(1-\frac{K}{K_K}\right)K + \\
&\quad \frac{\frac{k_{KE}l_F}{d_F(e_F+T)}\left(\frac{2K+\alpha GK+3E+3\alpha GE}{3(1+\alpha G)}\right)T}{\frac{l_F}{d_F(e_F+T)}\left(\frac{2K+\alpha GK+3E+3\alpha GE}{3(1+\alpha G)}\right)\left[\frac{3e_{KE}d_F(e_F+T)(1+\alpha G)}{l_F(2K+\alpha GK+3E+3\alpha GE)}+T\right]} \\
&= r_K\left(1-\frac{K}{K_K}\right)K + \frac{k_{KE}T}{\frac{3e_{KE}d_F(e_F+T)(1+\alpha G)}{l_F(2K+\alpha GK+3E+3\alpha GE)}+T} \\
&= r_K\left(1-\frac{K}{K_K}\right)K + \frac{k_{KE}T}{\frac{3e_{KE}d_F(e_F+T)\left(1+\frac{\alpha l_G}{d_G}T\right)}{l_F\left(2K+\frac{\alpha l_G}{d_G}TK+3E+\frac{3\alpha l_G}{d_G}TE\right)}+T}
\end{aligned}$$

by substituting (3.2) for G as in system (3.5)

Substituting (3.8) into the fourth equation, proceeding as we did above, and then substituting (3.1) for P as in system (3.5) gives

$$\frac{dE}{dt} = \frac{k_{KE}T}{\left(1+\frac{\beta l_P}{d_P}T\right)\left[\frac{3e_{KE}d_F(e_F+T)\left(1+\frac{\alpha l_G}{d_G}T\right)}{l_F\left(2K+\frac{\alpha l_G}{d_G}TK+3E+\frac{3\alpha l_G}{d_G}TE\right)}+T\right]} - d_E E$$

As mentioned earlier, as a person ages, the number of plasma cells increases slower and levels off later in life. Since the model assumes that the onset of the disease occurs at 70 years of age, the carrying capacity is reached at 84 years of age, and the plasma cell density increases slowly and levels off at these ages, we can assume that the plasma cell density is at equilibrium. Therefore, the number of equations can be reduced further by assuming that the second equation of system (3.5) is at equilibrium. This gives

$$\frac{dN}{dt} = l_N\left(1-\frac{N}{K_N}-\frac{T}{K_T}\right) = 0 \implies N = K_N - \frac{K_N}{K_T}T \tag{3.9}$$

Substituting (3.9) into the first equation gives

$$\begin{aligned}\frac{dT}{dt} &= \frac{k_T}{\frac{e_T d_I}{s l_I}\left(\frac{e_I+T}{e_I+8T}\right)+1}\left(1-\frac{T+(K_N-\frac{K_N}{K_T}T)}{K_T}\right)T-\frac{d_T(K+E)T}{g_T+T}\\ &= \frac{k_T}{\frac{e_T d_I}{s l_I}\left(\frac{e_I+T}{e_I+8T}\right)+1}\left(1-\frac{T}{K_T}-\frac{K_N}{K_T}+\frac{K_N}{K_T^2}T\right)T-\frac{d_T(K+E)T}{g_T+T}\end{aligned}$$

Having eliminated the I, F and N from the already reduce system (3.5) yields the following reduced system of four equations:

$$\begin{cases}\dfrac{dT}{dt} = \dfrac{k_T}{\frac{e_T d_I}{s l_I}\left(\frac{e_I+T}{e_I+8T}\right)+1}\left(1-\dfrac{T}{K_T}-\dfrac{K_N}{K_T}+\dfrac{K_N}{K_T^2}T\right)T-\dfrac{d_T(K+E)T}{g_T+T}\\[2ex] \dfrac{dK}{dt} = r_K\left(1-\dfrac{K}{K_K}\right)K+\dfrac{k_{KE}T}{\dfrac{3e_{KE}d_F(e_F+T)\left(1+\frac{\alpha l_G}{d_G}T\right)}{l_F\left(2K+\frac{\alpha l_G}{d_G}TK+3E+\frac{3\alpha l_G}{d_G}TE\right)}+T}\\[2ex] \dfrac{dE}{dt} = \dfrac{k_{KE}T}{\left(1+\frac{\beta l_P}{d_P}T\right)\left[\dfrac{3e_{KE}d_F(e_F+T)\left(1+\frac{\alpha l_G}{d_G}T\right)}{l_F\left(2K+\frac{\alpha l_G}{d_G}TK+3E+\frac{3\alpha l_G}{d_G}TE\right)}+T\right]}-d_E E\end{cases} \tag{3.10}$$

Again, numerical tests revealed no change in the qualitative behavior of the above reduced system.

3.4 Nondimensionalization of the Reduced System

Using the nondimensionalization in Table 2.6, we get the following:

$$t^* = k_T t \implies t = \frac{1}{k_T} t^* \implies \frac{d}{dt^*} = \frac{d}{dt}\frac{dt}{dt^*} = \frac{1}{k_T}\frac{d}{dt} \implies \frac{d}{dt} = k_T \frac{d}{dt^*}$$

$$T^* = \frac{T}{K_T} \implies T = K_T T^* \implies \frac{dT}{dt} = K_T \frac{dT^*}{dt} = k_T K_T \frac{dT^*}{dt^*}$$

$$K^* = \frac{K}{K_T} \implies K = K_T K^* \implies \frac{dK}{dT} = K_T \frac{dK^*}{dt} = k_T K_T \frac{dK^*}{dt^*}$$

$$E^* = \frac{E}{K_T} \implies E = K_T E^* \implies \frac{dE}{dt} = K_T \frac{dE^*}{dt} = k_T K_T \frac{dE^*}{dt^*}$$

Substituting these values into the first equation of the reduced system (3.10) gives

$$k_T K_T \frac{dT^*}{dt^*} = \frac{k_T}{\frac{e_T d_I}{s l_I}\left(\frac{e_I + K_T T^*}{e_I + 8 K_T T^*}\right) + 1}\left(1 - T^* - \frac{K_N}{K_T} + \frac{K_N}{K_T} T^*\right) K_T T^* - \frac{d_T K_T^2 (K^* + E^*) T^*}{g_T + K_T T^*}$$

$$\implies \frac{dT^*}{dt^*} = \frac{1}{\frac{e_T d_I}{s l_I}\left(\frac{e_I + K_T T^*}{e_I + 8K_T T^*}\right) + 1}\left((1 - \frac{K_N}{K_T}) - (1 - \frac{K_N}{K_T})T^*\right)T^*$$

$$- \frac{d_T K_T (K^* + E^*)T^*}{k_T(g_T + K_T T^*)}$$

The third equation of system (3.10) becomes

$$k_T K_T \frac{dK^*}{dt^*} = r_K\left(1 - \frac{K_T K^*}{K_K}\right)K_T K^* +$$

$$\frac{k_{KE} K_T T^*}{\frac{3e_{KE} d_F (e_F + K_T T^*)\left(1 + \frac{\alpha l_G}{d_G} K_T T^*\right)}{l_F K_T\left(2K^* + \frac{\alpha l_G}{d_G} K_T T^* K^* + 3E^* + \frac{3\alpha l_G}{d_G} K_T T^* E^*\right)} + K_T T^*}$$

$$\implies \frac{dK^*}{dt^*} = \frac{r_K}{k_T}\left(1 - \frac{K_T}{K_K} K^*\right)K^* +$$

$$\frac{k_{KE} T^*}{\frac{3k_T e_{KE} d_F (e_F + K_T T^*)\left(1 + \frac{\alpha l_G K_T}{d_G} T^*\right)}{l_F K_T\left(2K^* + \frac{\alpha l_G K_T}{d_G} T^* K^* + 3E^* + \frac{3\alpha l_G K_T}{d_G} T^* E^*\right)} + k_T K_T T^*}$$

The fourth equation of system (3.10) becomes

$$k_T K_T \frac{dE^*}{dt^*} =$$

$$\frac{k_{KE} K_T T^*}{\left(1 + \frac{\beta l_P}{d_P} K_T T^*\right) \left[\frac{3 e_{KE} d_F (e_F + K_T T^*) \left(1 + \frac{\alpha l_G}{d_G} K_T T^*\right)}{l_F K_T \left(2K^* + \frac{\alpha l_G}{d_G} K_T T^* K^* + 3E^* + \frac{3\alpha l_G}{d_G} K_T T^* E^*\right)} + K_T T^*\right]}$$

$$- d_E K_T E^*$$

$$\implies \frac{dE^*}{dt^*} =$$

$$\frac{k_{KE} T^*}{\left(1 + \frac{\beta l_P K_T}{d_P} T^*\right) \left[\frac{3 k_T e_{KE} d_F (e_F + K_T T^*) \left(1 + \frac{\alpha l_G K_T}{d_G} T^*\right)}{l_F K_T \left(2K^* + \frac{\alpha l_G K_T}{d_G} T^* K^* + 3E^* + \frac{3\alpha l_G K_T}{d_G} T^* E^*\right)} + k_T K_T T^*\right]}$$

$$- \frac{d_E}{k_T} E^*$$

The resulting equations give the following nondimensional reduced system:

$$
\begin{cases}
\dfrac{dT^*}{dt^*} = \dfrac{\left((1-\frac{K_N}{K_T}) - (1-\frac{K_N}{K_T})T^*\right)T^*}{\frac{e_T d_I}{s l_I}\left(\dfrac{e_I + K_T T^*}{e_I + 8K_T T^*}\right) + 1} - \dfrac{d_T K_T (K^* + E^*) T^*}{k_T (g_T + K_T T^*)} \\[2ex]
\dfrac{dK^*}{dt^*} = \dfrac{r_K}{k_T}\left(1 - \dfrac{K_T}{K_K}K^*\right)K^* + \\[2ex]
\qquad\qquad \dfrac{k_{KE} T^*}{\dfrac{3k_T e_{KE} d_F (e_F + K_T T^*)\left(1 + \frac{\alpha l_G K_T}{d_G} T^*\right)}{l_F K_T \left(2K^* + \frac{\alpha l_G K_T}{d_G} K^* T^* + 3E^* + \frac{3\alpha l_G K_T}{d_G} E^* T^*\right)} + k_T K_T T^*} \\[2ex]
\dfrac{dE^*}{dt^*} = \\[2ex]
\dfrac{k_{KE} T^*}{\left(1 + \frac{\beta l_P K_T}{d_P} T^*\right)\left[\dfrac{3k_T e_{KE} d_F (e_F + K_T T^*)\left(1 + \frac{\alpha l_G K_T}{d_G} T^*\right)}{l_F K_T \left(2K^* + \frac{\alpha l_G K_T}{d_G} K^* T^* + 3E^* + \frac{3\alpha l_G K_T}{d_G} E^* T^*\right)} + k_T K_T T^*\right]} \\[2ex]
\qquad\qquad -\dfrac{d_E}{k_T} E^*
\end{cases}
\tag{3.11}
$$

Once again, numerical tests revealed no change in the qualitative behavior of the above reduced system.

The complex fractions in system (3.11) will be simplified to make the equations easier to handle analytically.

$$\begin{aligned}
\frac{dT^*}{dt^*} &= \frac{\left((1-\frac{K_N}{K_T})-(1-\frac{K_N}{K_T})T^*\right)T^*}{\frac{e_T d_I(e_I+K_T T^*)+sl_I(e_I+8K_T T^*)}{sl_I(e_I+8K_T T^*)}} - \frac{d_T K_T K^* T^* + d_T K_T E^* T^*}{k_T g_T + k_T K_T T^*} \\
&= \frac{sl_I(e_I+8K_T T^*)\left((1-\frac{K_N}{K_T})-(1-\frac{K_N}{K_T})T^*\right)T^*}{e_T d_I(e_I+K_T T^*)+sl_I(e_I+8K_T T^*)} \\
&\qquad - \frac{d_T K_T K^* T^* + d_T K_T E^* T^*}{k_T g_T + k_T K_T T^*} \\
&= \frac{(sl_I e_I T^* + 8sl_I K_T T^{*2})\left((1-\frac{K_N}{K_T})-(1-\frac{K_N}{K_T})T^*\right)}{e_T d_I e_I + e_T d_I K_T T^* + sl_I e_I + 8sl_I K_T T^*} \\
&\qquad - \frac{d_T K_T K^* T^* + d_T K_T E^* T^*}{k_T g_T + k_T K_T T^*}
\end{aligned}$$

$$= \frac{sl_I e_I(1-\frac{K_N}{K_T})T^* - sl_I e_I(1-\frac{K_N}{K_T})T^{*2} + 8sl_I K_T(1-\frac{K_N}{K_T})T^{*2} - 8sl_I K_T(1-\frac{K_N}{K_T})T^{*3}}{e_I(e_T d_I + sl_I) + (e_T d_I + 8sl_I)K_T T^*}$$

$$-\frac{d_T K_T K^* T^* + d_T K_T E^* T^*}{k_T g_T + k_T K_T T^*}$$

$$= \frac{\left[\begin{array}{r} sl_I e_I T^* - \frac{sl_I e_I K_N}{K_T} T^* - sl_I e_I T^{*2} + \frac{sl_I e_I K_N}{K_T} T^{*2} + 8sl_I K_T T^{*2} - 8sl_I K_N T^{*2} \\ -8sl_I K_T T^{*3} + 8sl_I K_N T^{*3} \end{array}\right]}{e_I(e_T d_I + sl_I) + (e_T d_I + 8sl_I) K_T T^*}$$

$$-\frac{d_T K_T K^* T^* + d_T K_T E^* T^*}{k_T g_T + k_T K_T T^*}$$

$$= \frac{sl_I e_I(1 - \frac{K_N}{K_T})T^* + sl_I(\frac{e_I K_N}{K_T} - e_I + 8K_T - 8K_N)T^{*2} + 8sl_I(K_N - K_T)T^{*3}}{e_I(e_T d_I + sl_I) + (e_T d_I + 8sl_I) K_T T^*}$$

$$-\frac{d_T K_T K^* T^* + d_T K_T E^* T^*}{k_T g_T + k_T K_T T^*}$$

$$\frac{dK^*}{dt^*} = \frac{r_K}{k_T}K^* - \frac{r_K K_T}{k_T K_K}K^{*2} + \frac{k_{KE}T^*}{\left(\begin{array}{c}\left[\begin{array}{c}3k_T e_{KE} d_F (e_F + K_T T^*)\left(1 + \frac{\alpha l_G K_T}{d_G}T^*\right) + \\ l_F k_T K_T^2 \left(2K^* + \frac{\alpha l_G K_T}{d_G}K^*T^* + 3E^* + \frac{3\alpha l_G K_T}{d_G}E^*T^*\right)T^*\end{array}\right] \\ \hline l_F K_T \left(2K^* + \frac{\alpha l_G K_T}{d_G}K^*T^* + 3E^* + \frac{3\alpha l_G K_T}{d_G}E^*T^*\right)\end{array}\right)}$$

$$= \frac{r_K}{k_T}K^* - \frac{r_K K_T}{k_T K_K}K^{*2} + \frac{k_{KE}l_F K_T\left(2K^* + \frac{\alpha l_G K_T}{d_G}K^*T^* + 3E^* + \frac{3\alpha l_G K_T}{d_G}E^*T^*\right)T^*}{\left[\begin{array}{c}3k_T e_{KE} d_F \left(e_F + \frac{\alpha e_F l_G K_T}{d_G}T^* + K_T T^* + \frac{\alpha l_G K_T^2}{d_G}T^{*2}\right) + 2l_F k_T K_T^2 K^*T^* \\ + \frac{\alpha l_F k_T l_G K_T^3}{d_G}K^*T^{*2} + 3l_F k_T K_T^2 E^*T^* + \frac{3\alpha l_F k_T l_G K_T^3}{d_G}E^*T^{*2}\end{array}\right]}$$

$$= \frac{r_K}{k_T}K^* - \frac{r_K K_T}{k_T K_K}K^{*2} + \frac{2k_{KE}l_F K_T K^*T^* + \frac{\alpha k_{KE}l_F l_G K_T^2}{d_G}K^*T^{*2} + 3k_{KE}l_F K_T E^*T^* + \frac{3\alpha k_{KE}l_F l_G K_T^2}{d_G}E^*T^{*2}}{\left[\begin{array}{c}3k_T e_{KE} d_F e_F + \frac{3k_T e_{KE} d_F K_T(\alpha e_F l_G + d_G)}{d_G}T^* + \frac{3\alpha k_T e_{KE} d_F l_G K_T^2}{d_G}T^{*2} + 2l_F k_T K_T^2 K^*T^* \\ + \frac{\alpha l_F k_T l_G K_T^3}{d_G}K^*T^{*2} + 3l_F k_T K_T^2 E^*T^* + \frac{3\alpha l_F k_T l_G K_T^3}{d_G}E^*T^{*2}\end{array}\right]}$$

Similarly,

$$\frac{dE^*}{dt^*} =$$

$$\frac{2k_{KE}l_F K_T K^* T^* + \frac{\alpha k_{KE} l_F l_G K_T^2}{d_G} K^* T^{*2} + 3k_{KE} l_F K_T E^* T^* + \frac{3\alpha k_{KE} l_F l_G K_T^2}{d_G} E^* T^{*2}}{\left(1 + \frac{\beta l_P K_T}{d_P} T^*\right) \left[\begin{array}{c} 3k_T e_{KE} d_F e_F + \frac{3k_T e_{KE} d_F K_T (\alpha e_F l_G + d_G)}{d_G} T^* + \frac{3\alpha k_T e_{KE} d_F l_G K_T^2}{d_G} T^{*2} \\ +2l_F k_T K_T^2 K^* T^* + \frac{\alpha l_F k_T l_G K_T^3}{d_G} K^* T^{*2} + 3l_F k_T K_T^2 E^* T^* \\ + \frac{3\alpha l_F k_T l_G K_T^3}{d_G} E^* T^{*2} \end{array}\right]}$$

$$-\frac{d_E}{k_T} E^*$$

The nondimensional reduced system can now be written as follows:

$$
\begin{cases}
\dfrac{dT^*}{dt^*} = \dfrac{sl_I e_I(1-\frac{K_N}{K_T})T^* + sl_I(\frac{e_I K_N}{K_T} - e_I + 8K_T - 8K_N)T^{*2} + 8sl_I(K_N - K_T)T^{*3}}{e_I(e_T d_I + sl_I) + (e_T d_I + 8sl_I)K_T T^*} \\
\qquad\qquad - \dfrac{d_T K_T K^* T^* + d_T K_T E^* T^*}{k_T g_T + k_T K_T T^*} \\
\dfrac{dK^*}{dt^*} = \dfrac{r_K}{k_T}K^* - \dfrac{r_K K_T}{k_T K_K}K^{*2} + \\
\dfrac{2k_{KE}l_F K_T K^* T^* + \frac{\alpha k_{KE} l_F l_G K_T^2}{d_G}K^* T^{*2} + 3k_{KE}l_F K_T E^* T^* + \frac{3\alpha k_{KE} l_F l_G K_T^2}{d_G}E^* T^{*2}}{\left[\begin{array}{c} 3k_T e_{KE} d_F e_F + \frac{3k_T e_{KE} d_F K_T(\alpha e_F l_G + d_G)}{d_G}T^* + \frac{3\alpha k_T e_{KE} d_F l_G K_T^2}{d_G}T^{*2} \\ +2l_F k_T K_T^2 K^* T^* + \frac{\alpha l_F k_T l_G K_T^3}{d_G}K^* T^{*2} + 3l_F k_T K_T^2 E^* T^* \\ +\frac{3\alpha l_F k_T l_G K_T^3}{d_G}E^* T^{*2} \end{array}\right]} \\
\dfrac{dE^*}{dt^*} = \\
\dfrac{2k_{KE}l_F K_T K^* T^* + \frac{\alpha k_{KE} l_F l_G K_T^2}{d_G}K^* T^{*2} + 3k_{KE}l_F K_T E^* T^* + \frac{3\alpha k_{KE} l_F l_G K_T^2}{d_G}E^* T^{*2}}{\left(1+\frac{\beta l_P K_T}{d_P}T^*\right)\left[\begin{array}{c} 3k_T e_{KE} d_F e_F + \frac{3k_T e_{KE} d_F K_T(\alpha e_F l_G + d_G)}{d_G}T^* + \frac{3\alpha k_T e_{KE} d_F l_G K_T^2}{d_G}T^{*2} \\ +2l_F k_T K_T^2 K^* T^* + \frac{\alpha l_F k_T l_G K_T^3}{d_G}K^* T^{*2} + 3l_F k_T K_T^2 E^* T^* \\ +\frac{3\alpha l_F k_T l_G K_T^3}{d_G}E^* T^{*2} \end{array}\right]} \\
\qquad\qquad - \dfrac{d_E}{k_T}E^*
\end{cases}
\tag{3.12}
$$

Group constants together by making the substitutions indicated in Table 3.3.

Table 3.3: Substitutions

$u_1 = sl_I e_I(1 - \frac{K_N}{K_T})$	$u_2 = sl_I(\frac{e_I K_N}{K_T} - e_I + 8K_T - 8K_N)$
$u_3 = 8sl_I(K_N - K_T)$	$u_4 = e_I(e_T d_I + sl_I)$
$u_5 = (e_T d_I + 8sl_I)K_T$	$u_6 = d_T K_T$
$u_7 = k_T g_T$	$u_8 = k_T K_T$
$v_1 = \frac{r_K}{k_T}$	$v_2 = \frac{r_K K_T}{k_T K_K}$
$v_3 = k_{KE} l_F K_T$	$v_4 = \frac{\alpha k_{KE} l_F l_G K_T^2}{d_G}$
$v_5 = 3k_T e_{KE} d_F e_F$	$v_6 = \frac{3k_T e_{KE} d_F K_T(\alpha e_F l_G + d_G)}{d_G}$
$v_7 = \frac{3\alpha k_T e_{KE} d_F l_G K_T^2}{d_G}$	$v_8 = l_F k_T K_T^2$
$v_9 = \frac{\alpha l_F k_T l_G K_T^3}{d_G}$	$v_{10} = \frac{\beta l_P K_T}{d_P}$
$v_{11} = \frac{d_E}{k_T}$	

This gives the following simpler-looking system:

$$
\begin{cases}
\dfrac{dT^*}{dt^*} = \dfrac{u_1T^* + u_2T^{*2} + u_3T^{*3}}{u_4 + u_5T^*} - \dfrac{u_6K^*T^* + u_6E^*T^*}{u_7 + u_8T^*} \\[2ex]
\dfrac{dK^*}{dt^*} = v_1K^* - v_2K^{*2} + \dfrac{2v_3K^*T^* + v_4K^*T^{*2} + 3v_3E^*T^* + 3v_4E^*T^{*2}}{v_5 + v_6T^* + v_7T^{*2} + 2v_8K^*T^* + v_9K^*T^{*2} + 3v_8E^*T^* + 3v_9E^*T^{*2}} \\[2ex]
\dfrac{dE^*}{dt^*} = \dfrac{2v_3K^*T^* + v_4K^*T^{*2} + 3v_3E^*T^* + 3v_4E^*T^{*2}}{(1 + v_{10}T^*)(v_5 + v_6T^* + v_7T^{*2} + 2v_8K^*T^* + v_9K^*T^{*2} + 3v_8E^*T^* + 3v_9E^*T^{*2})} \\[2ex]
\qquad\qquad\qquad\qquad\qquad\qquad\qquad\qquad\qquad\qquad\qquad\qquad\qquad\qquad -v_{11}E^*
\end{cases}
\tag{3.13}
$$

Numerical tests revealed no change in the qualitative behavior of the system (see Figure 3.3).

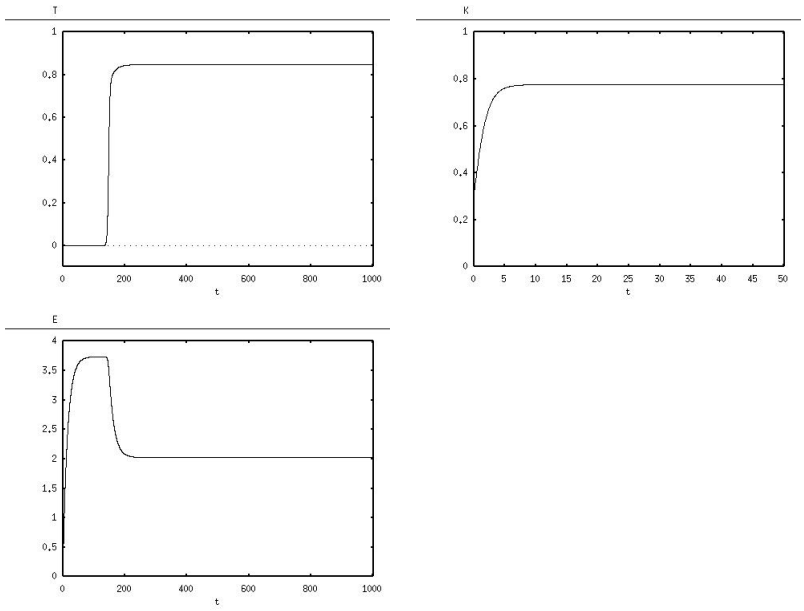

Figure 3.3: Plots of T^*, K^*, and E^* versus time t^*, using system (3.13). Note that the quantities have been scaled due to the nondimensionalization

3.5 Equilibria

When solving for equilibria, we must keep in mind that only the equilibria that lie in a valid region (all variables T, N, K, E, P, G, I, F non-negative, since they represent densities) are biologically valid. Therefore, when solving the system numerically, equilibria in which at least one variable is negative will be ignored. Similarly, complex equilibria will be ignored. Another thing to keep in mind is that due to unavoidable computational errors, such as *roundoff error* (error introduced by approximating a given number by a computer number [111]) and *truncation error* (error introduced by approximating a mathematical operation by computations directed by a program [111]), results obtained using a computer lose accuracy.

Using *Maple* to solve system (2.1) in Claim 3.1 which follows, resulted in a total of nineteen equilibria, only four of which were non-negative real numbers and thus lie in the valid region. Of these four, one of them was given by *Maple* as

$$\tilde{T} = 6.524858265 \times 10^7, \tilde{N} = -.0009483347431, \tilde{K} = 0, \tilde{E} = 0$$

$$\tilde{P} = 9.526450510 \times 10^9, \tilde{G} = 2.426996466 \times 10^7, \tilde{I} = 61599.30001, \tilde{F} = 0$$

However, the actual values of $\tilde{T}$ and $\tilde{N}$ should actually be

$$\tilde{T} = K_T = 7.7 \times 10^7 \text{ and } \tilde{N} = 0$$

Note that substituting these values of $\tilde{T}$ and $\tilde{N}$, along with the above values of $\tilde{K}, \tilde{E}, \tilde{P}, \tilde{G}, \tilde{I}, \tilde{F}$, into system (2.1) results in all derivatives being zero, and is therefore a valid equilibrium point. This result agrees with the corresponding equilibrium $\tilde{T^*} = 1, \tilde{K^*} = 0, \tilde{E^*} = 0$ of the nondimensional system (2.12) found in Claim 3.2, since $T^* = \dfrac{T}{K_T}$, so $T = K_T \implies T^* = 1$.

In the first claim which follows, we will find the equilibria of the original system (2.1) in case information is lost during the simplification process. Then, this result can be used to verify how accurately the nondimensional and/or reduced systems preserve the qualities of the original system. Only equilibria where $\tilde{T}, \tilde{N}, \tilde{K}, \tilde{E}, \tilde{P}, \tilde{G}, \tilde{I}, \tilde{F} \geq 0$ need to be considered.

Claim 3.1 *System (2.1), with parameter values from Table 2.2 (with* $g_T = 5 \times 10^9$*), contains the following four valid equilibria:*

1. $\tilde{T} = 0$, $\tilde{N} = 1.23 \times 10^7$, $\tilde{K} = 2.3 \times 10^7$,
   $\tilde{E} = 0$, $\tilde{P} = 0$, $\tilde{G} = 0$, $\tilde{I} = 7700$, $\tilde{F} = 0$

2. $\tilde{T} = 7.7 \times 10^7$, $\tilde{N} = 0$, $\tilde{K} = 0$, $\tilde{E} = 0$,
   $\tilde{P} = 9.526450510 \times 10^9$, $\tilde{G} = 2.426996466 \times 10^7$,
   $\tilde{I} = 61599.30001$, $\tilde{F} = 0$ *(see above explanation)*

3. $\tilde{T} = 0$, $\tilde{N} = 1.23 \times 10^7$, $\tilde{K} = 0$,
   $\tilde{E} = 0$, $\tilde{P} = 0$, $\tilde{G} = 0$, $\tilde{I} = 7700$, $\tilde{F} = 0$

4. $\tilde{T} = 6.524858265 \times 10^7$, $\tilde{N} = 1.877174457 \times 10^6$,
   $\tilde{K} = 5.987613009 \times 10^7$, $\tilde{E} = 1.558762754 \times 10^8$,
   $\tilde{P} = 8.072563553 \times 10^9$, $\tilde{G} = 2.056598435 \times 10^7$,
   $\tilde{I} = 6.159917394 \times 10^4$, $\tilde{F} = 2.292678211$

Proof: Substitute parameter values into system (2.1) and set the equations equal to zero.

$$\begin{cases} \dfrac{.44I(1-1.298701299\times10^{-8}T-1.298701299\times10^{-8}N)T}{2\times10^4+I}-\dfrac{(K+E)T}{5\times10^9+T}=0 \\ 983.77-7.998130081\times10^{-5}N-1.277623377\times10^{-5}T=0 \\ .09(1-4.347826087\times10^{-8}K)K+\dfrac{8.64\times10^6F}{70+F}=0 \\ \dfrac{8.64\times10^6F}{(70+F)(1+1.05\times10^{-10}P)}-.03E=0 \\ 14.5T-.1172P=0 \\ .0892T-.283G=0 \\ 7.7\times10^4+\dfrac{5.39\times10^5T}{1000+T}-10I=0 \\ \dfrac{50\left(\dfrac{K}{3}+\dfrac{K}{3+3.99\times10^{-6}G}+E\right)T}{1000+T}-2.16F=0 \end{cases} \tag{3.14}$$

Solving [1] the above system of equations results in the four valid equilibria stated in the claim. □

[1] *Maple* was used to aid in some of the calculations.

The first equilibrium is a tumor-free steady state of the system and is a good starting point for the model. It can be interpreted medically as the initial state of a healthy patient before the disease. It shows that the number of adaptive immune cells E is 0 because those adaptive immune cells that are circulating in the body at the onset of the disease do not recognize the cancer cells and can be disregarded. Only the new E cells are specifically created to target the cancer cells. The $\tilde{K}$ corrresponding to this equilibrium is the value used for $K(0)$.

The fourth equilibrium is tumor-positive. This equilibrium agrees with the plots in Figure 3.2.

As mentioned in Section 1.3, MGUS is characterized by an increase in M-protein due to an increase in plasma cells. As mentioned in Chapter 2, not all patients with MGUS develop MM (only a small fraction do). However, a person with more than 10% plasma cells is characterized as having MM. This is equivalent to a plasma cell density of 7.7×10^7, as calculated in Section 2.2. The above tumor-positive equilibrium gives a total plasma cell density (T and N cells) of approximately 6.7×10^7, which is less than this amount. Therefore, the above tumor-positive equilibrium can be interpreted as the person having MGUS.

The original system (2.1) contains eight equations and is too complicated to make studying the above equilibria possible. Therefore, to analyze the stability of the equilibria, it will be necessary to work with a simpler system.

Next, we find the equilibria of the full nondimensional system (2.12).

Claim 3.2 *System (2.12), with parameter values from Table 2.2 (with $g_T = 5 \times 10^9$), contains the following four valid equilibria:*

1. $\tilde{T}^* = 0$, $\tilde{N}^* = .1597402597$, $\tilde{K}^* = .2987012987$,
   $\tilde{E}^* = 0$, $\tilde{P}^* = 0$, $\tilde{G}^* = 0$, $\tilde{I}^* = 1$, $\tilde{F}^* = 0$

2. $\tilde{T}^* = 1$, $\tilde{N}^* = 0$, $\tilde{K}^* = 0$, $\tilde{E}^* = 0$, $\tilde{P}^* = 1$,
   $\tilde{G}^* = 1$, $\tilde{I}^* = 7.999909092$, $\tilde{F}^* = 0$

3. $\tilde{T}^* = 0$, $\tilde{N}^* = .1597402597$, $\tilde{K}^* = 0$,
   $\tilde{E}^* = 0$, $\tilde{P}^* = 0$, $\tilde{G}^* = 0$, $\tilde{I}^* = 1$, $\tilde{F}^* = 0$

4. $\tilde{T}^* = .8473841904$, $\tilde{N}^* = .02437888906$,
   $\tilde{K}^* = .7776120792$, $\tilde{E}^* = 2.024367213$,
   $\tilde{P}^* = .8473841904$, $\tilde{G}^* = .8473841904$,
   $\tilde{I}^* = 7.999892719$, $\tilde{F}^* = 2.292678211$

Proof: Substitute parameter values into system (2.12) and set the equations equal to zero.

$$\begin{cases} \dfrac{I^*(1-T^*-N^*)T^*}{2.597402597+I^*} - \dfrac{2.272727273(K^*+E^*)T^*}{64.93506494+T^*} = 0 \\ \\ 2.904368358\times 10^{-5} - 1.818181818\times 10^{-4}N^* - 2.904368358\times 10^{-5}T^* = 0 \\ \\ .2045454545(1-3.347826087K^*)K^* + \dfrac{.2550177096F^*}{3.927272727\times 10^{-8}+F^*} = 0 \\ \\ \dfrac{.2550177096F^*}{(3.927272727\times 10^{-8}+F^*)(1+1.000277304P^*)} - .06818181818E^* = 0 \\ \\ .2663636364T^* - .2663636364P^* = 0 \\ \\ .6431818182T^* - .6431818182G^* = 0 \\ \\ 22.72727273 + \dfrac{159.0909091T^*}{1.298701299\times 10^{-5}+T^*} - 22.72727273I^* = 0 \\ \\ \dfrac{4.909090909T^*\left(\dfrac{K^*}{3}+\dfrac{K^*}{3+96.83715900G^*}+E^*\right)}{1.298701299\times 10^{-5}+T^*} - 4.909090909F^* = 0 \end{cases} \tag{3.15}$$

Solving [2] the above system of equations results in the four valid equilibria stated in the claim. □

[2] *Maple* was used to aid in some of the calculations.

The accuracy of these results were verified several ways. First, the nondimensionalization in Table 2.6 that was used before was applied to the equilibria found for the original system in Claim 3.1 and values very close to these were obtained. Then, these equilibrium values were substituted into the equations of system (2.12) and results very close to zero were obtained, indicating that they are indeed equilibria (taking into account the fact that some computational error will always exist, as mentioned earlier).

Next, we find the equilibria of the nondimensional reduced system (3.13).

Claim 3.3 *System (3.13), with parameter values from Table 2.2 (with* $g_T = 5 \times 10^9$*), contains the following four valid equilibria:*

1. $\tilde{T}^* = 0$, $\tilde{K}^* = .2987012986$, $\tilde{E}^* = 0$
2. $\tilde{T}^* = 1$, $\tilde{K}^* = 0$, $\tilde{E}^* = 0$
3. $\tilde{T}^* = 0$, $\tilde{K}^* = 0$, $\tilde{E}^* = 0$
4. $\tilde{T}^* = .8473841905$, $\tilde{K}^* = .7776120789$, $\tilde{E}^* = 2.024367212$

Proof: Substitute parameter values into system (3.13) and set the equations equal to zero.

$$
\begin{cases}
\dfrac{6.47\times10^{7}T^{*}+3.985513530\times10^{13}T^{*2}-3.98552\times10^{13}T^{*3}}{2.77\times10^{8}+6.2832\times10^{13}T^{*}}- \\
\qquad\qquad \dfrac{7.7\times10^{7}K^{*}T^{*}+7.7\times10^{7}E^{*}T^{*}}{2.2\times10^{9}+3.388\times10^{7}T^{*}}=0 \\
\\
.2045454545K^{*}-.6847826087K^{*2}+ \\
\\
\dfrac{\begin{bmatrix} 6.6528\times10^{16}K^{*}T^{*}+1.073730419\times10^{18}K^{*}T^{*2} \\ +9.9792\times10^{16}E^{*}T^{*}+3.221191257\times10^{18}E^{*}T^{*2} \end{bmatrix}}{\begin{bmatrix} 1.99584\times10^{5}+1.537441038\times10^{10}T^{*} \\ +4.960634538\times10^{11}T^{*2}+2.60876\times10^{17}K^{*}T^{*} \\ +4.210415117\times10^{18}K^{*}T^{*2}+3.91314\times10^{17}E^{*}T^{*} \\ +1.263124535\times10^{19}E^{*}T^{*2} \end{bmatrix}}=0 \\
\\
\dfrac{\begin{bmatrix} 6.6528\times10^{16}K^{*}T^{*}+1.073730419\times10^{18}K^{*}T^{*2} \\ +9.9792\times10^{16}E^{*}T^{*}+3.221191257\times10^{18}E^{*}T^{*2} \end{bmatrix}}{(1+1.000277304T^{*})\begin{bmatrix} 1.99584\times10^{5}+1.537441038\times10^{10}T^{*} \\ +4.960634538\times10^{11}T^{*2}+2.60876\times10^{17}K^{*}T^{*} \\ +4.210415117\times10^{18}K^{*}T^{*2}+3.91314\times10^{17}E^{*}T^{*} \\ +1.263124535\times10^{19}E^{*}T^{*2} \end{bmatrix}} \\
\\
-.06818181818E^{*}=0
\end{cases}
\tag{3.16}
$$

Solving [3] the above system of equations results in the four valid equilibria stated in the claim. □

The accuracy of these results were verified several ways. First, the above equilibria was compared with the equilibria found in Claim 3.2 for the full nondimensional system (2.12) and the values were very close. Then, these equilibrium values were substituted into the equations of system (3.13) and results very close to zero were obtained. Also, note that these equilibria agree with the plots in Figure 3.3.

Therefore, the nondimensional reduced system (3.13) together with its equilibria just found above in Claim 3.3 will be used in the sability analysis which follows.

Another advantage to working with the reduced system, besides making it easier to handle analytically, is that being three-dimensional makes it possible to plot null-surfaces. By the T, K and E null-surface (asterisks omitted to simplify the notation), we mean the surface generated by plotting the values of T^*, K^* and E^*, where $\frac{dT^*}{dt^*} = 0$, $\frac{dK^*}{dt^*} = 0$ and $\frac{dE^*}{dt^*} = 0$, respectively. The intersection of all three null-surfaces indicates where equilibria exist (see Figure 3.4). The plot of the intersection of all three null-surfaces in still somewhat difficult to interpret. To simplify this, we can consider the intersection of two null-surfaces at a time. There are three possible pairs. Each intersection of two null-surfaces results in one or more curves in three-dimensional space.

[3] *Maple* was used to aid in some of the calculations.

Therefore, the points where these resulting three sets of curves intersect correspond to equilibrium points (see Figure 3.5). Figures 3.4 and 3.5 agree with the equilibria obtained in Claim 3.3.

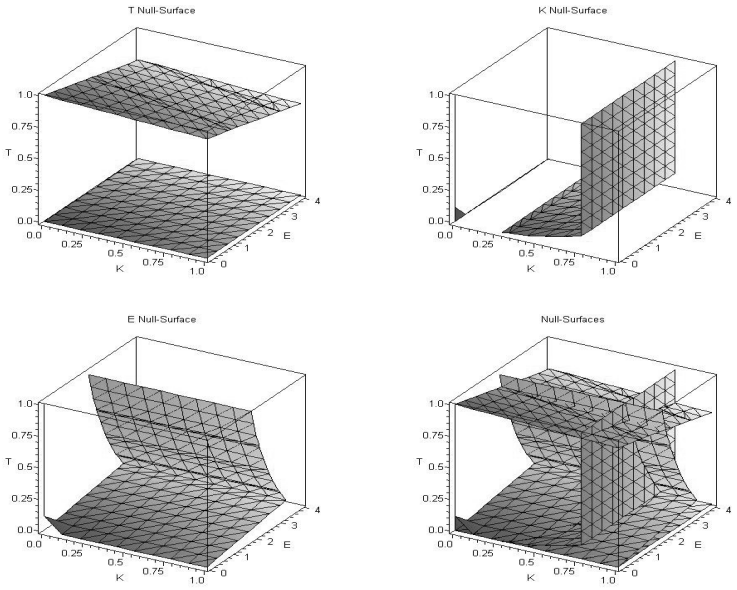

Figure 3.4: Plots of T, K and E null-surfaces of system (3.13) and the intersection of all three, which indicates where equilibria exist, generated using *Maple*. Some points which lie on an axis, such as $(T^*, K^*, E^*) = (T^*, 0, 0)$ and $(0, 0, E^*)$ on the K null-surface and $(T^*, K^*, E^*) = (T^*, 0, 0)$ and $(0, K^*, 0)$ on the E null-surface, do not clearly appear on the graphs.

3.6 Stability Analysis

Consider the following notation:

$$\vec{X} = (T^*, K^*, E^*)^T$$

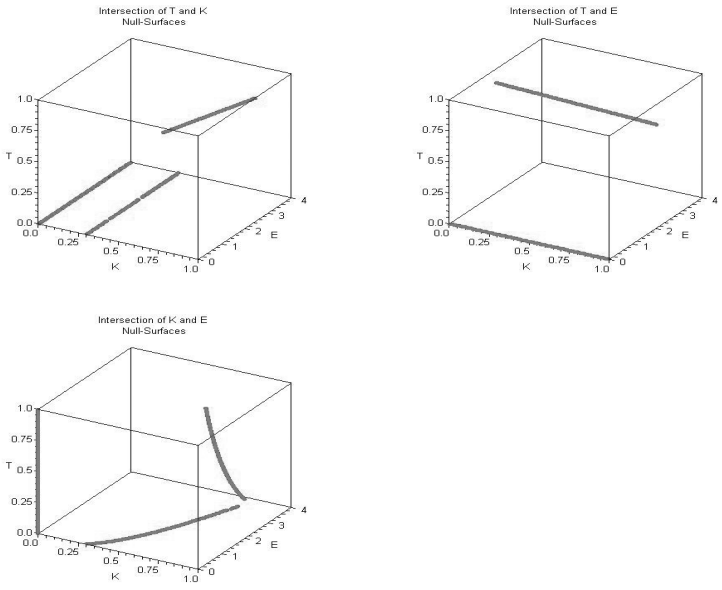

Figure 3.5: Plots of resulting curves from intersections of pairs of null surfaces from Figure 3.4, generated using *Maple*. The intersection of all three graphs indicates where equilibria exist. Point $(T^*, K^*, E^*) = (1, 0, 0)$ does not clearly appear on the graphs.

$$\vec{f}(\vec{X}) = (f_1(\vec{X}), f_2(\vec{X}), f_3(\vec{X}))^T$$

where the T superscript indicates *transpose* and

$$f_1 = \frac{u_1 T^* + u_2 T^{*2} + u_3 T^{*3}}{u_4 + u_5 T^*} - \frac{u_6 K^* T^* + u_6 E^* T^*}{u_7 + u_8 T^*} \ ,$$

$$f_2 = v_1 K^* - v_2 K^{*2} +$$

$$\frac{2v_3 K^* T^* + v_4 K^* T^{*2} + 3v_3 E^* T^* + 3v_4 E^* T^{*2}}{v_5 + v_6 T^* + v_7 T^{*2} + 2v_8 K^* T^* + v_9 K^* T^{*2} + 3v_8 E^* T^* + 3v_9 E^* T^{*2}}$$

and

$$f_3 = \frac{2v_3K^*T^* + v_4K^*T^{*2} + 3v_3E^*T^* + 3v_4E^*T^{*2}}{(1+v_{10}T^*)(v_5 + v_6T^* + v_7T^{*2} + 2v_8K^*T^* + v_9K^*T^{*2} + 3v_8E^*T^* + 3v_9E^*T^{*2})}$$

$$-v_{11}E^*$$

Using the above notation, system (3.13) can be written

$$\dot{\vec{X}} = \vec{f}(\vec{X}), \tag{3.17}$$

where the dot denotes differentiation.

In order to determine the local stability of the nonlinear system (3.17) (and hence system (3.13)) at each equilibrium point, the system must first be linearized by calculating the *Jacobian* matrix $J = (a_{ij})$, where $a_{ij} = \dfrac{\partial f_i}{\partial X_j}$ and $i, j \in \{1, 2, 3\}$, and evaluating it at each equilibrium value.

By *Hartman's Theorem* (see [81]), in a small neighborhood about a *hyperbolic* (eigenvalues of $J\mid_{(\tilde{T^*},\tilde{K^*},\tilde{E^*})}$ have nonzero real parts) equilibrium point $(\tilde{T^*}, \tilde{K^*}, \tilde{E^*})$, the phase portraits of the nonlinear system (3.17) and the linearized system

$$\dot{\vec{X}} = A\vec{X} \ ,$$

where

$$A = J\,|_{(\tilde{T^*},\tilde{K^*},\tilde{E^*})}\ ,$$

are qualitatively equivalent.

Therefore, the local stability of system (3.13) can be determined by looking at the eigenvalues λ of A. The eigenvalues are found by solving the *characteristic equation* $det(A - \lambda I) = \vec{0}$ for λ. By substituting each eigenvalue λ into $(A - \lambda I)\vec{v} = \vec{0}$, the corresponding eigenvector $\vec{v}$ can be obtained.

For each eigenvalue, the corresponding eigenvector gives information on the direction of the *stable* (if $\lambda < 0$) or *unstable* (if $\lambda > 0$) *subspace* of the linearized system. In a small neighborhood about each equilibrium point, the *stable* and *unstable manifolds* of the nonlinear system are tangent to the *stable* and *unstable subspaces*, respectively.

Proposition 3.1 *The local stability of the equilibria* $(\tilde{T^*}, \tilde{K^*}, \tilde{E^*})$ *given in Claim 3.3 and pertaining to system (3.13) is as follows:*

1. *(0,.2987012986,0) is a saddle point.*
2. *(1,0,0) is a saddle point.*
3. *(0,0,0) is a saddle point.*
4. *(.8473841905,.7776120789,2.024367212) is a stable node.*

Proof: Solve for and evaluate [4] the Jacobian at each equilibrium point and find the corresponding eigenvalues to determine the stability of each equilibrium.

[4] *Matlab* was used to aid in some of the calculations.

1. $J\,|_{(0,.2987012986,0)}=$

$$\begin{pmatrix} .2231194617692166 & 0 & 0 \\ 9.956709953333331 \times 10^{10} & -.2045454544067193 & 0 \\ 9.956709953333331 \times 10^{10} & 0 & -.06818181818181818 \end{pmatrix}$$

The matrix is triangular, so the eigenvalues are the diagonal entries. The eigenvalues and corresponding eigenvectors of the linearized system are

$\lambda_1 = -.06818181818181818 < 0$, $\vec{v_1} = (0,0,1)^T$

$\lambda_2 = -.2045454544067193 < 0$, $\vec{v_2} = (0,1,0)^T$

$\lambda_3 = .2231194617692166 > 0$,

$\vec{v_3} = (2.418034022990183 \times 10^{-12}, .5629562424592380, .8264867022984553)^T$

The eigenvalues $\lambda_1, \lambda_2 < 0$ and $\lambda_3 > 0$, so the equilibrium is a saddle point.

2. $J\,|_{(1,0,0)}=$

$$\begin{pmatrix} -.6343119588042305 & -.03446917470947410 & -.03446917470947410 \\ 0 & 2.229514392625560 \times 10^{6} & 6.493422163348529 \times 10^{6} \\ 0 & 1.114602552303918 \times 10^{6} & 3.246260913313697 \times 10^{6} \end{pmatrix}$$

The eigenvalues and corresponding eigenvectors are

$\lambda_1 = -.6343119588042305 < 0$, $\vec{v_1} = (1, 0, 0)^T$

$\lambda_2 = .0935019357129931 > 0$,

$\vec{v_2} = (.02940069473617550, -.9453940772606504, .3246007360273754)^T$

$\lambda_3 = 5.475775212437321 \times 10^6 > 0$,

$\vec{v_3} = (8.445268167641915 \times 10^{-9}, -.8944519985834053, -.4471639768923160)^T$

The eigenvalues $\lambda_1 < 0$ and $\lambda_2, \lambda_3 > 0$, so the equilibrium is a saddle point.

3.

$$J\,|_{(0,0,0)} = \begin{pmatrix} .2335740072202166 & 0 & 0 \\ 0 & .2045454545454546 & 0 \\ 0 & 0 & -.06818181818181818 \end{pmatrix}$$

The eigenvalues and corresponding eigenvectors are

$\lambda_1 = -.06818181818181818 < 0$, $\vec{v_1} = (0, 0, 1)^T$

$\lambda_2 = .2045454545454546 > 0$, $\vec{v_2} = (0, 1, 0)^T$

$\lambda_3 = .2335740072202166 > 0$, $\vec{v_3} = (1, 0, 0)^T$

The eigenvalues $\lambda_1 < 0$ and $\lambda_2, \lambda_3 > 0$, so the origin is a saddle point.

4. $J\,|_{(.8473841905,.7776120789,2.024367212)} =$

$$\begin{pmatrix} a_{11} & a_{12} & a_{13} \\ a_{21} & a_{22} & a_{23} \\ a_{31} & a_{32} & a_{33} \end{pmatrix}$$

where

$a_{11} = -.5362583205138792$

$a_{12} = -.02927639797282682$

$a_{13} = -.02927639797282682$

$a_{21} = -1.975175578650124 \times 10^{-11}$

$a_{22} = -.8604450006818201$

$a_{23} = 1.905322649653485 \times 10^{-9}$

$a_{31} = -.07472498343299178$

$a_{32} = 3.558675680526147 \times 10^{-10}$

$a_{33} = -.06818181715058691$

The eigenvalues and corresponding eigenvectors are

$\lambda_1 = -.5408863245448642 < 0,$

$\vec{v_1} = (.9877348054682283, 8.699157782163793 \times 10^{-10}, .1561408148647922)^T$

$\lambda_2 = -.06355381313417109 < 0,$

$\vec{v_2} = (.06181538238174657, -2.387904275840206 \times 10^{-9}, -.9980876006147950)^T$

$\lambda_3 = -.8604450006672509 < 0,$

$\vec{v_3} = (-.09070422940445617, -.9958411286164547, -.008555075923067444)^T$

The eigenvalues $\lambda_1, \lambda_2, \lambda_3 < 0$, so the equilibrium is a stable node.

□

Refer to Figure 3.6, where several trajectories corresponding to system (3.13), have been plotted.

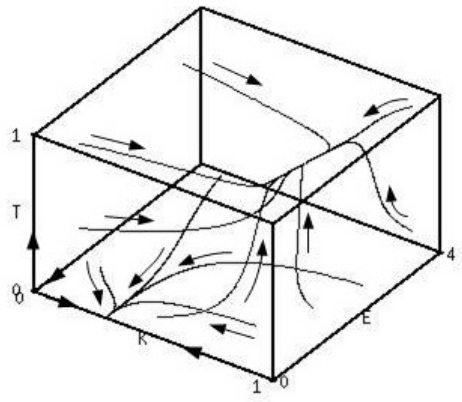

Figure 3.6: Plot of several trajectories of system (3.13) generated using *XPPAUT*. The arrows indicate the direction of the flow. The initial values off the coordinate axes are (T^*, K^*, E^*)=(0,.9,2.7), (0,.75,1), (0,.1,1), (0,.1,3.9), (.9,.1,3), (.9,.1,.5), (.2,.01,1), (.1,.5,.1), (.1,.9,1.5), (.1,.9,3.9), and (.9,.9,3.9).

3.7 The Effects of Varying Parameters

To facilitate calculating equilibria and their stability, the nondimensional reduced system (3.13) will be used from now on. In this system, parameters were grouped together to simplify the notation. the $u's$ and $v's$ have the original parameters embedded in them. When parameters are varied in the discussion which follows, we refer to the original parameters and let the computer do the necessary substitutions into the $u's$ and $v's$ of the system.

Certain parameters that are thought to play an important role in the development of the disease were varied numerically in order to observe how strong of an influence they have on the dynamics of the system. However, if most parameters are varied by a large enough amount, something is bound to happen. So the difficulty lies in determining what is a reasonable amount of variation for each parameter. Assuming

that the original parameter values used are relatively accurate, we did not want to vary them so much that they would become medically unrealistic. The following approach was taken. Unless there was a reason to believe that the original parameter value was unreliable, such as the case with g_T, parameters were only varied a relatively small amount. In the next section, when we search for bifurcations, parameter values will similarly be restricted to a certain range to make sure they remain realistic.

Each parameter in question was varied and plots of T^* vs t^* were generated, and when necessary, equilibria were calculated. The results fall into one of three groups.

The first group includes those parameters which have either no perceivable or very little effect on the system. The following fall into this group:

l_F - rate of $IFN-\gamma$ production by immune cells

l_P - M-protein production rate

d_P - M-protein degradation rate

l_G - tumor-derived glycolipid production rate

d_G - tumor-derived glycolipid degradation rate

$IFN-\gamma$ attracts immune cells to the tumor site. Therefore, when l_F was increased, a significant decrease in tumor density was expected. However, this did not

happen. Even when l_F was increased from the default value of 50 to 250, no perceivable change was observed in the plot.

M-protein causes a deletion of certain $CD4^+T$ cells and hence is a mechanism which supports tumor progression. Therefore, we expected that varying l_P and d_P, which control P, would alter the outcome noticeably. Varying these parameters would require varying β as well, since they are related, as explained later. However, instead of varying the parameters which control P, we decided to let P be identically zero ($P \equiv 0$) in the original system (2.1). This produced very little change (see Figure 3.7).

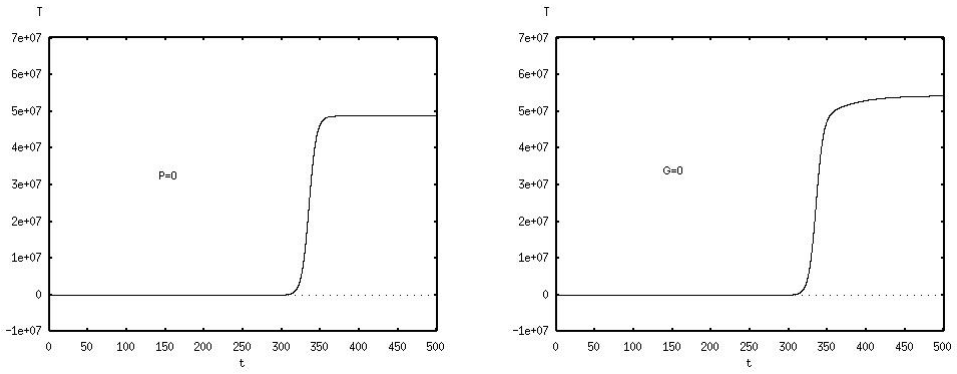

Figure 3.7: Plots of T vs t resulting from setting $P \equiv 0$ and $G \equiv 0$, respectively, in system (2.1).

Tumor-derived glycolipids cause a disruption in $IFN-\gamma$ production by NKT cells. Therefore, we expected that varying l_G and d_G, which control G, would alter the outcome noticeably. Varying these parameters would require varying α as well, since they are related, as explained later. However, as in the case above, we decided to instead let G be identically zero ($G \equiv 0$) in the original system (2.1). In this case also, very little change was observed (see Figure 3.7).

Surprisingly, it can be concluded from the above numerical experiments that the production of $IFN - \gamma$, M-protein and tumor-derived glycolipids do not play as important a role in the development of MGUS/MM as expected.

The second group includes those parameters which seem to simply delay or speed up the time at which the rapid increase in tumor cells occurs. This is important, since the disease occurs late in life, so a long enough delay in the increase in tumor cells can be almost as good as a cure. The following parameter falls into this group:

r_K - proliferation rate of innate immune system cells

Parameter r_K is related to K_K as explained in Section 2.1 and this dependency must be observed if either is varied.

$K_K = \frac{r_K}{c}$, where $c > 0$

Using the default values $K_K = 2.30 \times 10^7$ and $r_K = .09$ gives $c = 3.91 \times 10^{-9}$. Therefore, we get

$K_K = \frac{r_K}{3.91 \times 10^{-9}}$, or equivalently, $r_K = 3.91 \times 10^{-9} K_K$

Increasing r_K from its default value of .09 to .45, and hence increasing K_K from 2.30×10^7 to 1.15×10^8, delays the time at which the increase in tumor cells occurs and the density of tumor cells levels off at a lower number (see Figure 3.8).

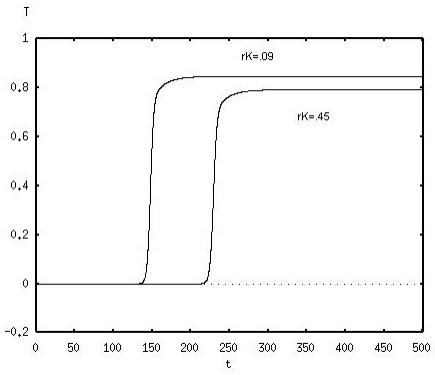

Figure 3.8: Plots of T^* vs t^* resulting from varying parameter r_K in system (3.13).

The third group includes those parameters which affect the dynamics significantly by, for instance, seemingly eliminating or creating an equilibrium in the (non-negative) valid region. The following parameters fall into this group:

g_T - half-saturation constant

d_T - rate of destruction of tumor cells by the immune system

k_T and K_T - proliferation rate and carrying capacity of tumor cells

k_{KE} - recruitment rate of immune cells

l_I - rate of $IL-6$ production by stromal cells

The effect that varying g_T has on the system was briefly addressed in Section 3.2. In that section we discussed why the original value used, 1×10^5, was suspected of being inaccurate and gave reasons why 5×10^9 might be more realistic. Since we have no medical evidence to support either choice, we will explore the entire range of possibilities between these two values. A plot of T vs t as g_T is varied in the original system (2.1) is given in Figure 3.1. As g_T was decreased from 5×10^9 to 3.5×10^9, the increase in T occurred at a later time. When it was decreased further to 3.4×10^9, the tumor growth seemed to be almost 0. And the same occurred when it was decreased to 1×10^5. However, calculating the equilibria revealed that $g_T = 3.4 \times 10^9$ and $g_T = 1 \times 10^5$ produced different results.

$g_T = 3.4 \times 10^9$ gave the following tumor-positive equilibrium:

$$\tilde{T} = 5.924491790 \times 10^7,\ \tilde{N} = 2.836201424 \times 10^6,$$
$$\tilde{K} = 5.987613010 \times 10^7,\ \tilde{E} = 1.627460770 \times 10^8,$$
$$\tilde{P} = 7.329789331 \times 10^9,\ \tilde{G} = 1.867366317 \times 10^7,$$
$$\tilde{I} = 61599.09023,\ \tilde{F} = 4.247088114 \times 10^9$$

This equilibrium is similar to the one obtained with the default parameter values, except with this new value of g_T, the time at which the rapid increase in tumor cells occurs is delayed and the density of tumor cells levels off at a lower number.

However, when $g_T = 1 \times 10^5$, no tumor positive equilibrium exits. So g_T has a threshold effect on the density of tumor cells, as suspected.

In the next section, when we look for possible bifurcations, this parameter will be studied in greater detail using the nondimensional reduced system (3.13).

As d_T was increased from 1 to 1.4, the increase in T^* occurred at a later time. And when d_T was increased to 1.5 or 2, the tumor growth seemed to be almost 0 (see Figure 3.9).

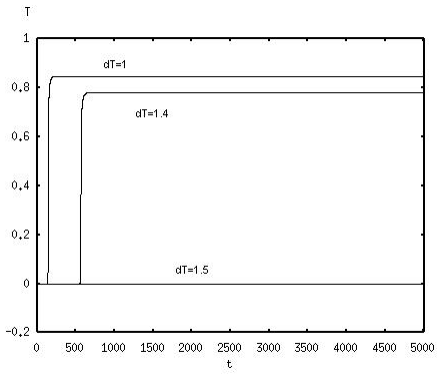

Figure 3.9: Plots of T^* vs t^* resulting from varying parameter d_T in system (3.13).

However, it was not clear if extending the graph far enough would result in T^* decreasing to zero eventually or increasing rapidly at some point. Therefore, the equilibria of the system was calculated as in Claim 3.1 and it was determined that the tumor-positive equilibrium in question still existed but had a lower tumor density and the following two new tumor-positive equilibria were obtained:

Equilibria at $d_T = 1.5$:

1. $\tilde{T^*} = 7.01659550110 \times 10^{-12}$,
   $\tilde{K^*} = .7725393882$,

$\tilde{E}^* = 3.676501469$

2. $\tilde{T}^* = 4.01156838110 \times 10^{-8}$,
   $\tilde{K}^* = .7776111965$,
   $\tilde{E}^* = 3.740248389$

Similarly, $d_T = 2$ gave the following equilibria:

1. $\tilde{T}^* = 3.999713833 \times 10^{-13}$,
   $\tilde{K}^* = .6844998498$,
   $\tilde{E}^* = 2.652272201$

2. $\tilde{T}^* = .1145964401 \times 10^{-5}$,
   $\tilde{K}^* = .7776120504$,
   $\tilde{E}^* = 3.740255028$

Parameter k_T is related to K_T as explained in Section 2.1 and this dependency must be observed if either is varied.

$K_T = \frac{k_T}{c}$, where $c > 0$

Using the default values $K_T = 7.7 \times 10^7$ and $k_T = .44$ gives $c = 5.71 \times 10^{-9}$. Therefore, we get

$K_T = \frac{k_T}{5.71 \times 10^{-9}}$, or equivalently, $k_T = 5.71 \times 10^{-9} K_T$

Also, α and β depend on K_T as follows (see Section 2.2):

$$\alpha = \frac{32.33 d_G}{l_G K_T}$$

and

$$\beta = \frac{d_P}{l_P K_T}$$

We have an estimate of how high K_T can go. In Section 2.2, we stated that K_T can go as high as 7.68×10^8, the bone marrow carrying capacity.

Therefore, increasing K_T from a default value of 7.7×10^7 to 7.68×10^8 and hence k_T from .44 to 4.39, α from 1.33×10^{-6} to 1.34×10^{-7} and β from 1.05×10^{-10} to 1.05×10^{-11}, makes the increase in tumor cells occur earlier and the density of tumor cells levels off at a higher number (see Figure 3.10). This results in a total bone marrow plasma cell content of approximately 10%, the threshold that distinguishes MGUS from MM. So only increasing parameter K_T will not result in MM.

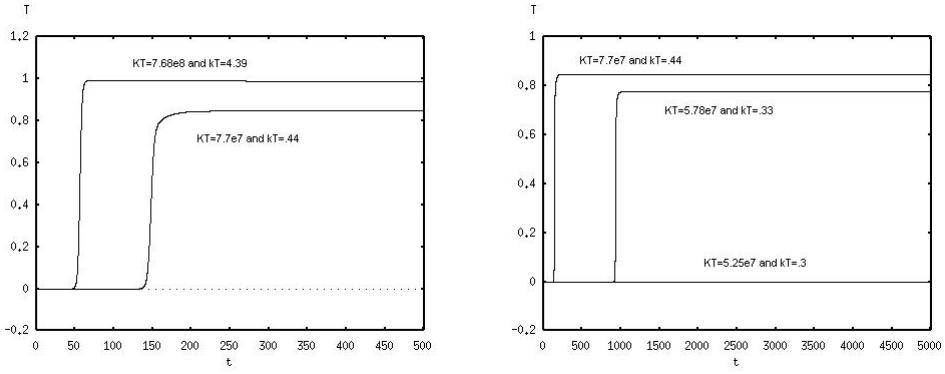

Figure 3.10: Plots of T^* vs t^* resulting from varying parameters k_T and K_T in system (3.13).

Next, k_T was decreased from .44 to .33 (and the corresponding changes in K_T, α and β were made). This resulted in the increase in T^* occurring at a later time. And when k_T was decreased to .3 or .1, the tumor growth seemed to be almost 0 (see Figure 3.10) . However, it was not clear if extending the graph far enough would result in T^* decreasing to zero eventually or increasing rapidly at some. Therefore, the equilibria of the system was calculated and it was determined that, when $k_T = .3$, the tumor-positive equilibrium in question still existed but had a lower tumor density and, when $k_T = .1$, it disappeared. Also, the tumor-free equilibrium that was originally at $(0, .2987012986, 0)$ shifted to a higher K^* density. For both of these values of k_T, the following new tumor-positive equilibria were obtained:

Equilibria at $k_T = .3$:

1. $\tilde{T^*} = 1.898034954 \times 10^{-12}$,
   $\tilde{K^*} = 1.099664608$,
   $\tilde{E^*} = 4.981823757$

2. $\tilde{T^*} = 3.561606134 \times 10^{-7}$,
   $\tilde{K^*} = 1.140497505$,
   $\tilde{E^*} = 5.485709575$

Letting $k_T = .1$ gave only one new equilibrium:

$\tilde{T^*} = 2.787639164 \times 10^{-13}$,
$\tilde{K^*} = 1.545264235$,
$\tilde{E^*} = .8147151941$

As k_{KE} was increased from 8.64×10^6 to 1.3×10^7, the increase in T^* occurred at a later time. And when k_{KE} was increased to 1.4×10^7 or 1×10^8, the tumor growth seemed to be almost 0 (see Figure 3.11).

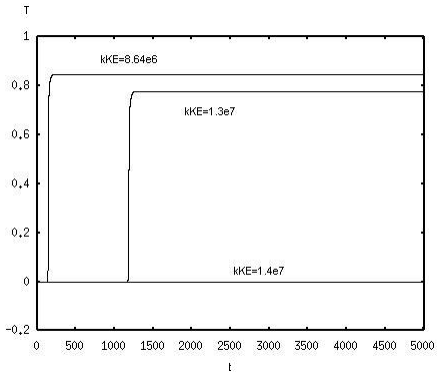

Figure 3.11: Plots of T^* vs t^* resulting from varying parameter k_{KE} in system (3.13).

However, it was not clear if extending the graph far enough would result in T^* decreasing to zero eventually or increasing rapidly at some point. Therefore, the equilibria of the system was calculated and it was determined that, when $k_{KE} = 1.4 \times 10^7$, the tumor-positive equilibrium in question still existed but had a lower tumor density and, when $k_{KE} = 1 \times 10^8$, it disappeared. For both of these values of k_{KE} the following new tumor-positive equilibria were obtained:

Equilibria at $k_{KE} = 1.4 \times 10^7$:

1. $\tilde{T^*} = 1.49711272110 \times 10^{-12}$,
   $\tilde{K^*} = .9207731158$,
   $\tilde{E^*} = 5.752773836$

2. $\tilde{T}^* = 1.29792448210 \times 10^{-7}$,

   $\tilde{K}^* = .9403893496$,

   $\tilde{E}^* = 6.060601677$

Letting $k_{KE} = 1 \times 10^8$ gave only one new equilibrium:

$\tilde{T}^* = 1.227738279 \times 10^{-14}$,

$\tilde{K}^* = .9207728820$,

$\tilde{E}^* = 5.752770213$

Parameter l_I was first increased from its default value of 1 to 5. This resulted in the increase in tumor cells occurring earlier and the density of tumor cells to level off at a higher number (see Figure 3.12).

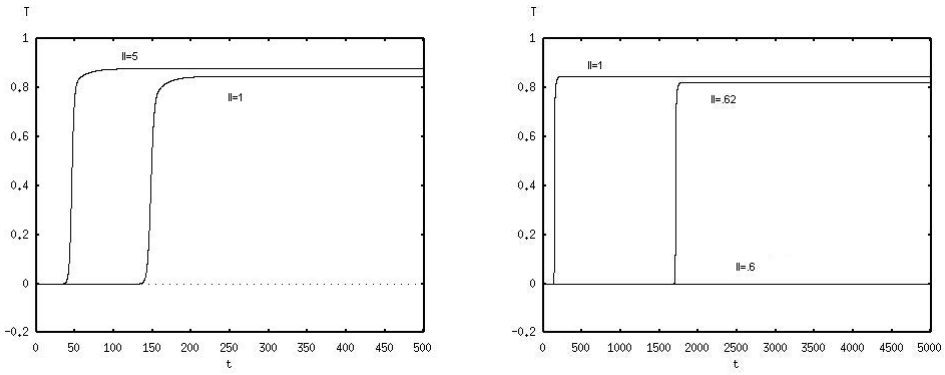

Figure 3.12: Plots of T^* vs t^* resulting from varying parameter l_I in system (3.13).

Next, as l_I was decreased from 1 to .62, the increase in T^* occurred at a later time. And when l_I was decreased to .6 or .5, the tumor growth seemed to be almost 0 (see Figure 3.12).

However, it was not clear if extending the graph far enough would result in T^* decreasing to zero eventually or increasing rapidly at some point. Therefore, the equilibria of the system was calculated and it was determined that the tumor-positive equilibrium in question still existed but had a lower tumor density and the following two new tumor-positive equilibria were obtained:

Equilibria at $l_I = .6$:

1. $\tilde{T}^* = 3.791368189 \times 10^{-11}$,
   $\tilde{K}^* = .7766753865$,
   $\tilde{E}^* = 3.728447560$
2. $\tilde{T}^* = 6.470583845 \times 10^{-9}$,
   $\tilde{K}^* = .7776065957$,
   $\tilde{E}^* = 3.740190453$

Similarly, $l_I = .5$ gave the following equilibria:

1. $\tilde{T}^* = 7.444163268 \times 10^{-13}$,
   $\tilde{K}^* = .7286753968$,
   $\tilde{E}^* = 3.146737707$
2. $\tilde{T}^* = 3.902477620 \times 10^{-7}$,
   $\tilde{K}^* = .7776119904$,

$\tilde{E}^* = 3.740257098$

Therefore, the the parameters, g_T, d_T, k_T (and K_T), k_{KE} and l_I need to be analyzed in greater detail, as they might possibly be bifurcation parameters.

As mentioned earlier, the system has a total of nineteen equilibria. However, many are not biologically valid because either they lie in a region where at least one of the variables, T^*, K^*, or E^*, which represent cell densities, is negative, or the equilibrium is complex. When certain parameters were varied and two new equilibria seemed to appear, the total number of equilibria remained at nineteen. The reason is that by varying the parameters, the two new equilibria which appeared were actually equilibria which originally resided outside the valid region (with at least one coordinate negative), but as the parameter was varied, the equilibria were translated to the valid region. Similarly, equilibria which existed with the original parameter values and seemed to disappear when parameters were varied, actually had shifted outside the valid region.

In the case of g_T, the tumor-positive equilibrium is translated in the direction of negative T and two new equilibria appear. By varying g_T in small decrements, the movement of the equilibria can be tracked. Also, the stability of the equilibria that lie in the valid region can be calculated for each value of g_T. We will proceed this way in the next section in an attempt to understand the effect that varying the parameter has on the system. In doing so, bifurcations can be revealed. The nondimensional reduced system (3.13) will continue to be used in the bifurcation analysis which follows.

3.8 Bifurcation Analysis

We are only concerned with the stability of those equilibria which lie in the valid region ($T^*, K^*, E^* \geq 0$).

In Claim 3.3 and Proposition 3.1, it was shown that system (3.13) had four equilibria lying in the valid region, one of which was a stable node and the other three were saddle points. By decreasing g_T in small decrements from 5×10^9 to 1×10^5 and calculating equilibria (as in the claim) and their stability (as in the proposition) along the way, we were able to determine the behavior of the system. Smaller steps were taken whenever necessary. The actual values of g_T used were: $5 \times 10^9, 4.5 \times 10^9, 4 \times 10^9, 3.5 \times 10^9, 3.4 \times 10^9, 3.35 \times 10^9, 3.3 \times 10^9, 3.25 \times 10^9, 3 \times 10^9, 2.5 \times 10^9, 2 \times 10^9, 1.9 \times 10^9, 1.8 \times 10^9, 1.7 \times 10^9, 1.6 \times 10^9, 1.5 \times 10^9, 1.4 \times 10^9, 1.3 \times 10^9, 1.25 \times 10^9, 1.2 \times 10^9, 1.1 \times 10^9, 1 \times 10^9, 9 \times 10^8, 8 \times 10^8, 7 \times 10^8, 6 \times 10^8, 5 \times 10^8, 4 \times 10^8, 3 \times 10^8, 2.75 \times 10^8, 2.5 \times 10^8, 2.25 \times 10^8, 2.24 \times 10^8, 2.23 \times 10^8, 2.2 \times 10^8, 2.1 \times 10^8, 2 \times 10^8, 1.5 \times 10^8, 1 \times 10^8, 9 \times 10^7, 1 \times 10^6, 1 \times 10^5$. However, only trajectories at certain key values of g_T were plotted to illustrate the behavior. Refer to Figure 3.13 for *XPPAUT* plots of the resulting trajectories as g_T is decreased.

As g_T is decreased, the original three saddle points

$$SP1 = (\tilde{T}^*, \tilde{K}^*, \tilde{E}^*) = (0, .2987012986, 0),$$

$$SP2 = (1, 0, 0),$$

$$SP3 = (0, 0, 0),$$

remain in their exact positions throughout.

However, the stable node

$$SN1 = (.8473841905, .7776120789, 2.024367212)$$

when $g_T = 5 \times 10^9$ begins to move in the negative T direction as g_T is decreased. By the time that $g_T = 3.35 \times 10^9$, the stable node $SN1$ has shifted to

$$(.7656478746, .7776120791, 2.118095020)$$

and two new equilibria come into the valid region from the $T < 0$ side. These are a stable node

$$SN2 = (1.037180156 \times 10^{-11}, .7741834150, 3.697108485)$$

and a saddle point

$$SP4 = (2.693235387 \times 10^{-8}, .7776107634, 3.740242973).$$

As g_T is decreased to 1.25×10^9, the original stable node $SN1$ has shifted to

$$(.02083465058, .7776120812, 3.663902409),$$

the new saddle point $SP4$ is at

$$(.001010620993, .7776120813, 3.736482490)$$

and the new stable node $SN2$ has now become a stable focus at

$$SF = (1.512899111 \times 10^{-13}, .5191263311, 1.149259533).$$

Decreasing g_T further to 1.2×10^9 causes the original stable node $SN1$ and the new saddle point $SP4$ to leave the valid region by moving into the $T < 0$ side. The stable focus SF is now at

$$(1.466586133 \times 10^{-13}, .5111315475, 1.090518879).$$

As g_T is decreased to 2.24×10^8, the stable focus becomes a stable node $SN2$ again and shifts to

$$(1.402695789 \times 10^{-16}, .2987696446, .2050846976 \times 10^{-3}).$$

As g_T is decreased still further, the stable node $SN2$ eventually collides with the original saddle point $SP1$ and a *transcritical bifurcation* occurs. When $g_T = 2.23 \times 10^8$, the saddle point $SP1$ has already switched stability and become a stable node and a saddle point has left the valid region from the same point into the region with $T, E < 0$.

Tracking the stability of the new stable node $SN2$ from the time that it emerged in the valid region until it collided with the saddle point $(0, .2987012986, 0)$ and the *transcritical bifurcation* occurred, gave the following results (only those values that correspond to plots in Figure 3.13 are given).

Eigenvalues and corresponding eigenvectors:

$g_T = 3.35 \times 10^9$:

$\lambda_1 = -.002518579426264989,$

$$\vec{v_1} = \begin{pmatrix} 2.309116696011637 \times 10^{-10} \\ .07673148004192766 \\ .9970517940260553 \end{pmatrix}$$

$\lambda_2 = -.06514900290243296,$

$$\vec{v_2} = \begin{pmatrix} -8.348202852800676 \times 10^{-12} \\ -.003836063906462556 \\ -.9999926422797847 \end{pmatrix}$$

$\lambda_3 = -.8551120968377294,$

$$\vec{v_3} = \begin{pmatrix} -6.330995533655018 \times 10^{-13} \\ -.9999996722463767 \\ .0008096339540205655 \end{pmatrix}$$

The eigenvalues are negative real numbers, so the equilibrium is a stable node.

$g_T = 1.25 \times 10^9$:

$\lambda_1 = -.02168746879033548 + .09384029714753124i,$

$\lambda_2 = -.02168746879033548 - .09384029714753124i,$

$\lambda_3 = -.4707381223633896,$

and the eigenvectors are complex in this case.

The eigenvalues are complex with negative real parts, so the equilibrium is a stable focus.

$g_T = 1.2 \times 10^9$:

$\lambda_1 = -.02156946069297827 + .09468000949812898i,$

$\lambda_2 = -.02156946069297827 - .09468000949812898i,$

$\lambda_3 = -.4591874188732668,$

and the eigenvectors are complex in this case.

The eigenvalues are complex with negative real parts, so the equilibrium is a stable focus.

$g_T = 2.24 \times 10^8$:

$\lambda_1 = -.0002144254855092620,$

$$\vec{v_1} = \begin{pmatrix} 6.462052110395747 \times 10^{-13} \\ .3155001124308840 \\ .9489255392580070 \end{pmatrix}$$

$\lambda_2 = -.06795058119214648,$

$$\vec{v_2} = \begin{pmatrix} -1.615451058598153 \times 10^{-15} \\ -.001691705570095869 \\ -.9999985690651082 \end{pmatrix}$$

$\lambda_3 = -.2045389917358546,$

$$\vec{v_3} = \begin{pmatrix} -5.353754689744907 \times 10^{-16} \\ -.9999997307253982 \\ .0007338590677618802 \end{pmatrix}$$

The eigenvalues are negative real numbers, so the equilibrium is a stable node.

$g_T = 2.23 \times 10^8$:

By the time that this value of g_T has been reached, the stable node that we have been tracking has collided with the saddle point $(0, .2987012986, 0)$ and emerged on the other side $(T, E < 0)$ as a saddle point. This point

$$(-5.474959999 \times 10^{-16}, .2984358021, -.0007957815632)$$

no longer lies in the valid region.

$\lambda_1 = .0008209482276856916,$

$$\vec{v_1} = \begin{pmatrix} 6.629681784585971 \times 10^{-13} \\ .3190079214135551 \\ .9477520488373544 \end{pmatrix}$$

$\lambda_2 = -.2045739812348497,$

$$\vec{v_2} = \begin{pmatrix} 2.106244548693402 \times 10^{-15} \\ -.9999958669152501 \\ -.002875091723287432 \end{pmatrix}$$

$\lambda_3 = -.06906706566695404 \times 10^{-2},$

$$\vec{v_3} = \begin{pmatrix} -6.179865583689437 \times 10^{-15} \\ -.006551677951559302 \\ .9999785375276907 \end{pmatrix}$$

The eigenvalues consist of one positive and two negative real numbers, so the equilibrium is a saddle point. The flow along $\vec{v_1}$ has reversed directions and is now outgoing as indicated by the sign of λ_1.

Next, we will show that the equilibrium $(0, .2987012986, 0)$ has now become a stable node by computing the eigenvalues and corresponding eigenvectors as follow:

$\lambda_1 = -.06818181818181818,$

$$\vec{v_1} = \begin{pmatrix} 0 \\ 0 \\ 1 \end{pmatrix}$$

$\lambda_2 = -.2045454544067193,$

$$\vec{v_2} = \begin{pmatrix} 0 \\ 1 \\ 0 \end{pmatrix}$$

$\lambda_3 = -.0008328414569134246,$

$$\vec{v_3} = \begin{pmatrix} 6.422296374582806 \times 10^{-13} \\ .3138978058851025 \\ .9494567749300220 \end{pmatrix}$$

The flow along $\vec{v_3}$ is now into the equilibrium as indicated by the sign of λ_3. Note that $\vec{v_3}$ for this equilibrium corresponds to $\vec{v_1}$ for the equilibrium that we have been tracking.

Therefore, a *transcritical bifurcation* has occurred at the bifurcation point $2.23 \times 10^8 \leq g_T \leq 2.24 \times 10^8$. This result will be verified analytically in the following proposition and corollary by applying the *Routh-Hurwitz Criterion* (Theorem A.1 in Appendis A), and in the process, a better estimate of the bifurcation point will be obtained.

To make system (3.13) easier to handle, rewrite it in the following form:

$$\begin{cases} \dfrac{dT^*}{dt^*} = \dfrac{u_1 T^* + u_2 T^{*2} + u_3 T^{*3}}{u_4 + u_5 T^*} - \dfrac{u_6 K^* T^* + u_6 E^* T^*}{u_7 + u_8 T^*} \\ \dfrac{dK^*}{dt^*} = v_1 K^* - v_2 K^{*2} + A \\ \dfrac{dE^*}{dt^*} = \dfrac{A}{1 + v_{10} T^*} - v_{11} E^* \end{cases} \tag{3.18}$$

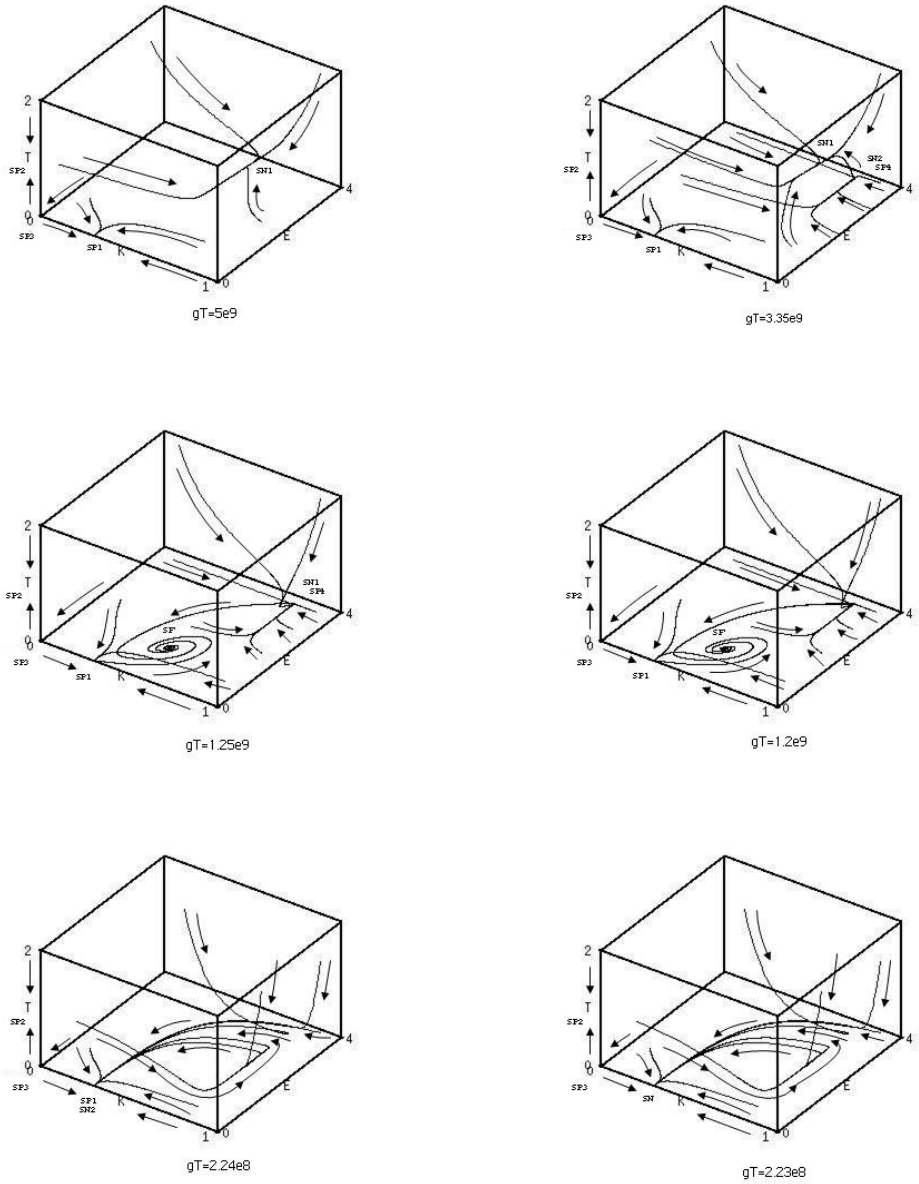

Figure 3.13: Plots of trajectories of system (3.13) as g_T is decreased.

where

$$A = \frac{2v_3K^*T^* + v_4K^*T^{*2} + 3v_3E^*T^* + 3v_4E^*T^{*2}}{v_5 + v_6T^* + v_7T^{*2} + 2v_8K^*T^* + v_9K^*T^{*2} + 3v_8E^*T^* + 3v_9E^*T^{*2}} \tag{3.19}$$

Proposition 3.2 *The equilibrium point* $(\tilde{T}^*, \tilde{K}^*, \tilde{E}^*) = (0, .2987012986, 0)$ *of system (3.18) and hence of system (3.13) is stable if the parameters satisfy the following inequalities* [5]*:*

$$a_1 > 0 \ , \ a_3 > 0 \ \textit{and} \ a_1 a_2 > a_3$$

where

$$a_1 = -\frac{u_1}{u_4} + \frac{.2987012986u_6}{u_7} - v_1 + .5974025972v_2 + v_{11}$$

$$a_2 = \frac{u_1 v_1}{u_4} - \frac{.5974025972u_1 v_2}{u_4} + \frac{.1784449316u_6 v_2}{u_7} - \frac{.2987012986u_6 v_1}{u_7} - \frac{u_1 v_{11}}{u_4}$$
$$+\frac{.2987012986u_6 v_{11}}{u_7} - v_1 v_{11} + .5974025972v_2 v_{11}$$

$$a_3 = \frac{u_1 v_1 v_{11}}{u_4} - \frac{.5974025972u_1 v_2 v_{11}}{u_4} + \frac{.1784449316u_6 v_2 v_{11}}{u_7} - \frac{.2987012986u_6 v_1 v_{11}}{u_7}$$

Proof: Using system (3.18), let

$$f_1 = \frac{dT^*}{dt^*} \ , \ f_2 = \frac{dK^*}{dt^*} \ , \ f_3 = \frac{dE^*}{dt^*}$$

[5]Note that these values are numerical approximations obtained with *Maple* and/or *Matlab*.

Furthermore, let

$$a_{11} = \frac{\partial f_1}{\partial T^*}$$

$$= \frac{u_1 + 2u_2T^* + 3u_3T^{*2}}{u_4 + u_5T^*} - \frac{(u_1T^* + u_2T^{*2} + u_3T^{*3})u_5}{(u_4 + u_5T^*)^2} - \frac{u_6K^* + u_6E^*}{u_7 + u_8T^*}$$

$$+ \frac{(u_6K^*T^* + u_6E^*T^*)u_8}{(u_7 + u_8T^*)^2}$$

$$a_{12} = \frac{\partial f_1}{\partial K^*} = -\frac{u_6T^*}{u_7 + u_8T^*}$$

$$a_{13} = \frac{\partial f_1}{\partial E^*} = -\frac{u_6T^*}{u_7 + u_8T^*}$$

$$a_{21} = \frac{\partial f_2}{\partial T^*} = \frac{\partial A}{\partial T^*}$$

$$a_{22} = \frac{\partial f_2}{\partial K^*} = v_1 - 2v_2K^* + \frac{\partial A}{\partial K^*}$$

$$a_{23} = \frac{\partial f_2}{\partial E^*} = \frac{\partial A}{\partial E^*}$$

$$a_{31} = \frac{\partial f_3}{\partial T^*} = \frac{\dfrac{\partial A}{\partial T^*}}{1 + v_{10}T^*} - \frac{Av_{10}}{(1 + v_{10}T^*)^2}$$

$$a_{32} = \frac{\partial f_3}{\partial K^*} = \frac{\dfrac{\partial A}{\partial K^*}}{1 + v_{10}T^*}$$

$$a_{33} = \frac{\partial f_3}{\partial E^*} = \frac{\dfrac{\partial A}{\partial E^*}}{1 + v_{10}T^*} - v_{11}$$

where

$$\frac{\partial A}{\partial T^*} = \frac{2v_3K^* + 2v_4K^*T^* + 3v_3E^* + 6v_4E^*T^*}{v_5 + v_6T^* + v_7T^{*2} + 2v_8K^*T^* + v_9K^*T^{*2} + 3v_8E^*T^* + 3v_9E^*T^{*2}}$$

$$-\frac{\begin{pmatrix} 2v_3K^*T^* + v_4K^*T^{*2} + \\ 3v_3E^*T^* + 3v_4E^*T^{*2} \end{pmatrix}\begin{pmatrix} v_6 + 2v_7T^* + 2v_8K^* + 2v_9K^*T^* \\ +3v_8E^* + 6v_9E^*T^* \end{pmatrix}}{(v_5 + v_6T^* + v_7T^{*2} + 2v_8K^*T^* + v_9K^*T^{*2} + 3v_8E^*T^* + 3v_9E^*T^{*2})^2}$$

$$\frac{\partial A}{\partial K^*} = \frac{2v_3T^* + v_4T^{*2}}{v_5 + v_6T^* + v_7T^{*2} + 2v_8K^*T^* + v_9K^*T^{*2} + 3v_8E^*T^* + 3v_9E^*T^{*2}}$$

$$-\frac{(2v_3K^*T^* + v_4K^*T^{*2} + 3v_3E^*T^* + 3v_4E^*T^{*2})(2v_8T^* + v_9T^{*2})}{(v_5 + v_6T^* + v_7T^{*2} + 2v_8K^*T^* + v_9K^*T^{*2} + 3v_8E^*T^* + 3v_9E^*T^{*2})^2}$$

$$\frac{\partial A}{\partial E^*} = \frac{3v_3T^* + 3v_4T^{*2}}{v_5 + v_6T^* + v_7T^{*2} + 2v_8K^*T^* + v_9K^*T^{*2} + 3v_8E^*T^* + 3v_9E^*T^{*2}}$$

$$-\frac{(2v_3K^*T^* + v_4K^*T^{*2} + 3v_3E^*T^* + 3v_4E^*T^{*2})(3v_8T^* + 3v_9T^{*2})}{(v_5 + v_6T^* + v_7T^{*2} + 2v_8K^*T^* + v_9K^*T^{*2} + 3v_8E^*T^* + 3v_9E^*T^{*2})^2}$$

Evaluating [6] the Jacobian matrix J at equilibrium

$$(\tilde{T^*}, \tilde{K^*}, \tilde{E^*}) = (0, .2987012986, 0)$$

gives

$$J\mid_{(0,.2987012986,0)} = \begin{pmatrix} \frac{u_1}{u_4} - \frac{.2987012986u_6}{u_7} & 0 & 0 \\ \frac{.5974025972v_3}{v_5} & v_1 - .5974025972v_2 & 0 \\ \frac{.5974025972v_3}{v_5} & 0 & -v_{11} \end{pmatrix}$$

The corresponding *characteristic equation* is given by

$$\lambda^3 + a_1\lambda^2 + a_2\lambda + a_3 = 0 \tag{3.20}$$

where

$$a_1 = -\frac{u_1}{u_4} + \frac{.2987012986u_6}{u_7} - v_1 + .5974025972v_2 + v_{11}$$

$$a_2 = \frac{u_1v_1}{u_4} - \frac{.5974025972u_1v_2}{u_4} + \frac{.1784449316u_6v_2}{u_7} - \frac{.2987012986u_6v_1}{u_7} - \frac{u_1v_{11}}{u_4}$$

$$+\frac{.2987012986u_6v_{11}}{u_7} - v_1v_{11} + .5974025972v_2v_{11}$$

[6] *Matlab* and *Maple* were used to aid in some of the calculations

$$a_3 = \frac{u_1 v_1 v_{11}}{u_4} - \frac{.5974025972 u_1 v_2 v_{11}}{u_4} + \frac{.1784449316 u_6 v_2 v_{11}}{u_7} - \frac{.2987012986 u_6 v_1 v_{11}}{u_7}$$

By Corollary A.1 in Appendix A, all eigenvalues λ have negative real parts if

$$a_1 > 0 \ , \ a_3 > 0 \text{ and } a_1 a_2 > a_3$$

□

Corollary 3.1 *Using parameter values* [7] *from Table 2.2 (with the exception of* g_T*), the equilibrium point* $(\tilde{T}^*, \tilde{K}^*, \tilde{E}^*) = (0, .2987012986, 0)$ *of system (3.18) and hence of system (3.13) is stable if parameter* g_T *satisfies the following inequality* [8]*:*

$$0 < g_T < 2.237951382 \times 10^8$$

Proof: By Proposition 3.2, the equilibrium is stable if

$$a_1 > 0 \ , \ a_3 > 0 \text{ and } a_1 a_2 > a_3$$

where, after substituting parameter values,

$$a_1 = .03915326548 + \frac{5.227272726 \times 10^7}{g_T}$$

$$a_2 = -.04975572098 + \frac{1.425619834 \times 10^7}{g_T}$$

[7] Parameter values from the table are substituted into the u's and v's of the equations.

[8] Note that these limits are numerical approximations obtained with *Maple* and/or *Matlab*.

$$a_3 = -.003257488735 + \frac{7.290101417 \times 10^5}{g_T}$$

$$a1 > 0 \implies g_T \in (-\infty, -1.335079632 \times 10^9) \cup (0, \infty)$$

$$a3 > 0 \implies g_T \in (0, 2.237951382 \times 10^8)$$

$$a_1 a_2 > a_3 \implies$$

$$g_T \in (-\infty, 0) \cup (0, 3.160531797 \times 10^8) \cup (1.800734879 \times 10^9, \infty)$$

Therefore, all three inequalities are satisfied if

$$g_T \in (0, 2.237951382 \times 10^8)$$

□

By the above corollary, the equilibrium point $(\tilde{T^*}, \tilde{K^*}, \tilde{E^*}) = (0, .2987012986, 0)$ undergoes the *transcritical bifurcation* at the bifurcation point $g_T = 2.237951382 \times 10^8$.

Next, we will look at the remaining parameters of interest.

As d_T is increased, first to 1.5 and then to 2, the original three saddle points, $(0, .2987012986, 0)$, $(1, 0, 0)$, and $(0, 0, 0)$, remain in their exact positions and the original stable node,

$$(.8473841905, .7776120789, 2.024367212),$$

moves in the negative T^* direction, first to

$$(.7628378710, .7776120791, 2.121471842)$$

when $d_T = 1.5$, and then to

$$(.6705327373, .7776120793, 2.238713033)$$

when $d_T = 2$.

We saw in Section 3.7 that when $d_T = 1.5$, two new tumor-positive equilibria appeared in the valid region. Calculating their stability, it turns out that the first one,

$$(7.01659550110 \times 10^{-12}, .7725393882, 3.676501469),$$

is a stable node and the second one,

$$(4.01156838110 \times 10^{-8}, .7776111965, 3.740248389),$$

is a saddle point.

When $d_T = 2$, the two new equilibria have shifted and one has changed from a stable node to a stable focus. The first equilibria, now located at

$$(3.999713833 \times 10^{-13}, .6844998498, 2.652272201)$$

has become a stable focus (see Figure 3.14) and the second one, now at

$$(.1145964401 \times 10^{-5}, .7776120504, 3.740255028)$$

remains a saddle point.

This is similar to what happened when g_T was varied, except in this case, the stable focus moves very slowly as d_T is varied.

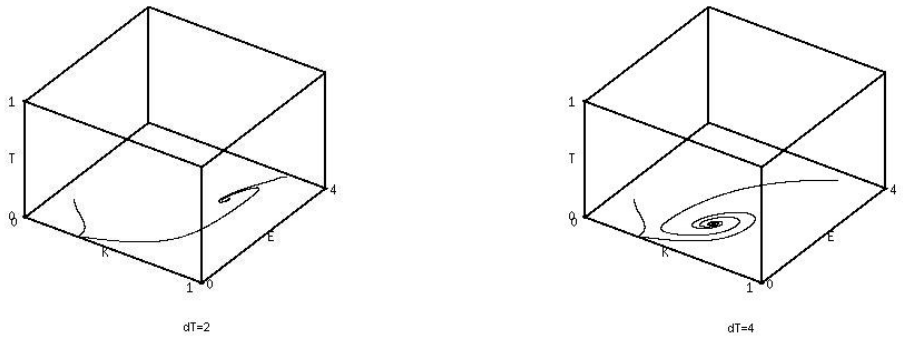

Figure 3.14: Stable focus obtained by setting parameter $d_T = 2$ and then $d_T = 4$ in system (3.13).

As k_T (and hence K_T) is decreased, first to .3 and then to .1, one of the original saddle points, $(0, .2987012986, 0)$, first moves to $(0, .4380952381, 0)$ when $k_T = .3$, and then to $(0, 1.31428574, 0)$ when $k_T = .1$. The other two saddle points, $(1, 0, 0)$ and $(0, 0, 0)$ remain in their exact positions. The original stable node,

$$(.8473841905, .7776120789, 2.024367212),$$

first moves to

$$(.7423334914, 1.140497716, 3.148114973)$$

when $k_T = .3$, and then leaves the valid region when $k_T = .1$.

We saw in Section 3.7 that when $k_T = .3$, two new tumor-positive equilibria appeared in the valid region. It turns out that the first one,

$$(1.898034954 \times 10^{-12}, 1.099664608, 4.981823757)$$

is a stable node and the second one,

$$(3.561606134 \times 10^{-7}, 1.140497505, 5.485709575)$$

is a saddle point.

When $k_T = .1$, the new stable node has become a stable focus (see Figure 3.15) at

$$(2.787639164 \times 10^{-13}, 1.545264235, .814715194)$$

and the new saddle point has left the valid region.

The trajectory initially moves in the direction of an equilibrium outside of the valid region ($T^* < 0$) and then goes to the stable focus. However, the initial increase in E^* can almost reach a value of 12 (see Figure 3.15). Converting the nondimensional variable E^* back into the dimensional variable E gives

$$E = K_T E^* = (7.7 \times 10^7)(12) = 9.24 \times 10^8 \tfrac{cells}{ml}$$

This is a value greater than the bone marrow cell density $7.68 \times 10^8 \tfrac{cells}{ml}$, which was previously calculated. Therefore, for the model to be realistic, the minimum value that k_T can be must be greater than .1.

As k_{KE} is increased, first to 1.4×10^7 and then to 1×10^8, the original three saddle points, $(0, .2987012986, 0)$, $(1, 0, 0)$, and $(0, 0, 0)$, remain in their exact positions and the original stable node,

$$(.8473841905, .7776120789, 2.024367212),$$

first moves to

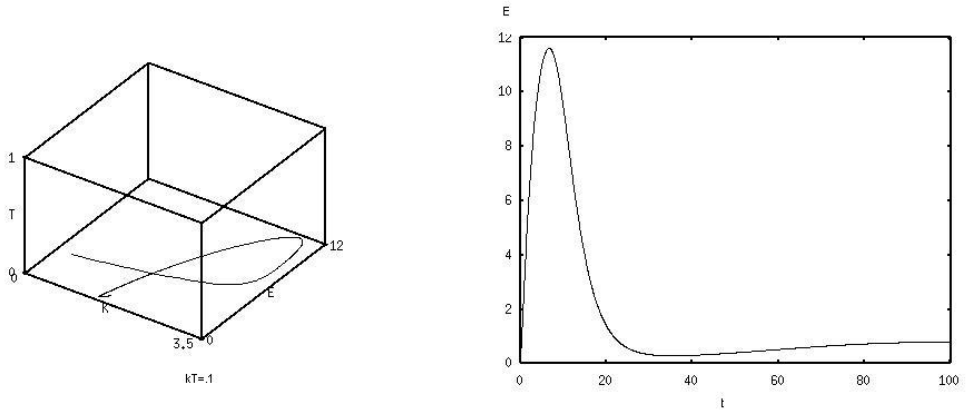

Figure 3.15: Stable focus obtained by setting parameter $k_T = .1$ in system (3.13) and a plot of E^* vs t^*.

$$(.7610401310, .9403895720, 3.441079897)$$

when $k_{KE} = 1.4 \times 10^7$ and then leaves the valid region when $k_{KE} = 1 \times 10^8$.

We saw in Section 3.7 that when $k_{KE} = 1.4 \times 10^7$, two new tumor-positive equilibria appeared in the valid region. It turns out that the first one,

$$(1.49711272110 \times 10^{-12}, .9207731158, 5.752773836)$$

is a stable node and the second one,

$$(1.29792448210 \times 10^{-7}, .9403893496, 6.060601677)$$

is a saddle point.

When $k_{KE} = 1 \times 10^8$, the new stable node has become a stable focus (see Figure 3.16) at

$$(1.227338279 \times 10^{-14}, .9207728820, 5.752770213)$$

and the new saddle point has left the valid region.

However, the oscillations of the stable focus reach a value of $E^* > 12$ (see Figure 3.16), which is greater than the bone marrow cell density. Therefore, for the model to be realistic, the minimum value that k_{KE} can be must be greater than 1×10^8.

These large oscillations indicate the possible existence of a *Hopf bifurcation* and will be explored later.

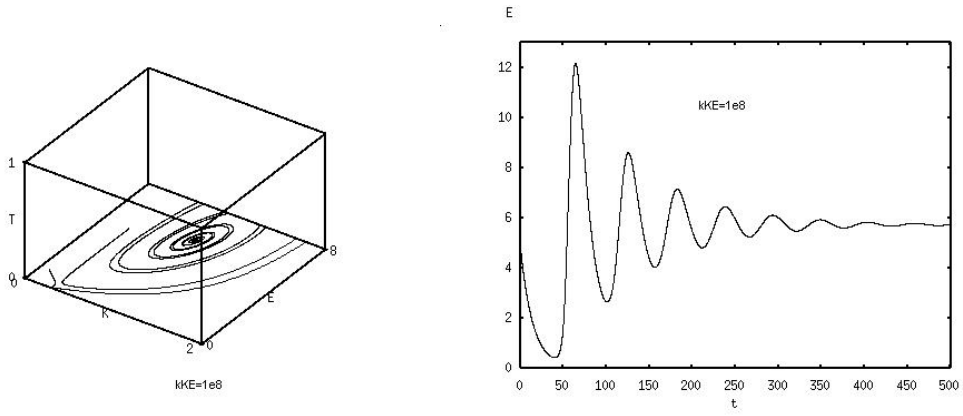

Figure 3.16: Stable focus obtained by setting parameter $k_{KE} = 1 \times 10^8$ in system (3.13) and a plot of E^* vs t^* showing the corresponding oscillations.

As l_I is decreased, first to .6 and then to .5, the original three saddle points, $(0, .2987012986, 0)$, $(1, 0, 0)$, and $(0, 0, 0)$, remain in their exact positions and the original stable node,

$$(.8473841905, .7776120789, 2.024367212),$$

first moves to

$$(.8204769741, .7776120790, 2.054292547)$$

when $l_I = .6$, and then to

$$(.8067722842, .7776120790, 2.069877114)$$

when $l_I = .5$.

We saw in Section 3.7 that when $l_I = .6$, two new tumor-positive equilibria appeared in the valid region. It turns out that the first one,

$$(3.791368189 \times 10^{-11}, .7766753865, 3.728447560)$$

is a stable node, and the second one,

$$(6.470583845 \times 10^{-9}, .7776065957, 3.740190453)$$

is a saddle point.

When $l_I = .5$, the new stable node has become a stable focus (see Figure 3.17) at

$$(7.444163268 \times 10^{-13}, .7286753968, 3.146737707)$$

and the new saddle point has moved to

$$(3.902477620 \times 10^{-7}, .7776119904, 3.740257098).$$

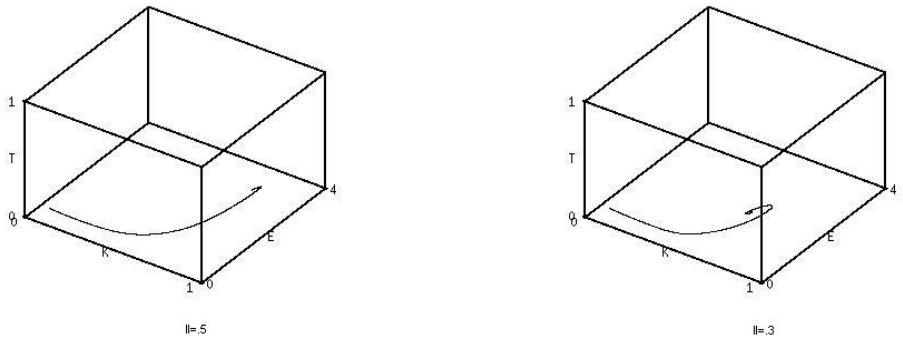

Figure 3.17: Stable focus obtained by setting parameter $l_I = .5$ and then $l_I = .3$ in system (3.13).

We now return to the possible existence of a *Hopf bifurcation* when large oscillations arise. First, parameters such as k_{KE}, g_T, d_T, k_T and l_I, which lead to oscillatory behavior, were varied one at a time experimentally to see how the oscillations are affected. Plots of T^*, K^*, and E^* versus t^* and plots of trajectories (starting close to and far from the equilibrium in question) were generated and analyzed. This proce-

dure was repeated, only this time several parameters were systematically varied. The results seem to indicate that no *Hopf bifurcation* exists in the valid region (T^*, K^*, $E^* > 0$).

Next, the $AUTO$[9] feature of $XPPAUT$ was also employed in the search for a *Hopf bifurcation* and none was found in this region.

The following result, which is a consequence of the *Hopf Bifurcation Theorem*, Theorem B.1 in Appendix B, was used in order to find a *Hopf bifurcation* analytically.

Proposition 3.3 *System (3.13) undergoes a Hopf bifurcation with respect to a bifurcation parameter p at an equilibrium point* $(\tilde{T}^*, \tilde{K}^*, \tilde{E}^*)$ *if the following conditions are satisfied:*

1. $AB - C = 0$
2. $-2A'B^2 + 2BC' - 2ABB' \neq 0$

where

$$A = -a_{11} - a_{22} - a_{33},$$

$$B = a_{11}a_{22} + a_{11}a_{33} + a_{22}a_{33} - a_{23}a_{32} - a_{12}a_{21} - a_{13}a_{31},$$

[9] $AUTO$ refers to a library of routines used to generate bifurcation diagrams by applying a process, known as *continuation*, in which a particular solution is followed as parameters vary.

$$C = -a_{11}a_{22}a_{33} + a_{11}a_{23}a_{32} + a_{12}a_{21}a_{33} - a_{12}a_{23}a_{31} - a_{13}a_{21}a_{32} + a_{13}a_{31}a_{22},$$

are evaluated at the equilibrium point, a_{ij} $(i, j \in \{1, 2, 3\})$ *are defined as in the proof of Proposition 3.2 and the prime (') denotes differentiation with respect to the bifurcation parameter p.*

Proof: Suppose that the Jacobian matrix J, evaluated at an equilibrium point $(\tilde{T}^*, \tilde{K}^*, \tilde{E}^*)$, is given by

$$J = J\,|_{(\tilde{T}^*, \tilde{K}^*, \tilde{E}^*)} = \begin{pmatrix} a_{11} & a_{12} & a_{13} \\ a_{21} & a_{22} & a_{23} \\ a_{31} & a_{32} & a_{33} \end{pmatrix}$$

Then,

$$det(J - \lambda I) = 0$$
$$\implies (a_{11} - \lambda)[(a_{22} - \lambda)(a_{33} - \lambda) - a_{23}a_{32}] - a_{12}[a_{21}(a_{33} - \lambda) - a_{23}a_{31}]$$
$$+a_{13}[a_{21}a_{32} - a_{31}(a_{22} - \lambda)] = 0$$

resulting in the *characteristic equation*

$$\lambda^3 + (-a_{11} - a_{22} - a_{33})\lambda^2 + (a_{11}a_{22} + a_{11}a_{33} + a_{22}a_{33} - a_{23}a_{32} - a_{12}a_{21} - a_{13}a_{31})\lambda$$
$$+(-a_{11}a_{22}a_{33} + a_{11}a_{23}a_{32} + a_{12}a_{21}a_{33} - a_{12}a_{23}a_{31} - a_{13}a_{21}a_{32} + a_{13}a_{31}a_{22}) = 0$$

Substituting A, B and C as indicated in the statement of the proposition gives

$$\lambda^3 + A\lambda^2 + B\lambda + C = 0 \tag{3.21}$$

The first necessary condition for the existence of a *Hopf bifurcation* is the existence of two purely imaginary eigenvalues. This implies that a *limit cycle* (*periodic orbit*) exists.

Equation 3.21 has two purely imaginary roots if and only if

$$AB = C$$

or equivalently

$$AB - C = 0 \tag{3.22}$$

In this case, the equation becomes

$$\lambda^3 + A\lambda^2 + B\lambda + AB = 0$$

$$\implies (\lambda^2 + B)(\lambda + A) = 0$$

$$\implies \lambda_{1,2} = \pm i\sqrt{B} \text{ and } \lambda_3 = -A \tag{3.23}$$

In general, the above roots can be written

$$\lambda_1 = u(p) + iv(p) \tag{3.24}$$

$$\lambda_2 = u(p) - iv(p)$$

$$\lambda_3 = w(p)$$

where in our case

$$u(p) = 0$$

$$v(p) = \sqrt{B}$$

$$w(p) = -A$$

The second necessary condition for the existence of a *Hopf bifurcation* is that the following *transversality condition* hold:

$$\frac{du}{dp} \mid_{p = p^*} \neq 0,$$

where p^* is the value of p at which the bifurcation occurs.

Substituting $\lambda = \lambda_1$ from (3.24) into (3.21) gives

$$(u + iv)^3 + A(u + iv)^2 + B(u + iv) + C = 0$$

$$\implies u^3 + 3iu^2v - 3uv^2 - iv^3 + Au^2 + 2iAuv - Av^2 + Bu + iBv + C = 0$$

Differentiating with respect to p gives

$$3u^2u' + 6iuu'v + 3iu^2v' - 3u'v^2 - 6uvv' - 3iv^2v' + A'u^2 + 2Auu' + 2iA'uv +$$

$$2iAu'v + 2iAuv' - A'v^2 - 2Avv' + B'u + Bu' + iB'v + iBv' + C' = 0$$

Setting $u = 0$ (since we want λ to be purely imaginary) gives

$$-3u'v^2 - 3iv^2v' + 2iAu'v - A'v^2 - 2Avv' + Bu' + iB'v + iBv' + C' = 0$$

$$\implies [-3u'v^2 - 2Avv' + Bu'] + i[-3v^2v' + 2Au'v + Bv']$$

$$= [A'v^2 - C'] + i[-B'v]$$

$$\implies [u'(-3v^2 + B) + v'(-2Av)] + i[u'(2Av) + v'(-3v^2 + B)]$$

$$= [A'v^2 - C'] + i[-B'v]$$

Equating real and imaginary parts gives the following system of equations

$$\begin{cases} (-3v^2 + B)u' + (-2Av)v' = A'v^2 - C' \\ \\ (2Av)u' + (-3v^2 + B)v' = -B'v \end{cases} \tag{3.25}$$

By applying *Cramer's Rule* to find u' and v', we get

$$u' = \frac{det\begin{pmatrix} A'v^2 - C' & -2Av \\ -B'v & -3v^2 + B \end{pmatrix}}{det\begin{pmatrix} -3v^2 + B & -2Av \\ 2Av & -3v^2 + B \end{pmatrix}}$$

$$= \frac{-3A'v^4 + A'Bv^2 + 3C'v^2 - BC' - 2AB'v^2}{9v^4 - 6Bv^2 + B^2 + 4A^2v^2}$$

and similarly,

$$v' = \frac{det\begin{pmatrix} -3v^2 + B & A'v^2 - C' \\ 2Av & -B'v \end{pmatrix}}{9v^4 - 6Bv^2 + B^2 + 4A^2v^2}$$

$$= \frac{3B'v^3 - BB'v - 2AA'v^3 + 2AC'v}{9v^4 - 6Bv^2 + B^2 + 4A^2v^2}$$

The *transversality condition*, $\frac{du}{dp} \mid_p = p^* \neq 0$, is satisfied when

$$-3A'v^4 + A'Bv^2 + 3C'v^2 - BC' - 2AB'v^2 \neq 0$$

In our case, $v = \sqrt{B}$, so we get

$$-2A'B^2 + 2BC' - 2ABB' \neq 0$$

If this is satisfied, then the *transversality condition* is satisfied.

□

To see if a *Hopf bifurcation* occurs when a single parameter is varied, Proposition 3.3 can be used. Out of several parameters that were tested (one at a time), g_T was the only one that resulted in a *Hopf bifurcation*, although it occurs outside of the valid region that we have been considering.

Using the numeric and symbolic capabilities of *Maple*, we were able to solve the following system of four equations consisting of the first condition of Proposition 3.3 together with the three equations that need to be satisfied for an equilibrium of system (3.13) to exist:

$$
\begin{cases}
AB - C = 0 \\
\\
\dfrac{u_1 T^* + u_2 T^{*2} + u_3 T^{*3}}{u_4 + u_5 T^*} - \dfrac{u_6 K^* T^* + u_6 E^* T^*}{u_7 + u_8 T^*} = 0 \\
\\
v_1 K^* - v_2 K^{*2} + \\
\qquad \dfrac{2v_3 K^* T^* + v_4 K^* T^{*2} + 3v_3 E^* T^* + 3v_4 E^* T^{*2}}{v_5 + v_6 T^* + v_7 T^{*2} + 2v_8 K^* T^* + v_9 K^* T^{*2} + 3v_8 E^* T^* + 3v_9 E^* T^{*2}} = 0 \\
\\
\dfrac{2v_3 K^* T^* + v_4 K^* T^{*2} + 3v_3 E^* T^* + 3v_4 E^* T^{*2}}{(1 + v_{10} T^*)(v_5 + v_6 T^* + v_7 T^{*2} + 2v_8 K^* T^* + v_9 K^* T^{*2} + 3v_8 E^* T^* + 3v_9 E^* T^{*2})} \\
\\
-v_{11} E^* = 0
\end{cases}
\tag{3.26}
$$

Only one solution was found. The approximate solution of the above system is

$g_T = 1.247074306 \times 10^9$

$T^* = -.1155278794$

$K^* = .7776120813$

$E^* = 4.228957701$

Substituting these values back into the left-hand-side of system (3.26) resulted in values close to zero, indicating that this is a good approximation to the solution of the system.

This point lies outside of the realm of what is biologically feasible, since T^* represents cell density per time and thus cannot be negative. However, for the sake of completion, this result was explored further, although it has no biological relevance.

The stability of equilibrium point

$$(\tilde{T^*}, \tilde{K^*}, \tilde{E^*}) = (-.1155278794, .7776120813, 4.228957701)$$

when

$$g_T = 1.247074306 \times 10^9$$

was computed using *Matlab* and it was determined that the above point is a stable focus. Using this as a starting point, the $AUTO$ feature of $XPPAUT$ was employed to find the *Hopf bifurcation*. This resulted in a *Hopf bifurcation* occurring at approximately

$$g_T = 1.247087900895566 \times 10^9$$

$$T^* = -.1155278803476433$$

$K^* = .7776120814774132$

$E^* = 4.228957707020461$

where a stable *limit cycle* (*periodic orbit*) surrounds an unstable focus. *Matlab* was used to confirm the existence of the above unstable focus by computing the stability of the above equilibrium at the given value of g_T. The second (*transversality*) condition of the proposition was also satisfied. Therefore, the bifurcation is a *supercritical Hopf bifurcation*. *XPPAUT* was used to plot the stable limit cycle (see Figure 3.18).

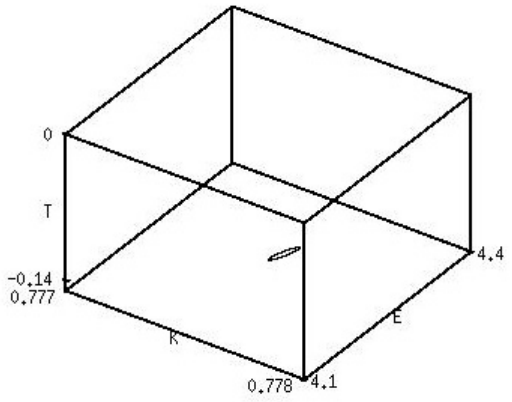

Figure 3.18: Plot of the stable *limit cycle* resulting from the *Hopf bifurcation*. The *limit cycle* was traced out by a trajectory starting close to it.

By varying g_T in small steps while computing equilibria, it was possible to track the movement of the above equilibrium. It was determined that this equilibrium came

from saddle point $SP4$ (see Figure 3.13), which changes stability when it crosses the $T^* = 0$ plane. At $g_T = 1.2 \times 10^9$ it is a stable node in the region where $T^* < 0$ and $K^*, E^* > 0$. At $g_T = 1.247074306 \times 10^9$, it is a stable focus and, at $g_T = 1.247087900895566 \times 10^9$, it is an unstable focus due to the *Hopf bifurcation* that occurs.

3.9 Conclusions and Medical Implications

Using the default parameter values from Table 2.2 (with $g_T = 5 \times 10^9$) gives only one stable equilibrium point (see Sections 3.5 and 3.6), a stable node with a tumor cell density of $6.524858265 \times 10^7 \frac{cells}{ml}$ and a normal plasma cell density of $1.877174457 \times 10^6 \frac{cells}{ml}$. This gives a combined plasma cell density of $6.712575711 \times 10^7 \frac{cells}{ml}$, which is less than $7.7 \times 10^7 \frac{cells}{ml}$, the threshold at which the patient is characterized as having MM (see Section 2.2). Even when the carrying capacity K_T of tumor cells was increased to the value of the bone marrow carrying capacity, this only resulted in an increase in the total bone marrow plasma cell content to approximately the 10% threshold value that distinguishes MGUS from MM. Therefore, the model predicts that the patient will eventually develop MGUS, but not MM.

At the beginning of Chapter 2, we stated that we would like the model to determine how much of an influence the production of M-protein and glycolipids by tumor cells has on the development of the disease. As mentioned in Section 1.3, M-protein causes a deletion of certain $CD4^+T$ cells by the same mechanism which is responsible for the prevention of autoimmunity and tumor-derived glycolipids cause a (medically

reversible) disruption in the ability of NKT cells to produce $IFN-\gamma$ (which attracts immune cells to the tumor site). Therefore, the production of M-protein and glycolipids supports tumor progression. However, numerical experiments (see Section 3.7) showed that setting the production of either to zero produced very little change in the progression or outcome of the disease. Also, $IFN-\gamma$ production was increased in numerical experiments. We expected this to cause a decrease in tumor density. However, no perceivable change in the progression or outcome of the disease was observed. Therefore, it can be concluded that the production of M-protein, tumor-derived glycolipids and $IFN-\gamma$ do not play as significant a role in tumor progression as expected.

In Chapter 2, we stated that since MGUS/MM is a disease which usually occurs late in life, a long enough delay in the increase in tumor cell density to the MGUS or MM level might be as good as a cure. We saw in Section 3.7 that an increase in the proliferation rate (and carrying capacity, since both parameters are interdependent) of innate immune system cells causes such a delay. Increasing the proliferation rate r_K from .09 to .45 (and hence the carrying capacity K_K from 2.30×10^7 to 1.15×10^8) delayed the increase in tumor cells by approximately 75. Since t^* is nondimensional and $t = \frac{t^*}{k_t}$, then this is equilvalent to a delay of $\frac{75}{.44} \approx 170$ days. Also, the number of tumor cells levels off at a lower number. However, this delay in not significant enough to be considered important.

We also saw in Section 3.7 that certain parameters, especially half-saturation constant g_T, play an important role in both the progression and the outcome of the disease. These parameters are d_T (the rate of destruction of tumor cells by the immune system), the interdependent parameters k_T and K_T (the proliferation rate and

carrying capacity of tumor cells, respectively), k_{KE} (the recruitment rate of immune cells due to the presence of $IFN-\gamma$), and l_I (the rate of $IL-6$ production by stromal cells). Varying any of these parameters slightly causes a delay in the increase in the density of tumor cells and the density of tumor cells levels off at a lower number. However, varying the parameters further produces more significant results.

Decreasing parameter k_T from .44 to .33 (and hence K_T from 7.7×10^7 to 5.78×10^7) causes a delay in the increase in tumor cell density by approximately 750. This is equivalent to (using the new k_T value) $\frac{t^*}{k_T} = \frac{750}{.33} \approx 2273$ days. However, we saw in Section 3.8 that k_T (and hence K_T) could not be decreased too much, say to .1, or an unrealistically large value of adaptive immune system cell density would occur. Therefore, it is important to obtain accurate estimates for the proliferation rate and carrying capacity of tumor cells.

Increasing k_{KE} from 8.64×10^6 to 1.3×10^7 causes a delay in the increase in tumor cells by approximately 1000. this is equivalent to $\frac{t^*}{k_T} = \frac{1000}{.44} \approx 2273$ days. However, increasing k_{KE} too much, say to 1×10^8, results in unrealistically large oscillations in adaptive immune system cell density. So it is also necessary to obtain an accurate estimate of the recruitment rate of immune cells due to the presence of $IFN-\gamma$.

The remaining parameters of interest, g_T, d_T and l_I, did not produce unrealistically large values when varied a reasonable amount.

Half-saturation constant g_T turned out to be an important bifurcation parameter. When $g_T = 5\times10^9$, there is only one stable equilibrium point, a stable node with a

nondimensional tumor density of $T^* = .8473841905$ or, equivalently,

$$T = 6.524858265 \times 10^7 \frac{cells}{ml}.$$

As mentioned earlier, a patient with this cell density is considered to have MGUS.

Decreasing g_T to 3.5×10^9 causes a delay in the increase in tumor cell density by approximately 1500 days and the density levels off at a lower value (see Section 3.2).

If g_T is decreased enough, say to 3.35×10^9, the above stable node shifts to a lower tumor density and another stable node emerges with a nondimensional tumor density of $T^* = 1.037180156 \times 10^{-11}$. This is equivalent to

$$T = K_T T^* = (7.7 \times 10^7)(1.037180156 \times 10^{-11}) = 7.986287201 \times 10^{-4} \frac{cells}{ml}$$

or, equivalently (using a bone marrow volume of 1042 ml),

$$(7.986287201 \times 10^{-4})(1042) = .8321711263 \text{ cells.}$$

Although in theory this is a positive tumor density with a fraction of one cell, this is impossible in reality and the number of tumor cells at this equilibrium will be zero. In this case, the tumor will be eradicated. Therefore, if the tumor density can be lowered to almost zero, it will settle at the lower stable equilibrium and the patient will remain tumor-free. However, if the tumor density is not decreased sufficiently, it will settle at the higher stable equilibrium with a positive tumor density.

If g_T is decreased still further, say to 1.25×10^9, the original stable node shifts to a lower tumor density and the new stable node becomes a stable focus. As g_T is decreased even more, say to 1.2×10^9, the original stable node disappears and the tumor density, regardless of its value, will be attracted to the only stable equilibrium remaining, the stable focus. The patient will then remain tumor-free. Decreasing g_T further causes the stable focus to become a stable node again and, eventually, at $g_T \approx 2.237951382 \times 10^8$, a *transcritical bifurcation* occurs and the saddle point (0,.2987012986,0) becomes a stable node. In this case, this tumor-free equilibrium is the only stable equilibrium and, once again, the patient will remain tumor-free.

In summary, decreasing g_T can lead to a lower tumor density or, if decreased enough, can lead to a cure. However, the reliability of this parameter is uncertain, so a better estimate, or at least range of possible values, must be obtained.

Another important parameter is d_T, the rate of destruction of tumor cells by immune cells. When $d_T = 1$, there is only one stable equilibrium point, a stable node with a positive tumor density. Increasing d_T to 1.4 causes a delay in the increase in tumor density by approximately 500 or, equivalently, $\frac{500}{.44} \approx 1136$ days and the density levels off at a lower value. However, as d_T continues to increase, say to 1.5, the tumor density of the stable node decreases and a new stable node with a tumor density of $7.01659550110 \times 10^{-12}$ emerges. This new stable node becomes a stable focus as d_T is increased further, say to 2. This is similar to what occurred when g_T was decreased. This makes sense, since d_T is in the numerator and g_T is in the denominator of the same term in the first equation of system (2.1). However, the difference is that, in

the case of d_T, the stable focus moves very slowly as d_T is increased further. As in the g_T case, lowering the tumor density enough can cause it to settle at the lower equilibrium and the patient will remain tumor-free.

The rate of $IL-6$ production l_I has similar results when varied. When $l_I = 1$, there is only one stable equilibrium point, a stable node with a positive tumor density. Decreasing l_I to .62 causes a delay in the increase in tumor cell density by approximately 1500 or, equivalently, $\frac{1500}{.44} \approx 3409$ days and the density levels off at a lower value. Decreasing l_I further, say to .6, causes the tumor density of the stable node to decrease and a new stable node with a tumor density of $3.791368189 \times 10^{-11}$ emerges. When l_I is decreased to .5, the new stable node becomes a stable focus. As in the d_T and g_T cases, lowering the tumor density enough can cause it to settle at the lower equilibrium and the patient will remain tumor-free.

Based on the parameter values used, the numerical experiments performed and the analysis, we can arrive at the following conclusions:

1. The model predicts that the patient will eventually develop MGUS.

2. The rate of production of M-protein, tumor-derived glycolipids and $IFN-\gamma$ do not play a significant role in the progression or outcome of the disease.

3. Decreasing the proliferation rate of tumor cells or increasing the recruitment rate of immune cells (due to the presence of $IFN-\gamma$) by a small amount causes a delay in the increase in tumor cell density to the MGUS level by approximately six years.

4. Decreasing either the half-saturation constant g_T or the rate of $IL{-}6$ production by stromal cells, or increasing the rate of destruction of tumor cells by the immune system causes a delay in the increase in tumor cell density to the MGUS level by three to four years if varied by a small amount or can lead to eradication of the tumor if varied by a greater amount.

However, whether or not these parameter values can be altered through medical intervention and, if so, by how much, remains uncertain.

3.10 Future Work

The complexity of system (3.18) has prevented us from doing more work analytically than has already been done. In order to proceed further, the system would have to be simplified even more. One thing that can be done is reduce the number of parameters. For instance, we can eliminate u_4 from the first equation in system (3.18), by multiplying the first term by $\frac{\frac{1}{u_4}}{\frac{1}{u_4}}$ and renaming the resulting parameter fractions. u_7 can be eliminated from the second term similarly. However, this alone will not simplify the system sufficiently. One major simplification that can make the system much more manageable analytically is replacing the A expression, which appears in the second and third equations of system (3.18), by a simpler expression. The difficulty in doing this lies in finding an expression which is simple enough to allow more work to be done analytically while, at the same time, preserving the dynamics of the system.

Simplifying system (3.18) has several advantages. For one thing, it might make it possible to work with several parameters at a time and, for instance, obtain a result

similar to Corollary 3.1, but with g_T in terms of, say d_T and l_I. This will help us determine if, instead of having to decrease g_T by a large amount in order to eradicate the tumor, it is possible to vary g_T, d_T and l_I by smaller amounts to achieve the same result.

Another benefit of working with a simpler system is that it might allow us to expand the model without it becoming overly complicated. For instance, a new tumor cell population can be introduced to include one of several possible mutations in an already existing cancer cell. By including some form of mutation-selection equation, we can study the role that a certain mutation plays in tumor development.

Another possibility is including some type of medical intervention by a treatment such as chemotherapy. In this case, it might be possible to apply optimal control theory to determine the best course of treatment.

However, before any of this can be achieved, we must first find a way to simplify the model.

Appendix A

Routh-Hurwitz Criterion

The *Routh-Hurwitz Criterion* is used to determine if all the roots of a polynomial have negative real parts. It can be stated as follows (refer to [61]):

Theorem A.1 ***(Routh-Hurwitz Criterion)***

Given the equation

$$x^n + a_1 x^{n-1} + \cdots + a_n = 0 \tag{A.1}$$

with real coefficients, construct Hurwitz matrices H_j, where $j = 1, \ldots, n$, by letting entry (l, m) in matrix H_j be defined by

$$a_{lm} = \begin{cases} a_{2l-m} \ , \ for \ 0 < 2l - m \leq n \\ \\ 1 \ , \ for \ 2l - m = 0 \\ \\ 0 \ , \ for \ 2l - m < 0 \ \ or \ 2l - m > n \end{cases} \tag{A.2}$$

That is

$$H_1 = (a_1)$$

$$H_2 = \begin{pmatrix} a_1 & 1 \\ a_3 & a_2 \end{pmatrix}$$

$$H_3 = \begin{pmatrix} a_1 & 1 & 0 \\ a_3 & a_2 & a_1 \\ a_5 & a_4 & a_3 \end{pmatrix}$$

$$\vdots$$

$$H_j = \begin{pmatrix} a_1 & 1 & 0 & 0 & \cdots & 0 \\ a_3 & a_2 & a_1 & 1 & \cdots & 0 \\ a_5 & a_4 & a_3 & a_2 & \cdots & 0 \\ \vdots & \vdots & \vdots & \vdots & \vdots & \vdots \\ a_{2j-1} & a_{2j-2} & a_{2j-3} & a_{2j-4} & \cdots & a_j \end{pmatrix}$$

$$\vdots$$

$$H_n = \begin{pmatrix} a_1 & 1 & 0 & \dots & 0 \\ a_3 & a_2 & a_1 & \dots & 0 \\ \vdots & \vdots & \vdots & \vdots & \vdots \\ 0 & \cdots & \cdots & \cdots & a_n \end{pmatrix}$$

A necessary and sufficient condition for the equation (A.1) to have only roots with negative real parts is that the determinants of the *Hurwitz matrices* H_j, for $j = 1, \dots, n$, all be positive.

In the special case of $n = 3$, we get the following corollary:

Corollary A.1 *Equation*

$$x^3 + a_1 x^2 + a_2 x + a_3 = 0 \tag{A.3}$$

has only roots with negative real parts if the determinants of the Hurwitz matrices, H_1*,* H_2 *and* H_3*, are all positive. That is,*

$$a_1 > 0 \ , \ a_3 > 0 \ \textit{and} \ a_1 a_2 > a_3$$

Appendix B

Hopf Bifurcation Theorem

A *Hopf bifurcation* occurs when a *limit cycle* (*periodic orbit*) emerges as a focus switches stability. The *Hopf Bifurcation Theorem* gives the conditions that are necessary and sufficient for this type of bifurcation to occur. It can be stated as follows (refer to [81]):

Theorem B.1 ***(Hopf Bifurcation Theorem)***

Suppose that the C^4*-system*

$$\dot{\vec{x}} = \vec{f}(\vec{x}, \mu) \tag{B.1}$$

with $\vec{x} \in \mathbb{R}^n$ *and* $\mu \in \mathbb{R}$ *has a critical point* $\vec{x}_0$ *for* $\mu = \mu_0$ *and that* $D\vec{f}(\vec{x}_0, \mu_0)$ *has a simple pair of pure imaginary eigenvalues and no other eigenvalues with zero real part. Then there is a smooth curve of equilibrium points* $\vec{x}(\mu)$ *with* $\vec{x}(\mu_0) = \vec{x}_0$ *and the eigenvalues,* $\lambda(\mu)$ *and* $\bar{\lambda}(\mu)$ *of* $D\vec{f}(\vec{x}(\mu), \mu)$*, which are pure imaginary at* $\mu = \mu_0$*, vary smoothly with* μ*. Furthermore, if*

$$\frac{d}{d\mu}\left[Re\lambda(\mu)\right]_{\mu=\mu_0} \neq 0, \tag{B.2}$$

then there is a unique two-dimensional center manifold passing through the point $(\vec{x}_0, \mu_0)$ *and a smooth transformation of coordinates such that (B.1) on the center manifold is transformed into the normal form*

$$\dot{x} = -y + ax(x^2 + y^2) - by(x^2 + y^2) + O(\mid \vec{x} \mid^4)$$

$$\dot{y} = x + bx(x^2 + y^2) + ay(x^2 + y^2) + O(\mid \vec{x} \mid^4)$$

in a neighborhood of the origin which, for $a \neq 0$*, has a weak focus of multiplicity one at the origin and*

$$\dot{x} = \mu x - y + ax(x^2 + y^2) - by(x^2 + y^2)$$

$$\dot{y} = x + \mu y + bx(x^2 + y^2) + ay(x^2 + y^2)$$

is a universal unfolding of this normal form in a neighborhood of the origin on the center manifold.

For more details on the *Hopf Bifurcation Theorem* and its variations, along with proofs, the reader can refer to [106] or [71].

By the above theorem, besides the necessary differentiability (on some sufficiently large open set containing the fixed point of interest), the system needs to satisfy two conditions in order for a *Hopf bifurcation* to occur. First, at the parameter value where the bifurcation occurs, the Jacobian, evaluated at the equilibrium point, must

have two purely imaginary eigenvalues. This guarantees the existence of a *limit cycle*. Second, the derivative of the real part of the eigenvalue with respect to the bifurcation parameter cannot be zero. In other words, the eigenvalue must cross the imaginary axis with non-zero speed. This condition is referred to as the *transversality condition*.

Bibliography

[1] Adam, J.A., Bellomo, N. (1997) *A Survey of Models for Tumor-Immune System Dynamics.* Birkhäuser.

[2] Alberts, B., Bray, D., Hopkin, K., Johnson, A., Lewis, J., Raff, M., Roberts, K., Walter, P. (2004) *Essential Cell Biology.* Garland Science.

[3] Arciero, J.C., Jackson, T.L., Kirschner, D.E. (2004) *A Mathematical Model of Tumor-Immune Evasion and siRNA Treatment.* Discrete and Continuous Dynamical Systems-Series B. vol. 4, no. 1. pp. 39-58.

[4] Asfaw, B., Schindler, D., Ledvinová, J., Černý, B., František Š., Conzelmann, E. (1998) *Degradation of Blood Group A Glycolipid A-6-2 by Normal and Mutant Human Skin Fibroblasts.* Journal of Lipid Research. vol. 39, pp. 1768-1780.

[5] Athreya, K.B., Ney, P.E. (2004) *Branching Processes.* Dover.

[6] Bhatt, B.S., Khan, Q.J.A., Jaju, R.P. (1999) *Switching Effect of Predation on Large Size Prey Species Exhibiting Group Defense.* Differential Equations and Control Processes. pp. 84-98.

[7] Bosmann, H.B., Winston, R.A. (1970) *Synthesis of Glycoprotein, Glycolipid, Protein, and Lipid in Synchronized L5178Y Cells.* The Journal of Cell Biology. vol. 45, pp. 23-33.

[8] Buckley, C.E., III, Dorsey, F.C. (1970) *The Effect of Aging on Human Serum Immunoglobulin Concentrations.* The Journal of Immunology. vol. 105, no. 4, pp. 964-972.

[9] Bürger, R. *The Mathematical Theory of Selection, Recombination, and Mutation.* Wiley.

[10] Caligaris-Cappio, F., Bergui, L., Gregoretti, M.G., Gaidano, G., Gaboli, M., Schena, M., Zallone, A.Z., Marchisio, P.C. (1991) *Role of Bone Marrow Stromal Cells in the Growth of Human Multiple Myeloma.* Blood. vol. 77, no. 12. pp. 2688-2693.

[11] Cantrel, R.S., Cosner, C. (2003) *Spatial Ecology via Reaction-Diffusion Equations.*, Wiley, England.

[12] Cavani, M., Lara, T., Romero, S. (2009) *Hopf Bifurcation for Simple Food Chain Model with Delay.* Electronic Journal of Differential Equations. vol. 2009, no. 76. pp. 1-10.

[13] Corso, A., Castelli, G., Pagnucco, G., Lazzarino, M., Bellio, L., Klersy, C., Bernasconi, C. (1997) *Bone Marrow T-Cell Subsets in Patients with Monoclonal Gammopathies: Correlation with Clinical Stage and Disease Status.* Haematologica. vol. 82, pp. 43-46.

[14] Cutler, A.J., Light, R.J. (1979) *Regulation of Hydroxydocosanoic Acid Sophoroside Production in Candida Bogoriensis by the Levels of Glucose and Yeast Extract in the Growth Medium.* The Journal of Biological Chemistry. vol. 254, no. 6. pp. 1944-1950.

[15] De Pillis, L.G., Radunskaya, A.E. (2002) *Non-Dimensionalization of Tumor-Immune ODE System.*

[16] De Pillis, L.G., Radunskaya, A. (2003) *A Mathematical Model of Immune Response to Tumor Invasion.* Second MIT Conference on Computational Fluid and Solid Mechanics. Elsevier Science Ltd. pp. 1661-1668.

[17] De Pillis, L.G., Radunskaya, A.E., Wiseman, C.L. (2005) *A Validated Mathematical Model of Cell-Mediated Immune Response to Tumor Growth.* Cancer Res. vol. 65, no. 17. pp. 7950-7958.

[18] Dhodapkar, M.V., Geller, M.D., Chang, D.H., Shimizu, K., Fujii, S., Dhodapkar, K.M., Krasovsky, J. (2003) *A Reversible Defect in Natural Killer T Cell Function Characterizes the Progression of Premalignant to Malignant Multiple Myeloma.* The Journal of Experimental Medicine. vol. 197, no. 12. pp. 1667-1676.

[19] Dhodapkar, M.V., Krasovsky, J., Osman, K., Geller, M.D. (2003) *Vigorous Premalignancy-Specific Effector T Cell Response in the Bone Marrow of Patients With Monoclonal Gammopathy.* The Journal of Experimental Medicine. vol. 198, no. 11. pp. 1753-1757.

[20] Dilly, S.A., Jagger, C.J., Sloane, J.P. (1990) *Lymphocyte Populations in Autopsy Bone Marrow Sections from Recipients of Allogeneic Marrow and Non-Transplant Sudden Death Cases.* Clin. Exp. Immunol. vol. 81, pp. 127-131.

[21] Dingli, D., Michor, F. (2006) *Successful Therapy Must Eradicate Cancer Stem Cells.* Stem Cells. pp. 2603-2610.

[22] Dunn, G.P., Bruce, A.T., Ikeda, H., Old, L.J., Schreiber, R.D. (2002) *Cancer Immunoediting: From Immunosurveillance to Tumor Escape.* Nature Publishing Group. vol. 3, no. 11. pp. 991-998.

[23] Dunn, G.P., Old, L.J., Schreiber, R.D. (2004) *The Three Es of Cancer Immunoediting.* Annual Review of Immunololgy. vol 22, pp. 329-360.

[24] Durie, B.G.M., Salmon, S.E. (1975) *A Clinical Staging System for Multiple Myeloma.* Cancer. 36, pp. 842-854.

[25] Ermentrout, B. (2002) *Simulating, Analyzing, and Animating Dynamical Systems.*, SIAM, Philadelphia.

[26] Ewens, W.J. (2004) *Mathematical Population Genetics.* Springer-Verlag.

[27] Fall, C.P., Marland, E.S. (2002) *Computational Cell Biology.* Springer.

[28] Feller, W., March, P. (1951) *Diffusion Processes in Genetics.* Proc. 2nd Berkeley Symp. on Math. Stat. and Prob. pp. 227-246.

[29] Foryś, U., Żolek, N. (1998) *A Model of the Immune System After Vaccinations.* ARI. 50, pp. 180-184.

[30] Franke, R. *A Precise Statement of the Hopf Bifurcation Theorem and Some Remarks.* Mathematical Methods: Dynamic Systems and Dynamic Optimization. pp. 1-6.

[31] Frassanito, M.A., Cusmai, A., Dammacco, F. (2001) *Deregulated Cytokine Network and Defective Th1 Immune Response in Multiple Myeloma.* Clinical and Experimental Immunololgy. vol 125, pp. 190-197.

[32] Freud, A.G., Becknell, B., Roychowdhury, S., Mao, H.C., Ferketich, A.K., Nuovo, G.J., Hughes, T.L., Marburger, T.B., Sung, J., Baiocchi, R.A., Guimond, M., Caligiuri, M.A. (2005) *A Human $CD34(+)$ Subset Resides in Lymph Nodes and Differentiates into $CD56^{bright}$ Natural Killer Cells.* Immunity. vol 22, pp. 295-304.

[33] Friedman, A. (1982) *Foundations of Modern Analysis.* Dover.

[34] Gadó, K., Domján, G., Hegyesi, H., Falus, A. (2000) *Role of Interleukin-6 in the Pathogenesis of Myltiple Myeloma.* Cell Biology International 2000. vol. 24, no. 4, pp. 195-209.

[35] Gershkevitsh, E. (2005) *Dose to Bone Marrow and Leukaemia Risk in External Beam Radiotherapy of Prostate Cancer.* Dissertationes Physicae Universitatis Tartuensis. Tartu University Press.

[36] Gollapudi, S.V.S., Kern, M. (1980) *Lipid A Induces Cells, Uniquely Present in Bone Marrow, to Secrete Proteins Other Than Immunoglobulins.* Eur. J. Biochem. vol. 108, pp. 233-237.

[37] Gopalsamy, K., Aggarwala, B.D. (1980) *Limit Cycles in Two Species Competition with Time Delays.* J. Austral. Math. Soc. vol. 22, Series B, pp. 148-160.

[38] Hale, J., Koçak, H. (1991) *Dynamics and Bifurcations.*, Springer-Verlag, New York.

[39] Harrison, W.J. (1962) *The Total Cellularity of the Bone Marrow in Man.* J. Clin. Path. 15, pp. 254-259.

[40] Hideshima, T., Bergsagel, P.L., Kuehl, W.M., Anderson, K.C. (2004) *Advances in Biology of Multiple Myeloma: Clinical Applications.* Blood. vol. 104, no. 3, pp. 607-618.

[41] Hoel, P.G., Port, S.C., Stone, C.J. (1972) *Introduction to Stochastic Processes.* Waveland Press.

[42] Höfer, T., Muehlinghaus, G., Moser, K., Yoshida, T., Mei, H.E., Hebel, K., Hauser, A., Hoyer, B., Luger, E.O., Dörner, T., Manz, R.A., Hiepe, F., Radbruch, A. (2006) *Adaptation of Humoral Memory.* Immunological Reviews. vol. 211, pp. 295-302.

[43] Horn, M.A., Webb, G. (2004) *Mathematical Models in Cancer.* Discrete and Continuous Dynamical Systems-Series B. vol. 4, no. 1.

[44] Iber, D., Maini, P.K. (2002) *A Mathematical Model of Germinal Centre Kinetics and Affinity Maturation.* J. Theor. Biol. 219, pp. 153-175.

[45] ICRP (1995) *Basic Anatomical and Physiological Data: The Skeleton.* Basic Anatomical and Physiological Data for Use in Radiological Protection. pub. 71.

[46] Iwasa, Y., Michor, F., Nowak, M.A. (2003) *Evolutionary Dynamics of Escape from Biomedical Intervention.* Proc.R. Soc. Lon. pp. 2573-2578.

[47] Iwasa, Y., Michor, F., Nowak, M.A. (2004) *Evolutionary Dynamics of Invasion and Escape.* Journal of Theoretical Biology. 226, pp. 205-214.

[48] Janeway, C.A., Travers, P., Walport, M., Shlomchik, M. (2001) *Immunobiology. The Immune System in Health and Disease.* Garland Publishing.

[49] Jarvis, L.J., LeBien, T.W. (1995) *Stimulation of Human Bone Marrow Stromal Cell Tyrosine Kinases and IL-6 Production by Contact with B Lymphocytes.* The Journal of Immunology. 155, pp. 2359-2368.

[50] Jinushi, M., Vanneman, M., Munshi, N.C., Tai, Y., Prabhala, R.H., Ritz, J., Neuberg, D., Anderson, K.C., Carrasco, D.R., Dranoff, G. (2008) *MHC Class I Chain-Related Protein A Antibodies and Shedding are Associated with the Progression of Multiple Myeloma.* PNAS. vol. 105, no. 4, pp. 1285-1290.

[51] Johnston, M.D., Edwards, C.M., Bodmer, W.F., Maini, P.K., Chapman, S.J. (2007) *Mathematical Modeling of Cell Population Dynamics in the Colonic Crypt and in Colorectal Cancer.* PNAS. vol. 104, no. 10, pp. 4008-4013.

[52] Kawano, M., Hirano, T., Matsuda, T., Taga, T., Horii, Y., Iwato, K., Asaoku, H., Tang, B., Tanabe, O., Tanaka, H., Kuramoto, A., Kishimoto, T. (1988) *Autocrine Generation and Requirement of BSF-2/IL-6 for Human Multiple Myelomas.* Nature. vol. 332, pp. 83-85.

[53] Keener, J., Sneyd, J. (1998) *Mathematical Physiology.*, Springer, New York.

[54] Kesmir, C., De Boer, R.J. (1999) *A Mathematical Model on Germinal Center Kinetics and Termination.* The Journal of Immunology. vol. 163 pp. 2463-2469.

[55] Kim, P.S., Lee, P.P., Levy, D. (2007) *Modeling Regulation Mechanisms in the Immune System.* Journal of Theoretical Biology. vol. no. 246, pp. 33-69.

[56] Kimmel, M., Axelrod, D.E. (2002) *Branching Processes in Biology.* Springer-Verlag.

[57] Kirschner, D., Panetta, J.C. (1998) *Modeling Immunotherapy of the Tumor-Immune Interaction.* Journal of Mathematical Biology. vol. 37, pp. 235-252.

[58] Klein, B., Zhang, X., Jourdan, M., Content, J., Houssiau, F., Aarden, L. Piechaczyk, M., Battaille, R. (1989) *Paracrine Rather Than Autocrine Regulation of Myeloma-Cell Growth and Differentiation by Interleukin-6.* Blood. vol. 73, no. 2, pp. 517-526.

[59] Klein, B., Zhang, X., Lu, Z., Bataille, R. (1995) *Interleukin-6 in Human Multiple Myeloma.* Blood. vol. 85, no. 4, pp. 863-872.

[60] Kondaiah, P. (2003) *Bone Marrow Stromal Cells and Multi-Lineage Differentiation.* J. Biosci. vol. 28, no. 6, pp. 651.

[61] Kot, M. (2001) *Elements of Mathematical Ecology.*, Cambridge University Press, UK.

[62] Kuehl, W.M., Bergsagel, P.L. (2002) *Multiple Myeloma: Evolving Genetic Events and Host Interactions.* Nature Reviews. vol. 2, pp. 175-187.

[63] Kwok, B.C.P., Dawson, G., Ritter, M.C. (1980) *Stimulation of Glycolipid Synthesis and Exchange by Human Serum High Density Lipoprotein-3 in Human Fibroblasts and Leukocytes.* The Journal of Biological Chemistry. vol. 256, no.1, pp. 92-98.

[64] Kyle, R.A., Rajkumar, S.V. (2003) *Monoclonal Gammopathies of Undetermined Significance: A Review.* Immunological Reviews. vo. 194, pp. 112-139.

[65] Lajtha, L.G. (1957) *Bone Marrow Cell Metabolism.* Radiobiology Laboratory, Department of Radiotherapy, Oxford, England.

[66] Lokhorst, H.M., Lamme, T., de Smet, M., Klein, S., de Weger, R.A., van Oers, R., Bloem, A.C. (1994) *Primary Tumor Cells of Myeloma Patients Induce Interleukin-6 Secretion in Long-Term Bone Marrow Cultures.* Blood. vol. 84, no. 7, pp. 2269-2277.

[67] Lust, J.A., Donovan, K.A., Hatcher M.J. *Biology of the Transition of Monoclonal Gammopathy of Undetermined Significance (MGUS) to Multiple Myeloma.* Mayo Clinic.

[68] Lynch, S. (2001) *Dynamical Systems with Applications Using Maple.*, Birkhäuser, Boston.

[69] Lynch, S. (2004) *Dynamical Systems with Applications Using Matlab.*, Birkhäuser, Boston.

[70] Manz, R.A., Arce, S., Cassese, G., Hauser, A.E., Hiepe, F., Radbruch, A. (2002) *Humoral Immunity and Long-Lived Plasma Cells.* Current Opinion in Immunlogy. 14, pp. 517-521.

[71] Marsden, J.E., McCracken, M. (1976) *The Hopf Bifurcation and its Applications.* Springer-Verlag, New York.

[72] Mendenhall, Scheaffer, Wackerly (1986) *Mathematical Statistics With Applications.* Duxbury Press.

[73] Michor, F., Iwasa, Y., Lengauer, C., Nowak, M.A. (2005) *Dynamics of Colorectal Cancer.* Seminars in Cancer Biology 15. pp. 484-493.

[74] Monteiro, J.P., Benjamin, A., Costa, E.S., Barcinski, M.A., Bonomo, A. (2005) *Normal Hematopoiesis is Maintained by Activated Bone Marrow $CD4^{+}T$ Cells.* Blood. vol. 105, no. 4. pp. 1484-1491.

[75] Moser, K., Tokoyoda, K., Radbruch, A., MacLennan, I., Manz, R.A. (2006) *Stromal Niches, Plasma Cell Differentiation and Survival.* Current Opinion in Immunology. 18, pp. 265-270.

[76] Nichols, G.E., Shiraishi, T., Young, Jr., W.W. (1988) *Polarity of Neutral Glycolipids, Gangliosides, and Sulfated Lipids in MDCK Epithelial Cells.* Journal of Lipid Research. vol. 29, pp. 1205-1213.

[77] O'Connor, B.P., Gleeson, M.W., Noelle, R.J., Erickson, L.D. (2003) *The Rise and Fall of Long-Lived Humoral Immunity: Terminal Differentiation of Plasma Cells in Health and Disease.* Immunological Reviews. vol. 194, pp. 61-76.

[78] Ogasawara, H., Takashi, T., Hirano, D., Aoki, Y., Nakamura, M., Kodama, H. (1996) *Induction of IL-6 Production by Bone Marrow Stromal Cells on the Adhesion of IL-6-Dependent Hematopoietic Cells.* Journal of Cellular Physiology. 169, pp. 209-216.

[79] *Pathology.* http://www.med-ed.virginia.edu/courses/path/innes/wcd/ leukmorph.cfm.

[80] Pecherstorfer, M., Seibel, M.J., Woitge, H.W., Horn, E., Schuster, J., Neuda, J., Sagaster, P., Köhn, H., Bayer, P., Thiébaud, D., Ludwig, H. (1997) *Bone Resorption in Multiple Myeloma and in Monoclonal Gammopathy of Undetermined Significance: Quantification by Urinary Pyridinium Cross-Links of Collagen.* Blood. vol. 90, no. 9. pp. 3743-3750.

[81] Perko, L. (2001) *Differential Equations and Dynamical Systems.*, Springer, New York.

[82] Pihlgren, M., Schallert, N., Tougne, C., Bozzotti, P., Kovarik, J., Fulurija, A., Kosco-Vilbois, M., Lambert, P., Siegrist, C. (2001) *Delayed and Deficient Establishment of the Long-Term Bone Marrow Plasma Cell Pool During Early Life.* Eur. J. Immunol. vol. 31, pp. 939-946.

[83] *Plasma Cell.* http://healthsystem.virginia.edu/internet/hematology/ HessEDD/Normal-hematopoietic-cells/Plasma-cell.cfm.

[84] Pribylova, L. (2009) *Bifurcation Routes to Chaos in an Extended Van Der Pol's Equation Applied to Economic Models.* Electronic Journal of Differential Equations. vol. 2009, no.53. pp. 1-21.

[85] Prikrylova, D., Jilek, M. *Mathematical Modeling of the Immune Response.* CRC Press.

[86] Rundell, A., HogenEsch, H., DeCarlo, R. (1995) *Enhanced Modeling of the Immune System to Incorporate Natural Killer Cells and Memory.* Proceedings of the American Control Conference. pp. 255-259.

[87] Sakiyama, H., Gross, S.K., Robbins, P.W. (1972) *Glycolipid Synthesis in Normal and Virus-Transformed Hamster Cell Lines.* Proc. Nat. Acad. Sci. vol. 69, no.4. pp. 872-876.

[88] San Miguel, J.F., García-Sanz, R., González, M., Moro, M.J., Hernández, J.M., Ortega, F., Borrego, D., Carnero, M., Casanova, F., Jiménez, R., Portero, J.A., Orfão, A. (1995) *A New Staging System for Multiple Myeloma Based on the Number of S-Phase Plasma Cells.* Blood. vol. 85, no. 2, pp. 448-455.

[89] Šátek, V., Kunovský, J., Petřek, J. (2008) *Multiple Arithmetic in Dynamic System Simulation.* IEEE.

[90] Segel, L.A. (1972) *Simplification and Scaling.* SIAM Review. vol. 14, no. 4. pp. 547-571.

[91] Shankaran, V., Ikeda, H., Bruce, A.T., White, J.M., Swanson, P.E., Old, L.J., Schreiber, R.D. (2001) $IFN-\gamma$ *and Lymphocytes Prevent Primary Tumour Development and Shape Tumour Immunogenicity.* Nature. vol. 410, pp. 1107-1111.

[92] Simmons, P.J., Torok-Storb, B. (1991) *Identification of Stromal Cell Precursors in Human Bone Marrow by a Novel Monoclonal Antibody, STRO-1.* Blood. vol. 78, no. 1, pp. 55-62.

[93] Smyth, M.J., Godfrey, D.I. (2000) *NKT Cells and Tumor Immunity - A Double-Edged Sword.* Nature Immunology. vol. 1, no. 6, pp. 459-460.

[94] Stengel, R.F., Ghigliazza, R., Kulkarni, N., Laplace, O. (2002) *Optimal Control of Innate Immune Response.* Optim. Control Appl. Meth. 23, pp. 91-104.

[95] Strobel, E., Strobel, H.G., Bross, K.J., Winterhalter, B., Fiebig, H., Schildge, J.U., Löhr, G.W. (1972) *Effects of Human Bone Marrow Stroma on the Growth of Human Tumor Cells.* Cancer Research. 49, pp. 1001-1007.

[96] Sud, D., Bigbee, C., Flynn, J. L., Kirschner, D. E. (2006) *Contribution of* $CD8^{+}T$ *Cells to Control of Mycobacterium Tuberculosis Infection.* The Journal of Immunology. pp. 4296-4314.

[97] Sullivan, P.W., Salmon, S.E., (1972) *Kinetics of Tumor Growth and Regression in IgG Multiple Myeloma.* The Journal of Clinical Investigation. vol. 51, pp. 1697-1708.

[98] Sulzer, B., Van Hemmen, J.L. (1999) *Adaptive Control: A Strategy to Treat Autoimmunity.* Journal of Theoretical Biology. 196, pp. 73-79.

[99] Suzuki, K., Hirokawa, K., Hatakeyama S. (1984) *Age-Related Change of Distribution of Immunoglobulin Containing Cells in Human Bone Marrow.* Virchows Arch, Pathol Anat. 404, pp. 243-251.

[100] Taneyhill, D.E., Dunn, A.M., Hatcher, M.J. (1999) *The Galton-Watson Branching Process as a Quantitative Tool in Parasitology.* Parasitology Today. vol. 15, no. 4.

[101] Tang, Y., Zhou, L. (2005) *Hopf Bifurcation and Stability of a Competition Diffusion System with Distributed Delay.* Publ. RIMS, Kyoto Univ. vol. 41, 2005, pp. 579-597.

[102] Terstappen, L.W.M.M., Johnsen, Steen., Segers-Nolten, I.M.J., Loken, M.R. (1990) *Identification and Characterization of Plasma Cells in Normal Human Bone Marrow by High-Resolution Flow Cytometry.* Blood. vol. 76, no. 9, pp. 1739-1747.

[103] Uchiyama, H., Barut, B.A., Mohrbacher, A.F., Chauhan, D., Anderson, K.C. (1993) *Adhesion of Human Myeloma-Derived Cell Lines to Bone Marrow Stromal Cells Stimulates Interleukin-6 Secretion.* Blood. vol. 82, no. 12, pp. 3712-3720.

[104] Walsh, M.C., Kim, N., Kadono, Y., Rho, J., Lee, S.J., Lorenzo, J., Choi, Y. (2006) *Osteoimmunology: Interplay Between the Immune System and Bone Metabolism.* Annu. Rev. Immunol. 24, pp. 33-63.

[105] Warrender, C.E. (2004) *Modeling Intercellular Interactions in the Peripheral Immune System.* Dissertation. Doctor of Philosophy. Computer Science. pp. 89.

[106] Wiggins, S. (1990) *Introduction to Applied Nonlinear Dynamical Systems and Chaos.* Springer-Verlag, New York.

[107] Wigginton, J.E., Kirschner, D. (2001) *A Model to Predict Cell-Mediated Immune Regulatory Mechanisms During Human Infection with Mycobacterium Tuberculosis.* The Journal of Immunology. pp. 1951-1967.

[108] Witzig, T.E., Timm, M., Larson, D., Therneau, T., Greipp, P.R. (1998) *Measurement of Apoptosis and Proliferation of Bone Marrow Plasma Cells in Patients With Plasma Cell Proliferative Disorders.* British Journal of Haematology. 104 pp. 131-137.

[109] Wols, H.A.M. (2005) *Plasma Cells.* Encyclopedia of Life Sciences. John Wiley & Sons, Ltd.

[110] Wols, H.A.M., Ippolito, J.A., Yu, Z., Palmer, J.L., White, F.A., Le, P.T., Witte, P.L. (2007) *The Effects of Microenvironment and Internal Programming on Plasma Cell Survival.* International Immunology 2007. pp. 1-10.

[111] Yakowitz, S., Szidarovszky, F. (1986) *An Introduction to Numerical Computations.*, Macmillan Publishing Company, New York.